α-Synuclein pathology and mitochondrial dysfunction

Studies in cell models for Parkinson's disease

Koen C. van Zomeren

Research described in this PhD dissertation was conducted at the Section Medical Physiology, Department of Neuroscience, University Medical Centre Groningen, University of Groningen, the Netherlands.

The research described in this PhD dissertation

Printing of this dissertation was supported by:

Universitair medisch centrum Groningen
Research School BCN
University of Groningen

Print: Ipskamp Printing

ISBN printed version: 978-94-034-0267-3

ISBN electronic version: 978-94-034-0268-0

rijksuniversiteit groningen

α-Synuclein pathology and mitochondrial dysfunction

Studies in cell models for Parkinson's disease

Proefschrift

ter verkrijging van de graad van doctor aan de
Rijksuniversiteit Groningen
op gezag van de
rector magnificus prof. dr. E. Sterken
en volgens besluit van het College voor Promoties.

De openbare verdediging zal plaatsvinden op

27-11-2017 om 12:45 uur

door

Koen Cornelis van Zomeren

geboren op 3 oktober 1985
te Apeldoorn

Promotor

Prof. H.W.G.M. Boddeke

Copromotor

Dr. J.C.V.M. Copray

Beoordelingscommissie

Prof. dr. H.H. Kampinga

Prof. dr. T. van Laar

Prof. dr. M.P. Smidt

Content

Chapter 1

General introduction

Preface

Although this year marks the celebration of two centuries of Parkinson's disease research, the disease still remains poorly understood. Neurodegenerative disorders put a growing strain on health care with increasing incidence in our ageing population. While much research is conducted, there have so far been few successes in preventing or delaying the onset of these diseases. It is hoped that at the start of the 21st century, with advancing technological assistance and biological understanding, scientists will finally be able to solve some of biology's major puzzles: to understand how the brain ages and how we can manage this process.

This thesis aims to elucidate a part of this puzzle with a focus on Parkinson's disease and by using the latest technological developments and scientific insights in the field of molecular neuroscience. Dopaminergic neurons derived from induced pluripotent stem cells (iPSCs), engineered from skin biopsies, allow us to study these neurons in the process of degeneration for the first time in decades after their implication in Parkinson's disease. Combining these techniques with advanced fluorescence microscopy allows us to follow the dynamics of mitochondrial trafficking in-vitro in neurons derived from Parkinson's patient skin biopsies. The following introduction aims to provide a concise background to the work presented in this thesis.

Parkinson's disease

Parkinson's disease (PD) is the second most common neurodegenerative and the most common movement disorder in the world, affecting around 2% of the population over the age of 60. First described in 1817 by James Parkinson as paralysis agitans [1], the work

of French neurologist Jean-Martin Charcot provided a landmark in the understanding of the disease nearly 50 years later. He described early motor symptoms including tremors, rigidity, bradykinesia and postural instability [2]. He also ascertained that the disease was not of pyramidal origin, but it took the work of Arvid Carlsson in the late 1950's to describe the underlying cellular processes using a model of monoamine depletion to immobilize animals [3, 4]. This pointed to the involvement of the dopaminergic system, specifically the substantia pars compacta (SNc), harboring the ventral midbrain A9 dopaminergic population. Progressive cell death of these neurons leads to diminished dopamine secretion in the putamen and caudate nucleus of the striatum, causing the underlying cause of the observed motor defects in PD. Onset of motor symptoms occurs when around 60% of the dopaminergic (DA) neuronal population and around 80% of dopamine is depleted [5]. This leads to a challenging conclusion, since it means that the disease is mostly studied at the end-stage when DA neurons are dying or dead and when most DA neurons are characterized by protein inclusions called Lewy bodies. Motor function deteriorates in most patients over a period of 10 years after diagnosis, during which non-motor effects like sleep disorders, depression and dementia can manifest [6]. This indicates that though DA neurons are mainly affected, other neuronal populations are also affected by the disease. In 2003, Braak et al. observed a specific pattern of disease spreading, now widely known as Braak staging of Parkinson's disease [7]. The accompanying Braak hypothesis stipulates that Lewy bodies spread throughout the brain via the olfactory bulb and/or gastrointestinal tract, entering the medulla oblongata and pontine tegmentum at stage 1 and 2. Stage 3 and 4 show spreading to the midbrain, leading to lesions in the substantia nigra. Finally, stages 5 and 6 show development of lesions and inclusions in the neocortex (see Figure 1) [8]. This is a critical observation, since it indicates that substantia nigra DA neurons are not the first cell type affected by disease, but are likely more vulnerable to the disease pathology. Indeed, many patients report bowel irritability or changes in

olfaction up to a decade prior to disease [9], as predicted by the Braak hypothesis [10]. The observation that many patients develop dementia or depression, also adds evidence for the later stages described by Braak et al. [11]. It should be noted, however, that many patients do not strictly follow the pathway delineated by Braak et al. and PD can be highly heterogeneous in both development and progression of disease [12]. For this reason, the Braak hypothesis is frequently debated, and careful considerations should be made concerning the cause of PD. Nevertheless, the observation that spreading of disease occurs in PD and that the disease is progressive remains a widely accepted view. In this thesis, Braak staging will be approached from the latter view, a piece of evidence for spreading of pathology and the progressive nature of the disease.

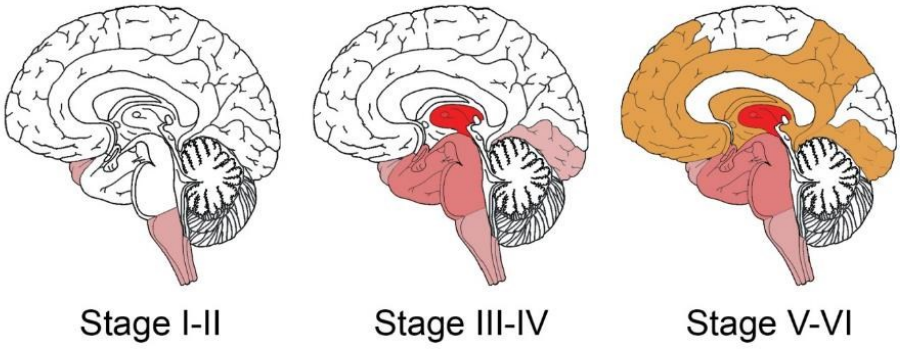

Figure 1. Braak staging of Parkinson's disease. *At stage I & II pathology spreading is observed in the pons and the olfactory bulb, after which disease pathology progresses towards the limbic systems (Stage III & IV). Finally, at stage V & VI disease pathology progresses to the neocortex. Modified after Braak* et al. *[8]*

Ageing and disease

For many prevalent diseases, the largest risk factor is age. With an increase in life-expectancy, the incidence of age-related disorders increases, placing a growing burden on society. To tackle this epidemic,

efforts to understand the biology of ageing is vital. For many years cellular ageing was approached from the concept of genetic control of ageing, which was supported by the Hayflick studies in the 1960s [13]. However, ageing is now widely considered to be a complex process consisting of both internal and external factors leading to loss of physiological integrity. This loss of physiological integrity in ageing is currently characterized by the following hallmarks: genomic instability, telomere attrition, epigenetic alterations, loss of proteostasis, deregulated nutrient sensing, mitochondrial dysfunction, cellular senescence, stem cell exhaustion and altered intercellular communication [14]. Many of the hallmarks mentioned in [14] are based on observations in cancer and stem cells, and may not be directly applicable to an ageing brain. In the brain, the cumulative acquisition of cellular damage under normal metabolic function is likely to result in cellular senescence. To assess hallmarks of PD, the next sections will discuss several contributors to this disease.

Genetic contributors to Parkinson's disease

Though familial PD cases have provided more insight into the disease development and contributors, the disease development of both idiopathic and familial Parkinson's remains poorly understood. Most PD cases (>90%) are thought to be sporadic, and some studies have linked the development of PD to environmental toxins [15] or genetic risk factors [16]. An overview of the most common genes involved in familial PD is depicted in Table 1.

Table 1. *Most common familial PD genes and mutations, gene names and mutations with reported age of onset. Disease progression and special remarks are stated in the last columns.*

Gene	Mutations	Average A/O	Progression	Remarks
SNCA	Duplication [17]	~50	Slow	Dosage effect
	Triplication [18]	~40	Rapid	Widespread pathology
	A53T [19]	40-50	Rapid	Dementia, prominent motor symptoms
	A30P [20]	~60	Slow	Mild dementia
	E46K [21]	~45	Rapid	Dementia, visual hallucinations
LRRK2	G2019S [22]	~60	Slow	Occasional absence of Lewy bodies
VPS 35	D620N [22]	~60	Slow	Resembles idiopathic PD
PARKIN	Many [23]	20-40	Slow	Absence of Lewy bodies
PINK1	Many [24]	20-50	Slow	Resembles idiopathic disease

In 1997, Polymeropoulos et al. discovered the mutation G209A in the *SNCA* gene in familial PD, leading to an A53T mutation in the protein α-synuclein [19]. Shortly thereafter, α-synuclein was discovered as a major constituent in Lewy bodies [25, 26]. Currently, seven α-synuclein related mutations are known, including the G88C (A30P) [20] and G188A (E46K) [21, 27] mutations or duplications [17] and triplications [18] of the *SNCA* genomic region. While these mutations are present in the same gene, these mutations have varying disease characteristics. A53T mutations are associated with rapid progression and widespread motor pathology [28]. A30P mutations on the other hand display a milder phenotype, with later age of onset and the occurrence of mild dementia

[29]. E46K mutations lead to rapidly progressing PD, similar to A53T mutations, but with added visual hallucinations [27].
Interestingly, triplication of the SNCA locus leads to earlier onset of disease compared to duplication, indicating there is a dosage effect in the expression of α-synuclein and disease onset [30]. A typical age of onset for SNCA triplication (four SNCA copies) is around 40 years, while SNCA duplication (three SNCA copies) onset is around 50 years of age. Disease progression in SNCA duplications is also slower and the disease pattern is highly heterogeneous [31], adding further evidence for a dosage effect.

In addition to α-synuclein, other familial PD genes have been identified, such as mutations in leucine-rich repeat kinase 2 (LRRK2), leading to autosomal dominant PD [22], or acting as risk factor depending on the mutations [32]. The fact that LRRK2 can also be a risk factor for PD, hints that both genetic and environmental cues can contribute to disease.

Vacuolar protein sorting-associated protein 35 (VPS35) mutations have only recently been discovered and interestingly lead to disease progression resembling idiopathic PD [33, 34]. As a major component of a membrane protein-recycling retromer complex, VPS35 is thought to play a role in mitochondrial turnover, causing mitochondrial fragmentation and cell death.

Juvenile PD with an onset below 30 years of age is mainly caused by homozygous PARK2 mutations [23]. Lewy bodies are absent in this form of PD and progression of disease is slow. The second largest cause for juvenile PD are mutations in the protein PINK1, with similar disease characteristics as idiopathic PD [24]. Both PARK2 and PINK1 are involved in mitochondrial turnover and lead to mitochondrial dysfunction at early age.

Synucleins

The synuclein family consists of the three genes *SNCA*, *SNCB* and *SNCG*, encoding the proteins α-, β- and γ-synuclein. Synucleins are

predominantly found in neural tissues, and are enriched at presynaptic nerve terminals [35]. In neurons they are abundantly expressed and by some estimates are thought to make up 1% of the cytosolic protein content [36]. Human α-synuclein has 140 amino acids, and is believed to be natively unfolded [35], although recent research has suggested it might be present in a tetrameric structure [37]. The structural properties of α-synuclein are depicted in figure 2.

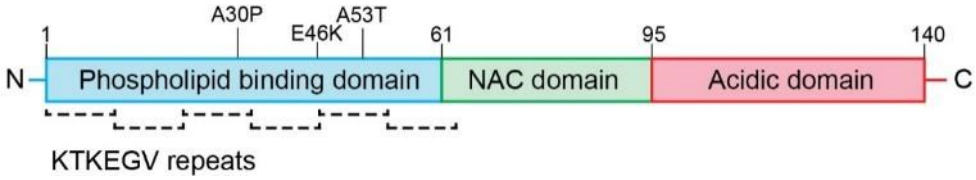

Figure 2. Structural properties of α-synuclein. *Known mutations are located in the N-terminal phospholipid domain, which is characterized by KTKEGV repeats. This is followed by the hydrophobic NAC domain and flanked by the acidic C-terminal domain.*

The central portion of the protein, called the non-amyloid-β component (NAC), is hydrophobic and prone to aggregation [38]. The C-terminus is highly acidic, and the N-terminus consists of 11-residue slightly dissimilar repeats (XKTKEGVXXXX), which influence α-synuclein aggregation properties. Interactions with acidic phospholipid surfaces are mediated via the N-terminal domain. Anionic solvents like sodium dodecyl sulfate (SDS) can also interact with this domain, making it more challenging to study these proteins in Western blot or immune labeling. Upon interaction with phospholipid surfaces, conformational changes cause synuclein to fold into an amphipathic α-helix. This property likely sensitizes α-synuclein to dimerization. Under normal physiological conditions α-synuclein can change from a membrane bound state to an unfolded state. The initial phase of dimerization that occurs is reversible, but dimers exhibit high stability and can act as a trigger in a self-assembly process [39]. This leads to a thermodynamically favorable state in which synuclein can form oligomers, and subsequently fibrils. Finally, the

formation of these fibrils is hypothesized to lead to the formation of Lewy bodies (see Figure 3.).

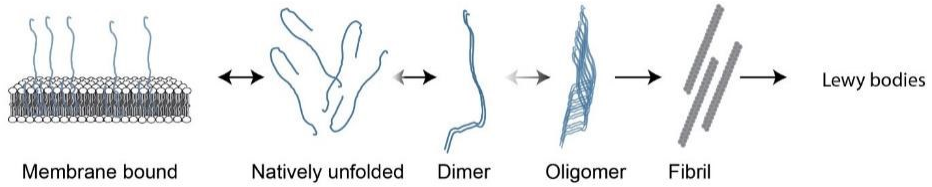

Figure 3. Model for α-synuclein aggregation. *Membrane bound state and natively unfolded monomers can dimerize, which leads to formation of oligomers. This is followed by the formation of fibrils, ultimately leading to the formation of Lewy bodies. Arrows indicate the favorable conformational state.*

The exact functions of the synuclein protein family remain to be elucidated, but involvement in vesicle snaring and exocytosis has been established [40]. Mouse α-synuclein knockout models display mild cognitive impairment [41], but even triple synuclein knockout mice show no morphological aberrations or decrease in synapse number [42]. This suggests that synucleins have a modulatory role and are not essential for neuronal function or survival. Considering its abundant expression pattern, it is likely that the synuclein family is involved in the modulation of many cellular processes.

α-Synuclein and protein inclusions

The propensity of α-synuclein to oligomerize, fibrillize and form aggregates has been studied in detail since its implication in PD. While Braak staging revealed a step-wise disease progression, the underlying mechanism for spreading pathology remained unknown. In 2008, Li et al. showed the presence of Lewy bodies in post mortem brains of PD patients that received embryonic nigral transplants 10 to 15 years before [43]; these findings indeed point to a spreading of pathology into the newly transplanted dopamine neurons from surrounding tissue. The transplanted fetal cells contained α-synuclein positive inclusions and additional experiments showed that this was the case only in long-term

grafts (>10 years after grafting) [44]. This spread of pathology is thought to be the result of prion-like properties of α-synuclein, which has been demonstrated in various model systems. The ability of α-synuclein to transfer from cell to cell has been demonstrated in cell models [45] and recently in rat models. By injecting rats with post mortem PD patient brain lysate or α-synuclein fibrils near the enteric plexus, α-synuclein was able to spread to the brain via the vagus nerve [46]. This find is supported by epidemiological evidence that shows chronic duodenal ulcer patients undergoing a truncal vagotomy have a reduced risk of developing PD [47].

Taken together, there is ample evidence that supports the Braak hypothesis, cell-to-cell transfer of α-synuclein, and gastro-intestinal involvement in the development of PD.

Protein homeostasis

Aberrant protein homeostasis leads to conformational changes in tertiary protein structure, incorrect folding of proteins or non-functional degradation of proteins. Each of these processes has been studied for PD, but no clear underlying mechanism has arisen to describe the development of disease. Chaperone folding proteins have been implicated in many neurodegenerative diseases and in PD it has been observed that heat shock proteins (HSP) are present in Lewy bodies [48, 49]. Apart from α-synuclein, Lewy bodies contain neurofilaments, various ubiquitinated proteins, and HSP70 and HSP90. Furthermore, proteasomal degradation of α-synuclein has been linked to HSP27, HSP40, HSP70, and HSP90 [49]. It is hypothesized that proper function of HSPs can prevent occurrence of inclusions and avert development of PD [50], but as of yet none of the HSP genes have been associated to PD risk in large GWAS studies. Further investigation is required to elucidate the causal relationship between HSPs and PD, and check their validity as a therapeutic target.

One prominent gene involved in protein degradation has been linked to PD. Mutations in glucocerebrosidase (GBA1) cause lysosomal

dysfunction and lead to increased risk for α-synuclein aggregation [51]. Currently, GBA1 mutations are considered the most widely distributed genetic risk factors for PD, with reported GBA1 mutations in over 5% of PD patients. Estimates conclude that GBA1 mutations can lead to a 20- or 30-fold increased risk for PD development [52]. GBA1 mutations are also implicated in Gaucher disease [53] in which recessive mutations can cause lipid storage disease. Heterozygous carriers of Gaucher disease associated GBA1 mutations have an increased risk for PD. Mutations in Gaucher disease are usually associated with loss of function or out of frame mutations that disrupt protein production. GBA1 mutations associated with PD, on the other hand, are hypothesized to induce a gain of function [51]. The underlying mechanism of GBA1-related PD is still debated, and it remains a protein of interest since disease closely mimics the pathology of idiopathic PD with a late onset and relatively slow disease progression.

Another protein implicated in PD involved in protein homeostasis is LRRK2. While being a major risk factor for PD, around 20% of heterozygous mutation carriers do not develop disease. Furthermore, carriers that do get PD can present highly heterogeneous disease patterns and display differences in neuropathology or even have an absence of Lewy bodies [30]. Apart from PD, LRRK2 mutations are also implicated in other neurodegenerative disorders, including Lewy body pathology, tauopathies, and Alzheimer's disease [54, 55].

Mitochondrial dysfunction in Parkinson's disease

The link between PD and mitochondrial dysfunction was elucidated by a chemistry student who attempted to produce synthetic opiates and injected himself with the substance 1-methyl-4-phenyl-1,2,3,6-tetrahydropyridine (MPTP) [56]. Several days after, he suffered from what appeared to be early onset PD, and the connection between drug use and the disease was made. MPTP is converted by glia cells into MPP+ by monoamine oxidase-B, and subsequently taken up by dopamine

transporters of DA neurons. The mechanism by which MPP+ exerts its effects is attributed to interference with complex I of the electron transport chain in mitochondria [56]. This leads to the production of reactive oxygen species (ROS), a decrease of ATP production and a subsequent toxic increase in cellular calcium levels. Several toxins causing mitochondrial respiratory chain inhibition have since been found to induce PD-like symptoms, such as the pesticide rotenone [57] and the herbicide paraquat [58]. Many pesticides are now epidemiologically linked to the development of PD and most are linked to dysfunction of complex I [15, 59]. The involvement of complex I is further supported by the finding that complex I activity is reduced in muscles and brain of PD patients [60-62]. Mild inhibition of complex I can lead to increased production of ROS, which can in turn lead to DNA damage, RNA damage, and protein damage.

Further evidence for mitochondrial dysfunction in PD is provided by mutations in the *PINK1* and *PARK2* genes, coding for the protein PINK1 and Parkin. In mitochondria with intact membrane potential, PINK1 is internalized into the inner mitochondrial membrane, where it is cleaved and inactivated by PARL [63, 64]. Mitochondria that lack sufficient membrane potential are unable to internalize PINK1 and, after recruitment of Parkin, can go into mitophagy or mitofission [65]. Mutations in either *PINK1* or *PARK2* lead to early onset (<40 years) PD with risk of additional features including depression and dementia [23, 24]. While non-motor symptoms are observed, the specific degeneration of DA neurons in the substantia nigra pars compacta emphasizes the vulnerability of these cells. A link between α-synuclein and ROS production has yet to be elucidated, but theories about underlying mechanisms are diverse, ranging from direct effects of α-synuclein oligomers on the mitochondrial membrane [66, 67], effects on mitophagy [68, 69], to indirect effects on mitochondrial trafficking in neurons [70, 71].

Environmental contributors to PD

The implication of mitochondrial toxins has led to the theory that environmental factors are contributors to the incidence of sporadic PD. While herbicides and pesticides show a clear connection to PD [58], other chemicals and heavy metals have also been implied in idiopathic PD [72, 73]. While not entirely conclusive, an etiologic study by Tanner et al. on monozygotic and dizygotic twin pairs established that a genetic component is not evident for idiopathic PD [74]. These results were confirmed in another twin cohort, suggesting environmental factors play an important role in the etiology of sporadic PD [75]. Indeed, the occurrence of PD has been linked to higher exposure to pesticides [76] and rural living [72]. Other chemicals implied in PD are organic solvents, such as the solvent trichloroethylene, which is associated with an increased risk of PD upon repeated exposure [77]. It should be noted that while evidence for an environmental disease component is strong, development of sporadic PD is likely attributable to a complex interplay between genetic susceptibility and environmental factors.

Axonal transport and Parkinson's disease

Neuronal axons can cover large distances and axonal trafficking to distal parts is essential to the function of neurons. The unique architecture of the neuronal cell requires information from the soma to be transported for lengths of over a meter in some neurons. The axonal trafficking process is complex and makes neuronal cells vulnerable to trafficking deficiencies. Many neurodegenerative diseases, including PD [78, 79], have been linked to altered axonal transport [80-82]. The basic mechanism for transport requires a cytoskeletal network and the presence of motor proteins. In neurons, long-range axonal transport is mainly dependent on microtubules, the presence of kinesins for anterograde and the presence of dyneins for retrograde trafficking. Cargo (e.g. vesicles, proteins, mitochondria) is bound to kinesins or dyneins and subsequently transported over microtubules. Direction is caused by polarity of the

microtubule, whereby kinesins move to the plus-end while dyneins moves to the minus-end. Transport rates can vary greatly from fast trafficking of organelles (~1 µm/s), to slow trafficking of structural proteins (<0.1 µm/s) (See also Figure 4) [83].

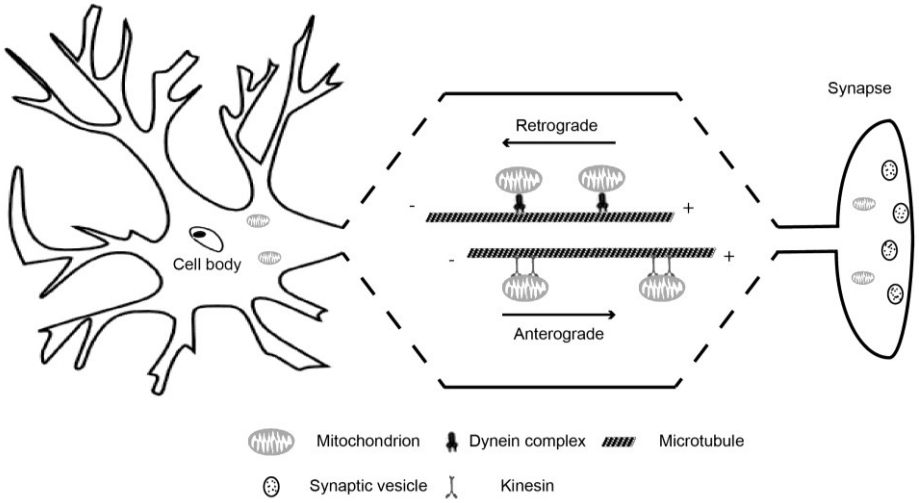

Figure 4. Schematic representation of axonal trafficking. *Anterograde trafficking takes place via kinesins, while retrograde trafficking is facilitated by dyneins. Trafficking takes place along microtubules, which are organized with a distal plus-end and minus-ends near the soma.*

Synucleins are predominantly transported via slow trafficking and axonal transport of synuclein slows significantly with ageing [84, 85]. This trafficking retardation was proposed to lead to α-synuclein aggregation formation over time, hampering normal axonal trafficking dynamics [86].

Selective vulnerability of SNc DA neurons likely arises from the size of their largely unmyelinated axonal arbor, estimated to be ten times larger compared to other neurons [87]. Apart from this complex axonal architecture, SNc DA neurons express L-type Ca^{2+} channels that regulate the robust pacemaker properties of these neurons resulting in high neuronal activity [88, 89]. Taken together, the cellular architecture and intrinsic pacemaking properties place SNc DA neurons under constant

high energy demand, which makes them more vulnerable to mitochondrial dysfunction and oxidative stress. Mitochondrial integrity in distal regions of neuronal cells is entirely dependent on proper retro- and anterograde trafficking of these organelles. Therefore, the complexity of the axonal arbor in SNc DA neurons makes these cells vulnerable to trafficking deficits. Another link is provided by the observation that PINK1 is involved in mitochondrial trafficking, fission and fusion through interaction with the MIRO/Milton complex [90]. The MIRO/Milton complex is an essential adaptor complex involved in mitochondrial trafficking, coupling mitochondria to kinesin 1 [91]. A link between mitochondrial trafficking, PINK1 mutations, and early onset PD provides evidence for mitochondrial trafficking involvement in this disease [92]. Equally important to anterograde trafficking is retrograde trafficking. Indeed, the implication of axonal trafficking in PD is supported by a heterozygous mutation in *DCTN1*, a subunit of the dynactin complex, which anchors vesicles to retrograde dynein motor proteins. Mutations in *DCTN1* lead to late onset PD with mild cognitive impairment [93]. While the process of mitophagy, i.e. the elimination of damaged mitochondria, can take place at distal regions of the axon [94], proper retrograde trafficking remains essential to remove dysfunctional or damaged mitochondria. Presence of damaged mitochondria at distal parts of the cell leads to oxidative damage at these sites, resulting in damaged mitochondrial DNA and oxidation of proteins at these sites. Presynaptic terminals, which are characterized by a high energy demand and Ca^{2+} accumulation, are crucially dependent on functional trafficking of mitochondria. The link between intracellular trafficking and α-synuclein pathology has been investigated, and trafficking has be shown to be impaired upon expression of α-synuclein [95]. The inhibiting effect of oligomergic α-synuclein on tubulin polymerization is a mechanism that has been proposed [96], and a recent study has shown a direct effect of α-synuclein on retrograde trafficking [97]. Lysosomal dysfunction in an iPS-based PD model is also demonstrated to occur through trafficking disruptions by α-synuclein [98],

further adding to the hypothesis that trafficking is impaired in PD pathology. The bridge between mitochondrial dysfunction and trafficking impairment has been illustrated by assessing the mitochondrial dynamics in mouse cortical neurons overexpressing human α-synuclein. In this model, overall transport velocity was reduced in axons of cells expressing A53T α-synuclein [99]. However, the underlying trafficking dynamics, i.e. retrograde and anterograde trafficking, and the presence of this deficiency has not yet been characterized in a human PD model. The focus of this thesis will be primarily on α-synuclein and mitochondrial trafficking in relation to PD.

Therapies for Parkinson's disease

Groundbreaking research in the early 1950s by Arvid Carlsson [3] showed a reduction of Parkinsonian symptoms by administering the dopamine precursor L-DOPA in a Parkinsonian animal model. The discovery led to the most common and effective line of therapy of PD [100]. While other drugs like monoamine oxidase B inhibitors [101] or dopamine agonists [102] are also used, the side effects associated with these treatments make them less suitable compared to L-DOPA [103-105]. Another line of therapy used is the surgical insertion of brain electrodes [106]. Deep brain stimulation has proven effective in patients with unstable L-DOPA responses, but possible complications during surgery and the fact that it merely treats symptoms of disease make it less commonly used. Addressing the underlying cause of PD symptoms, the loss of ventral midbrain DA neurons, was explored in the 80's by injecting fetal brain grafts into the brains of PD patients aiming to restore striatal DA levels [107]. While initial results were positive, later trials reported no significant benefit within a short period following engraftment [108]. Furthermore, the high demand for fetal tissue, six to eight embryos for one brain [109, 110], made the technique impractical for routine therapy. Due to side effects and ethical concerns, fetal transplant therapies in PD were put on halt for over a decade, but have recently gained renewed interest

[111]. Advancements in the stem cell field have provided methods that can provide a potential source for DA neurons. The introduction of DA neurons derived from embryonic stem cells (ESCs) in 2003 [112, 113], and the later discovery of induced pluripotent stem cells (iPSCs) [114] have created an inexhaustible source of new cells. The ability of these cells to differentiate into DA neurons makes them a suitable candidate for transplantation studies. Apart from stem cell based methods, transdifferentiation has also been proven feasible using skin fibroblasts [115, 116], providing an even more accessible source of DA neurons.

Cell models for Parkinson's disease research

PD disease models have contributed a large part of our understanding of the disease. These models range from animal models [117] and cell based models [118] to phospholipid membrane models [119]. Animal models have been extremely valuable in explaining PD pathogenesis [120], but there are limitations to these model organisms [121]. MPTP induced toxicity, for instance, presents a different pathology depending on the mouse strain used [122], and is different from human MPTP toxicity [121]. MPTP primate models offer a striking resemblance to human toxicity [123], but high costs and ethical concerns surrounding the use of these models limit their use. Rodent transgenic human α-synuclein models have produced mixed results, mainly display pathology outside the SNc, and do not cover all clinical aspects of PD pathology [124]. PD cell models overcome some of the challenges faced in PD animal experiments, and have been instrumental for discovering the complex pathways involved in the disease process [118]. A human genetic background, cost-effectiveness and the lack of ethical concerns create an advantage for PD cell-models compared to animal models. The most widely used cell line in PD research is the SH-SY5Y neuroblastoma cell line [125]. It is a subline of the SK-N-SH cell line, which was originally derived from a metastatic tumor biopsy [126]. While use of a mitotic tumor cell line might seem undesirable, SH-SY5Y cells can be differentiated to

a more neuronal state by using retinoic acid [120]. The resulting populations display a higher expression of dopaminergic markers, and subsequent treatment with phorbol esters increases this expression even further [127]. These properties, combined with the cost-effectiveness, ease of culturing and reproducibility make SH-SY5Y cells an excellent tool for the elucidation of biochemical pathways involved in PD [118]. However, SH-SY5Y cells do have shortcomings when used as a PD cell model. Endogenous expression of DA neuronal markers and expression of α-synuclein are low compared to SNc DA neurons [128], and the proliferative nature of these cells is in sharp contrast to a post-mitotic neuronal state. The discovery of ESCs and iPSCs have provided a solution for this problem, by being able to differentiate these cells into ventral midbrain DA neurons resembling their human counterparts [129]. Though this method is more laborious and more costly compared to SH-SY5Y cells, the ability to study endogenous expression of disease causing proteins in a PD patient genetic background holds great promise. The amount of publications using iPSCs and ESCs in the field of PD research is still relatively low, but with the arrival of new differentiation methods, the technique is bound to provide new insights into the disease process [130]. Additionally, transdifferentiation holds great promise as a source for DA neurons to be used in disease modeling. While the availability and the neuronal yield of direct reprogramming protocols is low, the presence of epigenetic marks associated with aging make these neurons more useful in the study of late onset disorders [131].

Generation of dopamine neurons

Animal studies have elucidated many of the pathways involved in embryogenesis and have been crucial in creating protocols to generate DA neurons from ESCs and iPSCs [132, 133]. The intrinsic and extrinsic signaling pathways involved can be reproduced by supplementing cell culture media with a variety of defined factors, thereby mimicking early embryogenesis. After formation of neuroepithelium in the neural tube,

regional specific generation of mesencephalic DA neurons takes place under the influence of two extrinsic signaling centers: fibroblast growth factor 8 (FGF-8) signaling from the isthmus induces the development of DA neurons at the anterior-posterior axis of the neural tube [134], while sonic hedgehog (SHH) signaling from the floor plate positions these neurons along the dorsal-ventral axis [135]. Additionally, early WNT signaling promotes early DA neurogenesis, proliferation and maturation (see Figure 5A).

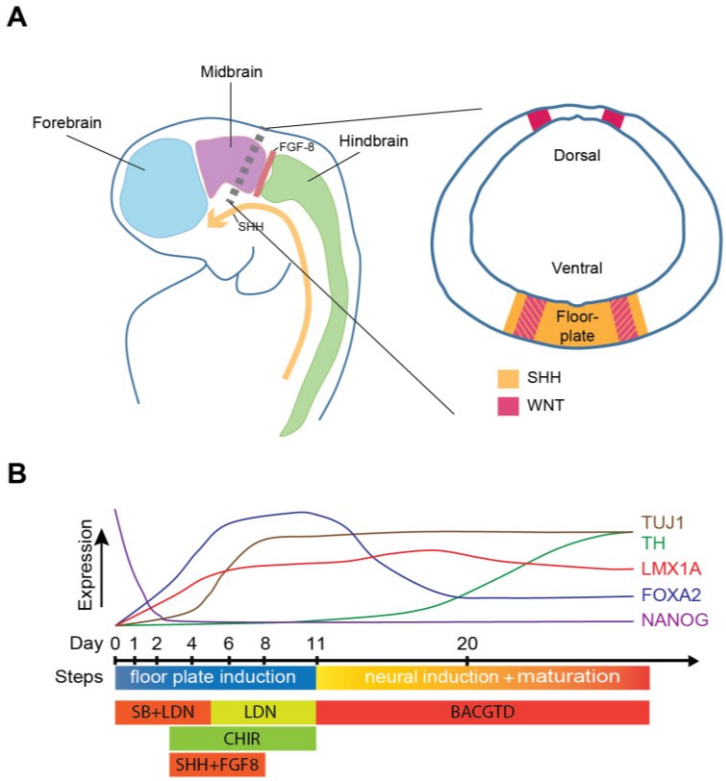

Figure 5. *(A) Generation of ventral midbrain DA neurons during development. While FGF-8 positions DA neurons along the anterior posterior axis, SHH positions these neurons on the ventral plane at the floor plate. WNT signaling promotes early DA neurogenesis and proliferation. (B) Schematics of dual-SMAD based dopaminergic differentiation of human pluripotent stem cells, coupled with a schematic plot illustrating changes in protein expression levels during this differentiation.*

Trophic factors like glial- [136] and brain- [137] derived neurotrophic factor (GDNF/BDNF), appear to be essential for the survival of these DA neurons as demonstrated in various mouse knockout studies [138, 139].

To mimic the in-vivo process of regional specification during in-vitro dopaminergic differentiation of ESCS a two-step protocol has been developed based on the signaling pathways employed by the above-described factors (Figure 5B) [129, 140]. The first step covers the neural induction of ESCs by dual inhibition of SMAD signaling with small molecules [140]. SB431542 blocks phosphorylation of the receptors ALK4, ALK5 and ALK7, inhibiting activin and TGFβ pathways. LDN-193189, a small molecule inhibitor of ALK2 and ALK3, blocks BMP signaling, promoting neuralization of primitive ectoderm. In the second step, the resulting neural stem cell-like populations are subjected to Wnt pathway inhibition using CHIR99021, a potent GSK3 inhibitor, and are supplemented with FGF-8 and SHH to increase the efficiency of DA cell differentiation [129]. During dual SMAD inhibition, expression of pluripotency markers such as *NANOG* and *OCT3/4* and *SOX2* decreases, while expression of midbrain marker *LMX1A* and *FOXA2* increases. At around 7 days, expression of the neuronal marker BIII-tubulin increases, and the cells start to display neuronal structures. This is followed by tyrosine hydroxylase (TH) expression around 15-20 days of differentiation, and increases until around day 30 of differentiation. Upon maturation, neurons become electrically active and start to display markers such as *GIRK2*. After maturation, the resulting DA neuron populations are supplemented with trophic factors BDNF, GDNF and the γ-secretase inhibitor DAPT [141] to sustain long-term in-vitro culture. Although this DA differentiation protocol has been shown to be the most effective in generating ventral midbrain DA neuronal populations, variability between different ESC and iPSC lines appears to be considerable [142], and are likely caused by differences in neural differentiation potential between iPSC lines [143].

Outline of the thesis

Parkinson's disease is associated with α-synuclein pathology and mitochondrial dysfunction, but the mechanisms linking these pathological aspects of PD are currently still unclear. The aim of this thesis is to elucidate part of these mechanisms using novel technologies and to determine how α-synuclein pathology contributes to mitochondrial dysfunction. For this purpose, we generated α-synuclein-overexpressing neuronal cell models to study mitochondrial function. Using iPSC technology, we further show that long-term in-vitro generated neurons show similar pathologies as those observed in our overexpressing cell models. Finally, to mimic age-associated pathology, we introduce an experimental model to effectively age cells derived from iPSCs, since these cells must be considered rejuvenated as a consequence of the iPSC induction process.

In **Chapter 2**, we have used SH-SY5Y cells overexpressing wild-type, A30P and A53T α-synuclein to examine the effect of α-synuclein on mitochondrial trafficking. We demonstrate that cells overexpressing A30P and A53T α-synuclein show an increase in ROS production and that trafficking in A53T α-synuclein expressing cells is significantly reduced, first in retrograde trafficking, and at a later stage also in anterograde trafficking. Treatment with davunetide, a microtubule-stabilizing peptide, rescues trafficking deficiency and decreases ROS production.

To validate the findings of our SH-SY5Y experiments, we use PD-patient derived iPSCs to study similar processes in the DA neurons produced from these iPSCs. To this aim, long-term culture protocols were used to prevent the usage of mitochondrial toxins and to study cells with endogenous α-synuclein expression. In order to be able to perform experiments on purified cell suspensions of DA neurons, we developed a new method to purify neuronal cells based on metabolic capacity, as described in **Chapter 3**. Using glucose deprivation and lactate supplementation effectively enriches neuronal populations, leading to

post-mitotic neuronal populations without the use of toxic mitotic inhibitors or need for strenuous cell sorting. The resulting neuronal cultures are functional and have a significantly higher percentage of neuronal cells. Crucially, the resulting populations can be cultured for prolonged periods of time without interference of proliferating cells.

Using our purified long-term cultured neurons, we show in **Chapter 4** that PD patient-derived neurons, obtained via iPSC technology present a similar mitochondrial deficiency as observed in the SH-SY5Y cells described in Chapter 2. The familial PD-derived iPSCs, from respectively a PD4 (SNCA triplication) and a PD1 (A53T mutation) patient, were successfully differentiated into DA neurons and were analyzed at 90 days in-vitro to assess mitochondrial trafficking. Mitochondrial trafficking appears to be significantly reduced in both PD1- and PD4- derived DA neurons compared to control, but not between PD1 and PD4 DA neurons.

The need to culture cells for prolonged periods of time when studying aging-related pathologies is challenging in in-vitro research using iPSCs, since they are known to generate rejuvenated differentiated cells. Also the need to use mitochondrial toxins, and proteasome inhibitors makes it a complicated model to work with. Therefore, we have used transgenic overexpression of progerin, the disease-causing protein in the accelerated aging Hutchinson-Gilford progeria syndrome, to “age” our rejuvenated, iPSC-derived DA neurons (**Chapter 5**). We show that progerin-overexpressing PD patient-derived DA neurons exhibit an increase in α-synuclein load. Unfortunately, these DA neurons appeared to be unsuitable to study the progerin-induced effects on mitochondrial activity and cellular aging features in detail as they are more difficult to culture. Therefore, we have included studies on cardiomyocytes, since these cells are relatively easy to differentiate and have high mitochondrial activity. The resulting cultures demonstrate that progerin-expressing cells have folded nuclei, a higher incidence of double stranded DNA breaks and a higher production of ROS.

Finally, in **Chapter 6** the results of the studies described in this thesis have been discussed. Furthermore, suggestions for future work are proposed and the relevance of this work in the stem cell field is discussed.

References

1. Parkinson J. An essay on the shaking palsy. 1817. **The Journal of neuropsychiatry and clinical neurosciences**. 2002;14:223-236; discussion 222.
2. Goetz CG. The history of Parkinson's disease: early clinical descriptions and neurological therapies. **Cold Spring Harbor perspectives in medicine**. 2011;1:a008862.
3. Carlsson A. Basic concepts underlying recent developments in the field of Parkinson's disease. **Contemporary neurology series**. 1971;8:1-31.
4. Carlsson A. Thirty years of dopamine research. **Advances in neurology**. 1993;60:1-10.
5. Cheng HC, Ulane CM, Burke RE. Clinical progression in Parkinson disease and the neurobiology of axons. **Annals of neurology**. 2010;67:715-725.
6. Chaudhuri KR, Healy DG, Schapira AH et al. Non-motor symptoms of Parkinson's disease: diagnosis and management. **The Lancet Neurology**. 2006;5:235-245.
7. Braak H, Del Tredici K, Rub U et al. Staging of brain pathology related to sporadic Parkinson's disease. **Neurobiology of aging**. 2003;24:197-211.
8. Braak H, Ghebremedhin E, Rub U et al. Stages in the development of Parkinson's disease-related pathology. **Cell and tissue research**. 2004;318:121-134.
9. Doty RL. Olfaction in Parkinson's disease and related disorders. **Neurobiology of disease**. 2012;46:527-552.
10. Braak H, de Vos RA, Bohl J et al. Gastric alpha-synuclein immunoreactive inclusions in Meissner's and Auerbach's plexuses in cases staged for Parkinson's disease-related brain pathology. **Neuroscience letters**. 2006;396:67-72.
11. Braak H, Rub U, Del Tredici K. Cognitive decline correlates with neuropathological stage in Parkinson's disease. **Journal of the neurological sciences**. 2006;248:255-258.

12. Burke RE, Dauer WT, Vonsattel JP. A critical evaluation of the Braak staging scheme for Parkinson's disease. **Annals of neurology**. 2008;64:485-491.
13. Hayflick L, Moorhead PS. The serial cultivation of human diploid cell strains. **Experimental cell research**. 1961;25:585-621.
14. Lopez-Otin C, Blasco MA, Partridge L et al. The hallmarks of aging. **Cell**. 2013;153:1194-1217.
15. Tanner CM. The role of environmental toxins in the etiology of Parkinson's disease. **Trends in neurosciences**. 1989;12:49-54.
16. Nalls MA, Pankratz N, Lill CM et al. Large-scale meta-analysis of genome-wide association data identifies six new risk loci for Parkinson's disease. **Nature genetics**. 2014;46:989-993.
17. Chartier-Harlin MC, Kachergus J, Roumier C et al. Alpha-synuclein locus duplication as a cause of familial Parkinson's disease. **Lancet**. 2004;364:1167-1169.
18. Singleton AB, Farrer M, Johnson J et al. alpha-Synuclein locus triplication causes Parkinson's disease. **Science**. 2003;302:841.
19. Polymeropoulos MH, Lavedan C, Leroy E et al. Mutation in the alpha-synuclein gene identified in families with Parkinson's disease. **Science**. 1997;276:2045-2047.
20. Kruger R, Kuhn W, Muller T et al. Ala30Pro mutation in the gene encoding alpha-synuclein in Parkinson's disease. **Nature genetics**. 1998;18:106-108.
21. Greenbaum EA, Graves CL, Mishizen-Eberz AJ et al. The E46K mutation in alpha-synuclein increases amyloid fibril formation. **The Journal of biological chemistry**. 2005;280:7800-7807.
22. Zimprich A, Biskup S, Leitner P et al. Mutations in LRRK2 cause autosomal-dominant parkinsonism with pleomorphic pathology. **Neuron**. 2004;44:601-607.
23. Shimura H, Hattori N, Kubo S et al. Familial Parkinson disease gene product, parkin, is a ubiquitin-protein ligase. **Nature genetics**. 2000;25:302-305.
24. Valente EM, Abou-Sleiman PM, Caputo V et al. Hereditary early-onset Parkinson's disease caused by mutations in PINK1. **Science**. 2004;304:1158-1160.
25. Spillantini MG, Schmidt ML, Lee VM et al. Alpha-synuclein in Lewy bodies. **Nature**. 1997;388:839-840.
26. Spillantini MG, Crowther RA, Jakes R et al. alpha-Synuclein in filamentous inclusions of Lewy bodies from Parkinson's disease and

dementia with lewy bodies. **Proceedings of the National Academy of Sciences of the United States of America**. 1998;95:6469-6473.
27. Zarranz JJ, Alegre J, Gomez-Esteban JC et al. The new mutation, E46K, of alpha-synuclein causes Parkinson and Lewy body dementia. **Annals of neurology**. 2004;55:164-173.
28. Markopoulou K, Dickson DW, McComb RD et al. Clinical, neuropathological and genotypic variability in SNCA A53T familial Parkinson's disease. Variability in familial Parkinson's disease. **Acta neuropathologica**. 2008;116:25-35.
29. Kruger R, Kuhn W, Leenders KL et al. Familial parkinsonism with synuclein pathology: clinical and PET studies of A30P mutation carriers. **Neurology**. 2001;56:1355-1362.
30. Lesage S, Brice A. Parkinson's disease: from monogenic forms to genetic susceptibility factors. **Human molecular genetics**. 2009;18:R48-59.
31. Nishioka K, Hayashi S, Farrer MJ et al. Clinical heterogeneity of alpha-synuclein gene duplication in Parkinson's disease. **Annals of neurology**. 2006;59:298-309.
32. Di Fonzo A, Wu-Chou YH, Lu CS et al. A common missense variant in the LRRK2 gene, Gly2385Arg, associated with Parkinson's disease risk in Taiwan. **Neurogenetics**. 2006;7:133-138.
33. Vilarino-Guell C, Wider C, Ross OA et al. VPS35 mutations in Parkinson disease. **American journal of human genetics**. 2011;89:162-167.
34. Zimprich A, Benet-Pages A, Struhal W et al. A mutation in VPS35, encoding a subunit of the retromer complex, causes late-onset Parkinson disease. **American journal of human genetics**. 2011;89:168-175.
35. Lavedan C. The synuclein family. **Genome research**. 1998;8:871-880.
36. Stefanis L. alpha-Synuclein in Parkinson's disease. **Cold Spring Harbor perspectives in medicine**. 2012;2:a009399.
37. Bartels T, Choi JG, Selkoe DJ. alpha-Synuclein occurs physiologically as a helically folded tetramer that resists aggregation. **Nature**. 2011;477:107-110.
38. Bisaglia M, Trolio A, Bellanda M et al. Structure and topology of the non-amyloid-beta component fragment of human alpha-synuclein bound to micelles: implications for the aggregation process. **Protein science : a publication of the Protein Society**. 2006;15:1408-1416.
39. Lyubchenko YL, Kim BH, Krasnoslobodtsev AV et al. Nanoimaging for protein misfolding diseases. **Wiley interdisciplinary reviews Nanomedicine and nanobiotechnology**. 2010;2:526-543.

40. Burre J, Sharma M, Tsetsenis T et al. Alpha-synuclein promotes SNARE-complex assembly in vivo and in vitro. **Science**. 2010;329:1663-1667.
41. Kokhan VS, Afanasyeva MA, Van'kin GI. alpha-Synuclein knockout mice have cognitive impairments. **Behavioural brain research**. 2012;231:226-230.
42. Greten-Harrison B, Polydoro M, Morimoto-Tomita M et al. alphabetagamma-Synuclein triple knockout mice reveal age-dependent neuronal dysfunction. **Proceedings of the National Academy of Sciences of the United States of America**. 2010;107:19573-19578.
43. Li JY, Englund E, Holton JL et al. Lewy bodies in grafted neurons in subjects with Parkinson's disease suggest host-to-graft disease propagation. **Nature medicine**. 2008;14:501-503.
44. Chu Y, Kordower JH. Lewy body pathology in fetal grafts. **Annals of the New York Academy of Sciences**. 2010;1184:55-67.
45. Desplats P, Lee HJ, Bae EJ et al. Inclusion formation and neuronal cell death through neuron-to-neuron transmission of alpha-synuclein. **Proceedings of the National Academy of Sciences of the United States of America**. 2009;106:13010-13015.
46. Holmqvist S, Chutna O, Bousset L et al. Direct evidence of Parkinson pathology spread from the gastrointestinal tract to the brain in rats. **Acta neuropathologica**. 2014;128:805-820.
47. Liu B, Fang F, Pedersen NL et al. Vagotomy and Parkinson disease: A Swedish register-based matched-cohort study. **Neurology**. 2017;88:1996-2002.
48. McNaught KS, Shashidharan P, Perl DP et al. Aggresome-related biogenesis of Lewy bodies. **The European journal of neuroscience**. 2002;16:2136-2148.
49. Ebrahimi-Fakhari D, Wahlster L, McLean PJ. Molecular chaperones in Parkinson's disease--present and future. **Journal of Parkinson's disease**. 2011;1:299-320.
50. Luo GR, Chen S, Le WD. Are heat shock proteins therapeutic target for Parkinson's disease? **International journal of biological sciences**. 2006;3:20-26.
51. Sidransky E, Nalls MA, Aasly JO et al. Multicenter analysis of glucocerebrosidase mutations in Parkinson's disease. **The New England journal of medicine**. 2009;361:1651-1661.
52. Sidransky E, Lopez G. The link between the GBA gene and parkinsonism. **The Lancet Neurology**. 2012;11:986-998.

53. Brady RO, Kanfer JN, Bradley RM et al. Demonstration of a deficiency of glucocerebroside-cleaving enzyme in Gaucher's disease. **The Journal of clinical investigation**. 1966;45:1112-1115.
54. Zhao Y, Ho P, Yih Y et al. LRRK2 variant associated with Alzheimer's disease. **Neurobiology of aging**. 2011;32:1990-1993.
55. Rajput A, Dickson DW, Robinson CA et al. Parkinsonism, Lrrk2 G2019S, and tau neuropathology. **Neurology**. 2006;67:1506-1508.
56. Langston JW, Ballard P, Tetrud JW et al. Chronic Parkinsonism in humans due to a product of meperidine-analog synthesis. **Science**. 1983;219:979-980.
57. Sherer TB, Kim JH, Betarbet R et al. Subcutaneous rotenone exposure causes highly selective dopaminergic degeneration and alpha-synuclein aggregation. **Experimental neurology**. 2003;179:9-16.
58. McCormack AL, Thiruchelvam M, Manning-Bog AB et al. Environmental risk factors and Parkinson's disease: selective degeneration of nigral dopaminergic neurons caused by the herbicide paraquat. **Neurobiology of disease**. 2002;10:119-127.
59. Tanner CM, Kamel F, Ross GW et al. Rotenone, paraquat, and Parkinson's disease. **Environmental health perspectives**. 2011;119:866-872.
60. Parker WD, Jr., Boyson SJ, Parks JK. Abnormalities of the electron transport chain in idiopathic Parkinson's disease. **Annals of neurology**. 1989;26:719-723.
61. Schapira AH, Cooper JM, Dexter D et al. Mitochondrial complex I deficiency in Parkinson's disease. **Journal of neurochemistry**. 1990;54:823-827.
62. Perier C, Vila M. Mitochondrial biology and Parkinson's disease. **Cold Spring Harbor perspectives in medicine**. 2012;2:a009332.
63. Poole AC, Thomas RE, Andrews LA et al. The PINK1/Parkin pathway regulates mitochondrial morphology. **Proceedings of the National Academy of Sciences of the United States of America**. 2008;105:1638-1643.
64. Geisler S, Holmstrom KM, Skujat D et al. PINK1/Parkin-mediated mitophagy is dependent on VDAC1 and p62/SQSTM1. **Nature cell biology**. 2010;12:119-131.
65. Scarffe LA, Stevens DA, Dawson VL et al. Parkin and PINK1: much more than mitophagy. **Trends in neurosciences**. 2014;37:315-324.
66. Camilleri A, Zarb C, Caruana M et al. Mitochondrial membrane permeabilisation by amyloid aggregates and protection by polyphenols. **Biochimica et biophysica acta**. 2013;1828:2532-2543.

67. Tosatto L, Andrighetti AO, Plotegher N et al. Alpha-synuclein pore forming activity upon membrane association. **Biochimica et biophysica acta**. 2012;1818:2876-2883.
68. Chinta SJ, Mallajosyula JK, Rane A et al. Mitochondrial alpha-synuclein accumulation impairs complex I function in dopaminergic neurons and results in increased mitophagy in vivo. **Neuroscience letters**. 2010;486:235-239.
69. Nakamura K, Nemani VM, Azarbal F et al. Direct membrane association drives mitochondrial fission by the Parkinson disease-associated protein alpha-synuclein. **The Journal of biological chemistry**. 2011;286:20710-20726.
70. Lee HJ, Khoshaghideh F, Lee S et al. Impairment of microtubule-dependent trafficking by overexpression of alpha-synuclein. **The European journal of neuroscience**. 2006;24:3153-3162.
71. Itoh K, Nakamura K, Iijima M et al. Mitochondrial dynamics in neurodegeneration. **Trends in cell biology**. 2013;23:64-71.
72. Lai BC, Marion SA, Teschke K et al. Occupational and environmental risk factors for Parkinson's disease. **Parkinsonism & related disorders**. 2002;8:297-309.
73. Pan-Montojo F, Reichmann H. Considerations on the role of environmental toxins in idiopathic Parkinson's disease pathophysiology. **Translational neurodegeneration**. 2014;3:10.
74. Tanner CM, Ottman R, Goldman SM et al. Parkinson disease in twins: an etiologic study. **Jama**. 1999;281:341-346.
75. Wirdefeldt K, Gatz M, Schalling M et al. No evidence for heritability of Parkinson disease in Swedish twins. **Neurology**. 2004;63:305-311.
76. Freire C, Koifman S. Pesticide exposure and Parkinson's disease: epidemiological evidence of association. **Neurotoxicology**. 2012;33:947-971.
77. Gash DM, Rutland K, Hudson NL et al. Trichloroethylene: Parkinsonism and complex 1 mitochondrial neurotoxicity. **Annals of neurology**. 2008;63:184-192.
78. Winklhofer KF, Haass C. Mitochondrial dysfunction in Parkinson's disease. **Biochimica et biophysica acta**. 2010;1802:29-44.
79. Irrcher I, Aleyasin H, Seifert EL et al. Loss of the Parkinson's disease-linked gene DJ-1 perturbs mitochondrial dynamics. **Human molecular genetics**. 2010;19:3734-3746.
80. Sheng ZH. Mitochondrial trafficking and anchoring in neurons: New insight and implications. **The Journal of cell biology**. 2014;204:1087-1098.

81. Oliveira JM. Nature and cause of mitochondrial dysfunction in Huntington's disease: focusing on huntingtin and the striatum. **Journal of neurochemistry**. 2010;114:1-12.
82. Reid E, Kloos M, Ashley-Koch A et al. A kinesin heavy chain (KIF5A) mutation in hereditary spastic paraplegia (SPG10). **American journal of human genetics**. 2002;71:1189-1194.
83. Maday S, Twelvetrees AE, Moughamian AJ et al. Axonal transport: cargo-specific mechanisms of motility and regulation. **Neuron**. 2014;84:292-309.
84. Roy S, Zhang B, Lee VM et al. Axonal transport defects: a common theme in neurodegenerative diseases. **Acta neuropathologica**. 2005;109:5-13.
85. Li W, Hoffman PN, Stirling W et al. Axonal transport of human alpha-synuclein slows with aging but is not affected by familial Parkinson's disease-linked mutations. **Journal of neurochemistry**. 2004;88:401-410.
86. Van Laar VS, Berman SB. Mitochondrial dynamics in Parkinson's disease. **Experimental neurology**. 2009;218:247-256.
87. Pissadaki EK, Bolam JP. The energy cost of action potential propagation in dopamine neurons: clues to susceptibility in Parkinson's disease. **Frontiers in computational neuroscience**. 2013;7:13.
88. Paladini CA, Robinson S, Morikawa H et al. Dopamine controls the firing pattern of dopamine neurons via a network feedback mechanism. **Proceedings of the National Academy of Sciences of the United States of America**. 2003;100:2866-2871.
89. Guzman JN, Sanchez-Padilla J, Chan CS et al. Robust pacemaking in substantia nigra dopaminergic neurons. **The Journal of neuroscience : the official journal of the Society for Neuroscience**. 2009;29:11011-11019.
90. Weihofen A, Thomas KJ, Ostaszewski BL et al. Pink1 forms a multiprotein complex with Miro and Milton, linking Pink1 function to mitochondrial trafficking. **Biochemistry**. 2009;48:2045-2052.
91. Sheng ZH, Cai Q. Mitochondrial transport in neurons: impact on synaptic homeostasis and neurodegeneration. **Nature reviews Neuroscience**. 2012;13:77-93.
92. Chung SY, Kishinevsky S, Mazzulli JR et al. Parkin and PINK1 Patient iPSC-Derived Midbrain Dopamine Neurons Exhibit Mitochondrial Dysfunction and alpha-Synuclein Accumulation. **Stem cell reports**. 2016;7:664-677.

93. Araki E, Tsuboi Y, Daechsel J et al. A novel DCTN1 mutation with late-onset parkinsonism and frontotemporal atrophy. **Movement disorders : official journal of the Movement Disorder Society**. 2014;29:1201-1204.
94. Ashrafi G, Schlehe JS, LaVoie MJ et al. Mitophagy of damaged mitochondria occurs locally in distal neuronal axons and requires PINK1 and Parkin. **The Journal of cell biology**. 2014;206:655-670.
95. Hunn BH, Cragg SJ, Bolam JP et al. Impaired intracellular trafficking defines early Parkinson's disease. **Trends in neurosciences**. 2015;38:178-188.
96. Chen L, Jin J, Davis J et al. Oligomeric alpha-synuclein inhibits tubulin polymerization. **Biochemical and biophysical research communications**. 2007;356:548-553.
97. Fang F, Yang W, Florio JB et al. Synuclein impairs trafficking and signaling of BDNF in a mouse model of Parkinson's disease. **Scientific reports**. 2017;7:3868.
98. Mazzulli JR, Zunke F, Isacson O et al. alpha-Synuclein-induced lysosomal dysfunction occurs through disruptions in protein trafficking in human midbrain synucleinopathy models. **Proceedings of the National Academy of Sciences of the United States of America**. 2016;113:1931-1936.
99. Li L, Nadanaciva S, Berger Z et al. Human A53T alpha-synuclein causes reversible deficits in mitochondrial function and dynamics in primary mouse cortical neurons. **PloS one**. 2013;8:e85815.
100. Fahn S, Oakes D, Shoulson I et al. Levodopa and the progression of Parkinson's disease. **The New England journal of medicine**. 2004;351:2498-2508.
101. Parkinson Study G. A controlled, randomized, delayed-start study of rasagiline in early Parkinson disease. **Archives of neurology**. 2004;61:561-566.
102. Rascol O, Brooks DJ, Korczyn AD et al. A five-year study of the incidence of dyskinesia in patients with early Parkinson's disease who were treated with ropinirole or levodopa. **The New England journal of medicine**. 2000;342:1484-1491.
103. Bostwick JM, Hecksel KA, Stevens SR et al. Frequency of new-onset pathologic compulsive gambling or hypersexuality after drug treatment of idiopathic Parkinson disease. **Mayo Clinic proceedings**. 2009;84:310-316.
104. Hauser RA, Rascol O, Korczyn AD et al. Ten-year follow-up of Parkinson's disease patients randomized to initial therapy with

ropinirole or levodopa. **Movement disorders : official journal of the Movement Disorder Society**. 2007;22:2409-2417.
105. Fernandez HH, Chen JJ. Monoamine oxidase-B inhibition in the treatment of Parkinson's disease. **Pharmacotherapy**. 2007;27:174S-185S.
106. Deuschl G, Schade-Brittinger C, Krack P et al. A randomized trial of deep-brain stimulation for Parkinson's disease. **The New England journal of medicine**. 2006;355:896-908.
107. Lindvall O, Brundin P, Widner H et al. Grafts of fetal dopamine neurons survive and improve motor function in Parkinson's disease. **Science**. 1990;247:574-577.
108. Freed CR, Greene PE, Breeze RE et al. Transplantation of embryonic dopamine neurons for severe Parkinson's disease. **The New England journal of medicine**. 2001;344:710-719.
109. Kordower JH, Freeman TB, Snow BJ et al. Neuropathological evidence of graft survival and striatal reinnervation after the transplantation of fetal mesencephalic tissue in a patient with Parkinson's disease. **The New England journal of medicine**. 1995;332:1118-1124.
110. Kordower JH, Rosenstein JM, Collier TJ et al. Functional fetal nigral grafts in a patient with Parkinson's disease: chemoanatomic, ultrastructural, and metabolic studies. **The Journal of comparative neurology**. 1996;370:203-230.
111. Abbott A. Fetal-cell revival for Parkinson's. **Nature**. 2014;510:195-196.
112. Ying QL, Stavridis M, Griffiths D et al. Conversion of embryonic stem cells into neuroectodermal precursors in adherent monoculture. **Nature biotechnology**. 2003;21:183-186.
113. Perrier AL, Tabar V, Barberi T et al. Derivation of midbrain dopamine neurons from human embryonic stem cells. **Proceedings of the National Academy of Sciences of the United States of America**. 2004;101:12543-12548.
114. Takahashi K, Tanabe K, Ohnuki M et al. Induction of pluripotent stem cells from adult human fibroblasts by defined factors. **Cell**. 2007;131:861-872.
115. Caiazzo M, Dell'Anno MT, Dvoretskova E et al. Direct generation of functional dopaminergic neurons from mouse and human fibroblasts. **Nature**. 2011;476:224-227.
116. Pfisterer U, Kirkeby A, Torper O et al. Direct conversion of human fibroblasts to dopaminergic neurons. **Proceedings of the National Academy of Sciences of the United States of America**. 2011;108:10343-10348.

117. Blesa J, Przedborski S. Parkinson's disease: animal models and dopaminergic cell vulnerability. **Frontiers in neuroanatomy**. 2014;8:155.
118. Alberio T, Lopiano L, Fasano M. Cellular models to investigate biochemical pathways in Parkinson's disease. **The FEBS journal**. 2012;279:1146-1155.
119. Jo E, McLaurin J, Yip CM et al. alpha-Synuclein membrane interactions and lipid specificity. **The Journal of biological chemistry**. 2000;275:34328-34334.
120. Duty S, Jenner P. Animal models of Parkinson's disease: a source of novel treatments and clues to the cause of the disease. **British journal of pharmacology**. 2011;164:1357-1391.
121. Bezard E, Yue Z, Kirik D et al. Animal models of Parkinson's disease: limits and relevance to neuroprotection studies. **Movement disorders : official journal of the Movement Disorder Society**. 2013;28:61-70.
122. Hamre K, Tharp R, Poon K et al. Differential strain susceptibility following 1-methyl-4-phenyl-1,2,3,6-tetrahydropyridine (MPTP) administration acts in an autosomal dominant fashion: quantitative analysis in seven strains of Mus musculus. **Brain research**. 1999;828:91-103.
123. Iravani MM, Syed E, Jackson MJ et al. A modified MPTP treatment regime produces reproducible partial nigrostriatal lesions in common marmosets. **The European journal of neuroscience**. 2005;21:841-854.
124. Dawson TM, Ko HS, Dawson VL. Genetic animal models of Parkinson's disease. **Neuron**. 2010;66:646-661.
125. Xicoy H, Wieringa B, Martens GJ. The SH-SY5Y cell line in Parkinson's disease research: a systematic review. **Molecular neurodegeneration**. 2017;12:10.
126. Biedler JL, Roffler-Tarlov S, Schachner M et al. Multiple neurotransmitter synthesis by human neuroblastoma cell lines and clones. **Cancer research**. 1978;38:3751-3757.
127. Presgraves SP, Ahmed T, Borwege S et al. Terminally differentiated SH-SY5Y cells provide a model system for studying neuroprotective effects of dopamine agonists. **Neurotoxicity research**. 2004;5:579-598.
128. Korecka JA, van Kesteren RE, Blaas E et al. Phenotypic characterization of retinoic acid differentiated SH-SY5Y cells by transcriptional profiling. **PloS one**. 2013;8:e63862.
129. Kriks S, Shim JW, Piao J et al. Dopamine neurons derived from human ES cells efficiently engraft in animal models of Parkinson's disease. **Nature**. 2011;480:547-551.

130. Avior Y, Sagi I, Benvenisty N. Pluripotent stem cells in disease modelling and drug discovery. **Nature reviews Molecular cell biology**. 2016;17:170-182.
131. Playne R, Connor B. Understanding Parkinson's Disease through the Use of Cell Reprogramming. **Stem cell reviews**. 2017;13:151-169.
132. Murry CE, Keller G. Differentiation of embryonic stem cells to clinically relevant populations: lessons from embryonic development. **Cell**. 2008;132:661-680.
133. Prakash N, Wurst W. Development of dopaminergic neurons in the mammalian brain. **Cellular and molecular life sciences : CMLS**. 2006;63:187-206.
134. Ye W, Shimamura K, Rubenstein JL et al. FGF and Shh signals control dopaminergic and serotonergic cell fate in the anterior neural plate. **Cell**. 1998;93:755-766.
135. Hynes M, Porter JA, Chiang C et al. Induction of midbrain dopaminergic neurons by Sonic hedgehog. **Neuron**. 1995;15:35-44.
136. Lin LF, Doherty DH, Lile JD et al. GDNF: a glial cell line-derived neurotrophic factor for midbrain dopaminergic neurons. **Science**. 1993;260:1130-1132.
137. Hyman BT, Wenniger JJ, Tanzi RE. Nonisotopic in situ hybridization of amyloid beta protein precursor in Alzheimer's disease: expression in neurofibrillary tangle bearing neurons and in the microenvironment surrounding senile plaques. **Brain research Molecular brain research**. 1993;18:253-258.
138. Patterson SL, Abel T, Deuel TA et al. Recombinant BDNF rescues deficits in basal synaptic transmission and hippocampal LTP in BDNF knockout mice. **Neuron**. 1996;16:1137-1145.
139. Baloh RH, Enomoto H, Johnson EM, Jr. et al. The GDNF family ligands and receptors - implications for neural development. **Current opinion in neurobiology**. 2000;10:103-110.
140. Chambers SM, Fasano CA, Papapetrou EP et al. Highly efficient neural conversion of human ES and iPS cells by dual inhibition of SMAD signaling. **Nature biotechnology**. 2009;27:275-280.
141. Crawford TQ, Roelink H. The notch response inhibitor DAPT enhances neuronal differentiation in embryonic stem cell-derived embryoid bodies independently of sonic hedgehog signaling. **Developmental dynamics : an official publication of the American Association of Anatomists**. 2007;236:886-892.

142. Torrent R, De Angelis Rigotti F, Dell'Era P et al. Using iPS Cells toward the Understanding of Parkinson's Disease. **Journal of clinical medicine**. 2015;4:548-566.
143. Hu BY, Weick JP, Yu J et al. Neural differentiation of human induced pluripotent stem cells follows developmental principles but with variable potency. **Proceedings of the National Academy of Sciences of the United States of America**. 2010;107:4335-4340.

Chapter 2

Impairment of mitochondria dynamics by human A53T α-synuclein and rescue by NAP (davunetide) in a cell model for Parkinson's disease.

Zomeren, K.C. van[1,a]; Melo, T.Q.[1,a,b]; Ferrari, M.F.R.[b]; Boddeke, H.W.G.M.[a] and Copray, J.C.V.M.[a]

[a] Department of Neuroscience, section Medical Physiology, University Medical Center Groningen, University of Groningen, the Netherlands

[b] Department of Genetics and Evolutionary Biology, Institute for Biosciences, University of Sao Paulo, Sao Paulo, Brazil

[1] These authors contributed equally to this work.

Exp. Brain Res. 2017; 235(3): 731–742

Abstract

The formation of oligomers and aggregates of overexpressed or mutant α-synuclein play a role in the degeneration of dopaminergic neurons in Parkinson's disease by causing dysfunction of mitochondria, reflected in their disturbed mobility and production of ROS. The mode of action and mechanisms underlying this mitochondrial impairment is still unclear.

We have induced stable expression of wild-type, A30P or A53T α-synuclein in neuronally differentiated SH-SY5Y neuroblastoma cells and studied anterograde and retrograde mitochondrial trafficking in this cell model for Parkinson's disease. In contrast to wild-type and A30P, A53T α-synuclein significantly inhibited mitochondrial trafficking, at first retrogradely and in a later stage anterogradely. Accordingly, A53T α-synuclein also caused the highest increase in ROS production in the dysmobilized mitochondria in comparison to wild-type or A30P α-synuclein. Treatment with NAP, the 8 amino acid peptide identified as the active component of activity-dependent neuroprotective protein (ADNP), completely annihilated the adverse effects of A53T on mitochondrial dynamics. Our results reveal that A53T α-synuclein (oligomers or aggregates) leads to the inhibition of mitochondrial trafficking, which can be rescued by NAP, suggesting the involvement of microtubule disruption in the pathophysiology of Parkinson's disease

Keywords: mitochondrial trafficking, α-synuclein, mitochondria dysfunction, neurodegeneration, Parkinson, SHSY5Y, microtubule, reactive oxygen species

Introduction

Parkinson's disease (PD) is the most common neurodegenerative movement disorder affecting 1% of people above 65 years of age [1]. The pathology of PD is characterized by the degeneration of dopaminergic neurons in the substantia nigra. This neurodegeneration is thought to be associated with the formation of aggregates containing α-synuclein [2] and with increased oxidative stress [3-5]. The vast majority of PD patients have the sporadic form of this disease which appears to be age-related. A small percentage of PD is familiar and caused by specific mutations. The α-synuclein gene (*SNCA*) was the first gene associated with familiar PD and there are 3 known missense point mutations, A53T and A30P and E46K, besides duplication and triplication of *SNCA*, that all lead to an early disease onset [6-9]. Various genome-wide association (GWAS) studies have shown that SNPs in *SNCA* (and *MAPT*) are also common risk factors for sporadic PD [10-12]. To date, there are three known missense mutations linked with autosomal dominant PD (A53T, A30P, E46K). The molecular mechanisms underlying the neurodegenerative effects of α-synuclein oligomers and aggregates seem to involve most prominently the mitochondria. Although direct damaging effects of α-synuclein oligomers and aggregates on mitochondria have been described, indirect effects on the processes of autophagy and trafficking of mitochondria may be involved as well. Alterations in intracellular degradation pathways, such as macro-autophagy, have been observed in many studies linking protein aggregation mechanisms with neurodegeneration [13]. It has been demonstrated that overexpression of α-synuclein can lead to inhibition of autophagy and concomitant α-synuclein accumulation, whereas the knockdown of α-synuclein resulted in autophagy enhancement, suggesting that α-synuclein may have a regulatory role in autophagy [14] The presence of damaged mitochondria by the direct action of (mutant) α-synuclein oligomers, on the contrary, appears to stimulate excessive mitophagy leading to mitochondrial fragmentation [15, 16].

Normal mitochondrial turnover depends on a proper balance between anterograde and retrograde trafficking [17]; in PD, this mitochondrial turnover appears to be impaired [5, 18]. In anterograde trafficking, mitochondria are transported from the soma to the axon up to the synaptic terminals; by retrograde trafficking, the mitochondria return to the cell soma for breakdown and re-entering the biogenesis cycle [19]. Retardation in anterograde transport can result in an abnormal cellular distribution of mitochondria and a decrease in ATP levels at the synapses [20]; impairment of retrograde transportation leads to an accumulation of mitochondria in the synaptic terminal interfering with proper synapse formation and function [21].

Alpha-synuclein oligomers and aggregates seem to interfere directly with normal mitochondrial turnover [4, 22]. Alterations in axonal transport and in the level of motor proteins, have been observed in transgenic *Drosophila* co-expressing tau and α-synuclein, in post mortem brain tissue of sporadic PD patients, in animal and cellular models of sporadic PD and in rats overexpressing α-synuclein [23-26]. Studies have shown the interaction between α-synuclein and tau [27, 28]. In neurons, tau is essential for stabilizing microtubules and so for enabling proper motor transport [29]. In case of overexpression of α-synuclein, tau is phosphorylated, leading to its loss of function and the subsequent impairment of trafficking [27, 30]. Esteves and coworkers [31] demonstrated that α-synuclein oligomers are able to disrupt microtubules, leading to abnormal axonal trafficking and consequently mitochondrial dysfunction. In particular, the α-synuclein gene mutation A53T is able to form oligomers and aggregates more easily and faster than other types of α-synuclein [32]. Accordingly, it was demonstrated that in particular A53T α-synuclein significantly reduced mitochondrial motility in cellular models for PD in which human A53T α-synuclein was expressed, i.e. in mouse hippocampal neurons and SH-SY5Y neuroblastoma cells [33] or in mouse cortical neurons [34].

Activity-dependent neuroprotective protein (ADNP) is essential for brain formation and provides neuroprotection throughout the entire adult brain; ADNP mRNA and protein expression responds to brain injury and a variety of cytotoxic insults. Structure-activity studies have identified a short 8 amino acid peptide in ADNP, NAPVSIPQ (abbreviated to NAP) that appears to be responsible for neuroprotection [35-37]. Treatment with NAP has been shown to restore microtubule integrity and to rescue microtubules-dependent axonal trafficking, and, with that, mitochondrial function [31, 35-37]. NAP also contributed to functional recovery in mice overexpressing α-synuclein by reducing hyperphosphorylated tau levels [30].

In the present study, we aimed to analyze in more detail the effects of A30P or A53T α-synuclein on anterograde and retrograde mitochondrial trafficking in SH-SY5Y neuroblastoma cells in which we managed to induce a stable expression of wild type, A30P or A53T α-synuclein. In addition, we have studied the effect of NAP treatment on the mitochondrial mobility and function in these cells.

Materials and methods

Cell culture

SH-SY5Y cells (passage 17), obtained from ATCC cell culture, were not used above passage 35 as these cells are reported to lose their neuronal phenotype after repeated passaging. Cells were maintained in DMEM (1x) supplemented with 15% FBS, 1% Pen/Strep, 100mM Na-pyruvate and 2mM Glutamax (DFCS) in tissue culture treated dishes or flasks. At 70-80% confluence, cells were passaged using trypsin/EDTA (Lonza) following general cell culture procedures. Split ratios ranging from 1/20 to 1/40 were used to ensure similar densities among transgenic lines. To initiate differentiation into neuron-like cells, SH-SY5Y cells were plated at a density of $2x10^4$ cells/cm^2 in wells pre-treated with poly-D-lysine (PDL). After 1 day, cells were exposed to 10μM retinoic acid (Sigma) in DMEM (1x) supplemented with 10% FBS for 5 days, after which medium

was replaced to DMEM 1X (High Glucose) containing 10ng/ml BDNF (Peprotech), in order to promote the outgrowth of neural extensions.

Construction of viral vectors

Viral vectors containing wild-type α-synuclein and mutant α-synuclein A30P or A53T (pENG1-3, a generous gift by Ellen Nollen) were constructed by PCR amplification (Phusion High-Fidelity DNA Polymerase, ThermoScientific) with overhangs for SpeI and NsiI. PCR amplicons and pSin-EF2-Nanog-Pur (Adgene plasmid 16578) were restricted using BcuI (SpeI, Thermo Scientific) and Mph1103I (NsiI, Thermo Scientific), and subsequently ligated using T4 ligase (Thermo Scientific) after which the product was transformed in DH5α competent cells. PCR screening was performed to select positive colonies, which were checked by restriction analysis. Correct plasmids were sent for sequencing and transfected in HEK293T to validate expression. Vector constructs are shown in Supplemental figure S1.

SH-SY5Y viral transduction and transfection

Lentiviral particles were generated using a modified protocol based on the protocol of Trono et al. (http://tcf.epfl.ch/page-6764-en.html). Briefly, HEK-293T cells were transfected when cells were 70-80% confluent. A mixture containing 100 µl OPTIMEM (Gibco) 1.4 µg viral vector, 0.4 µg pMD2-VSV-G and 1 µg pCMV-D8.91, was supplemented with 6 µl FUGENE HD (Lonza) and incubated for 15 min at room temperature (RT) to generate transfection complexes. The next day medium was changed with 2 ml OPTIMEM and viral particles were harvested between 36 and 48 h.

Viral supernatant was collected and sterilized using a 0.45 µm filter (Nalgene), mixed with 10%DFCS in a 1:1 ratio and supplemented with polybrene (8 µg/ml). This mixture was added to a 6-well plate and $1x10^5$ cells were added to be transduced in suspension. The next day media was changed to DFCS15% and cells were placed on puromycin (2-4

μg/ml, Sigma) selection three days after transduction. Puromycin selection was continued during cell culture of the lines.

Characterization of SH-SY5Y by immunofluorescence

Transgenic cell lines cultured on PDL coated coverslips were fixed in paraformaldehyde 4% for 20 min at RT and rinsed in PBS 3 times. Samples were permeabilized and blocked with PBS containing 0.1% Triton, 1% BSA and 5% normal goat serum for 60 min at RT.

Samples were incubated with rabbit anti-MAP2 (1:1000, Abcam), mouse anti-α-synuclein (1:500, Invitrogen) or rabbit anti-TOM20 (1:1000 Santa Cruz FL-145) antibodies at RT for 1h followed by incubation of fluorescent secondary antibodies (1:400) and Hoechst for 1h at RT. Images were acquired using a Leica AF-6000 fluorescent microscope.

Mitochondria mobility

SH-SY5Y were transfected with pDsRed2-Mito (Clontech Cat. nr: 632421) in OPTIMEM (Gibco) using Lipofectamine 2000 (Invitrogen), following manufacturer's instructions. After 1 day of transfection cells were exposed to 200μg/ml of G418 for 2 weeks in order to select for cell lines containing the plasmid. SH-SY5Y were differentiated as described above and mitochondrial mobility was measured in live cells after 4, 6 or 8 days of differentiation, using spinning disc confocal microscopy at 63x objective in a climate controlled chamber. The track was calculated by image comparison of the same field every 10 sec for 20 min. Single cell image stacks were analyzed using the ImageJ difference tracker plugin. Kymographs were generated using ImageJ (FIJI) Multi Kymograph plugin. The experiment was repeated 3 times independently.

ROS measurements

After 8 days of differentiation, ROS production was measured by incubating cells with CM-H_2DCFDA probe (Invitrogen) at 10μM for 1 min. Images were recorded using spinning disc confocal microscopy at a 63x

objective, and analyzed using ImageJ. We have used CM-H_2DCFDA (5-(and-6)-chloromethyl-2',7'-dichlorodihydrofluorescein diacetate, acetyl ester), an improved, more stable, derivative of DCFDA, as a detector of ROS; this dye is not fluorescent when chemically reduced, but after cellular oxidation and removal of acetate groups by cellular esterases it becomes fluorescent. We measured fluorescence intensity of the transgenic neurons (i.e. expressing A53T, A30P or a surplus of WT α-synuclein) and the control (transfected with an empty vector).

Mitochondria morphology and connectivity measurement

After 8 days of differentiation neurons were fixed and stained for mitochondria using TOM20 antibody. Mitochondria morphology and connectivity among fluorescent mitochondria were observed and compared through stained neurons or neurons expressing pDsRed2-Mito. Total amount of neurons containing normal mitochondria morphology was analyzed and quantified.

Treatment with NAP

NAP (Santa Cruz, sc361778A) was dissolved in ultrapure H_2O (Sigma Aldrich) at a stock concentration of 5mM. Cells were treated with 5nM NAP or vehicle, ultrapure H_2O, for 24h to evaluate rescuing of mitochondria trafficking.

Western Blotting

At 8 days of differentiation, protein was extracted using protein lysis buffer. Protein lysates were sonicated and centrifuged at 13000 rpm for 10 min. The supernatant was fractionated by SDS-PAGE (25μg or 50μg protein/lane) using a 12.5% tris-HCl gel at 100V for 1.5h. Proteins were transferred to immobilon membrane (FL-Millipore IPFL 00010) for 1h at 100V. Membranes were blocked using PBS with 0.5% Tween 20 and 5% milk for 30 min. The following antibodies were used directed against: β-actin (1:1000, 37 kDa, Abcam, #ab6276) and α-synuclein

(1:1000, 14kDa, Invitrogen, LB509). The blotted protein bands were visualized using Odyssey scanner (Li-Cor Biosciences, Lincoln, NE). Band density was quantified by computer assisted image analysis software (ImageJ). For reliable quantification of the Western blot data the defined methodology was followed as described by Taylor et al., 2013.

Real-time PCR

Total RNA and genomic DNA were collected using an AllPrep DNA/RNA/Protein Mini Kit. CDNA was reverse transcribed from 1 µg of RNA using M-MLV Reverse Transcriptase. GAPDH mRNA and genomic GAPDH were used as reference for normalization. For quantitative real-time PCR, primers were acquired from Biolegio and reactions were run on a Biorad C1000 Touch thermal cycler and analyzed with Biorad CFX manager software.

Statistical Analysis

Mitochondrial trafficking, immunofluorescence, Western Blotting and real-time PCR results were analyzed by one-way ANOVA followed by Tukey post hoc test. Neurons containing normal mitochondria morphology were analyzed by Student´s t-test. A p-value ≤ 0.05 was considered significantly different, using GraphPad Prism software (GraphPad Software Inc., version 5.00, CA).

Results

Characterization of differentiated, α-synuclein transgenic SH-SY5Y cells

After 4 days in-vitro (DIV) in the presence of retinoic acid and BDNF, the transgenic SH-SY5Y cells (i.e. expressing A53T, A30P or a surplus of WT α-synuclein) and the control SH-SY5Y cells (transfected with an empty vector) differentiated into neuron-like cells and formed small neurite-like extensions; at 6 DIV, these cells started to express the neuronal marker MAP2 and continued to grow their neurite-like

extensions reaching stable maturity at 8 DIV (Fig. 1A, B and C). No differences in the neuronal differentiation pattern were observed between the control cells and the ones expressing the α-synuclein variants (supplemental Fig. 2). Selective survival based on puromycine resistance resulted in a neuronally differentiated SH-SY5Y cell culture of which all cells expressed a high level either of A53T, A30P or WT α-synuclein; in the control SH-SY5Y cell cultures, expression of α-synuclein could not be detected through immunofluorescence (Fig. 1D). The expression of the α-synuclein variants in the differentiated transgenic and control SH-SY5Y cells was quantified at 8 DIV using qPCR (Fig. 1E). Results of qPCR showed that, although each of the transgenic cell lines contained a similar number of α-synuclein gene copies, transcriptional activity was lower in the cell lines containing mutant α-synuclein in comparison to those expressing wild type α-synuclein, suggesting interference of these α-synuclein mutants with transcription, nuclear shuttling, or cytoplasmic mRNA processing.

Analysis of α-synuclein linked to YFP corroborated the results of immunofluorescence, suggesting that A53T is more prone to aggregation since its pattern of labeling resembles that of small aggregates (Fig. 2). The expression of α-synuclein was quantified in Western blots demonstrating increased expression of A53T isoforms (Fig. 2). Our findings suggest a reduction in degradation, possibly due to the aggregated state of A53T α-synuclein.

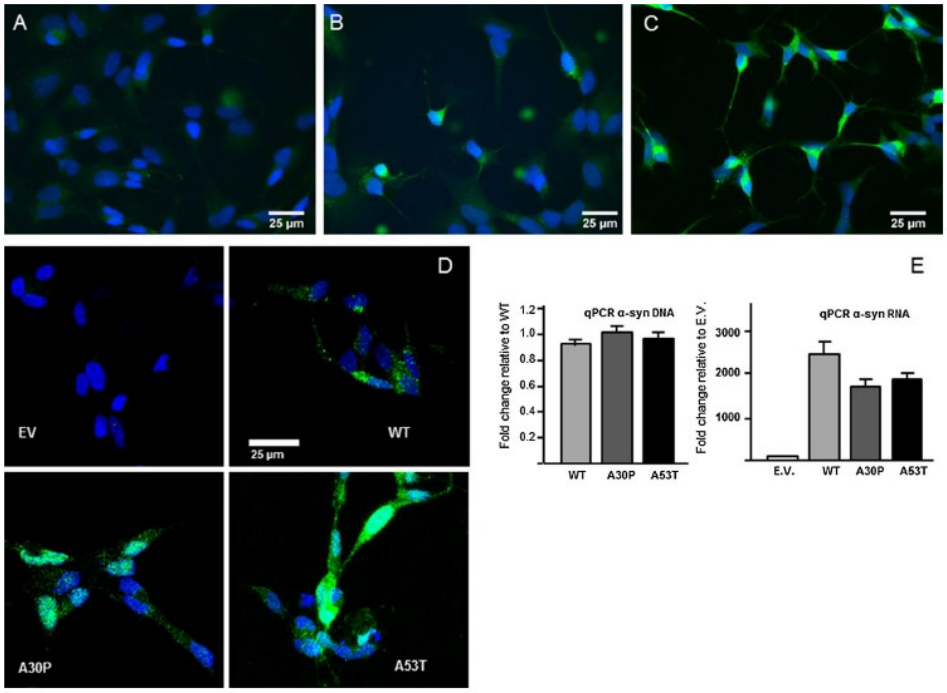

Figure 1. Characterization of differentiated, α-synuclein transgenic SH-SY5Y cells. *Immunofluorescence shows a positive stain for microtubule associated protein (MAP2) (green) at 4 days of differentiation (A), at 6 days of differentiation (B) and at 8 days of differentiation (C). Immunostaining for α-synuclein shows its expression in the α-synuclein transgenic SH-SY5Y cells (WT, A30P and A53T) but not in the control cells (transduced with an empty vector, EV) (D). Blue staining in A-D is Hoechst nuclear staining. Quantification of α-synuclein with q-PCR after 8 days of differentiation confirms the increased expression of α-synuclein (E).*

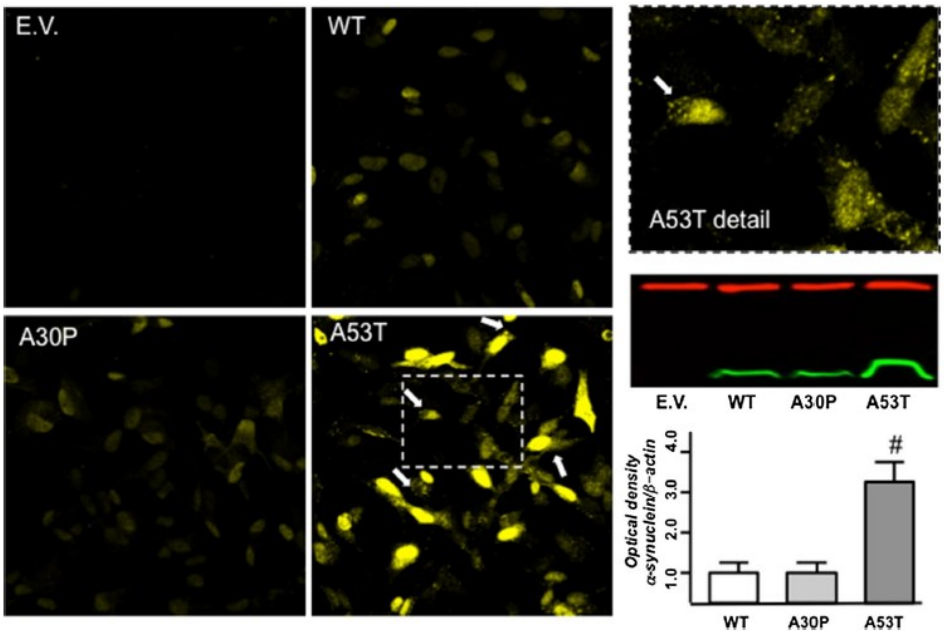

Figure 2: α-Synuclein expression*. Photomicrographs show homogeneous α-synuclein staining in neurons expressing WT or A30P YFP-α-synuclein. Neurons expressing A53T YFP-α-synuclein showed puncta accumulation of the protein at soma and neurites (arrows in magnification of boxed area). Blottings of insoluble protein fraction (red bands = β-actin; green bands = α-synuclein) reveal significantly higher levels of A53T α-synuclein compared to WT and A30P α-synuclein. Experiments were repeated 3 times. # p<0.001 as compared with WT according to one-way analysis of variance (ANOVA) followed by Tukey post-test.*

Mitochondrial trafficking in differentiated, α-synuclein transgenic SH-SY5Y cells

We transfected the various SH-SY5Y cell cultures with the pDsRed2-Mito plasmid: approximately 50% of the cells showed red staining in the cytosol that appeared to be confined to mitochondria and completely co-localized with the green immunostaining by the mitochondria-specific TOM20 antibody (Fig. 3). The strong specific staining by pDsRed2-Mito allowed us to investigate mitochondrial mobility in the neurite-like extensions in the neuronally differentiated SH-SY5Y

cells and the consequences of aberrant α-synuclein expression for mitochondrial trafficking.

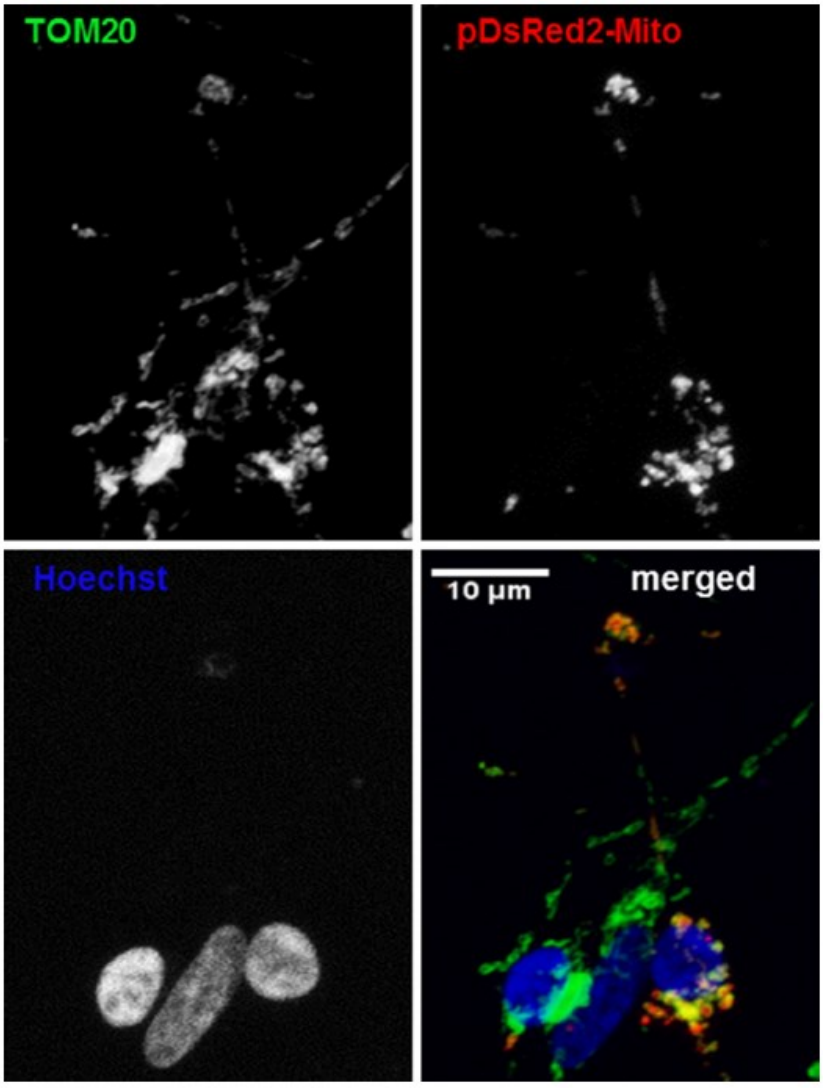

Figure 3. Mitochondrial labeling. *Immunofluorescence imaging shows the co-localization of fluorescent staining for the mitochondria-specific TOM20 (green) and pDsRed2-Mito (red). Nuclei were stained by Hoechst (blue).*

In order to examine if and when mitochondria trafficking was impaired by α-synuclein in SH-SY5Y cell cultures, we analyzed mitochondria mobility in the different transgenic and control SH-SY5Y cells at 4, 6 and 8 DIV in the presence of retinoic acid and BDNF representing different stages in differentiation. At 4 DIV, when the neuron-like cells were still immature and proper mitochondria trafficking was crucial for the outgrowth of the young “neurites”, a similar pattern of mitochondrial trafficking activity was observed in all the groups of SH-SY5Y-derived neuron-like cells. The first sign of disturbed mitochondrial mobility was observed at 6 DIV only in the A53T α-synuclein expressing SH-SY5Y cells where retrograde trafficking was significantly decreased in comparison to the control. Only later, at 8 DIV, also the anterograde trafficking of mitochondria was significantly decreased to almost 30%, again only, in the A53T α-synuclein expressing SH-SY5Y derived cells. No changes were observed in the other transgenic SH-SY5Y cell lines or in the control cells (Fig. 4). So, Figure 4 presents evidence for the presence of mitochondria trafficking during differentiation and shows that the disturbance in mitochondria trafficking is specific for neuronal cells, since it does not occur in undifferentiated SH-SY5Y cells.

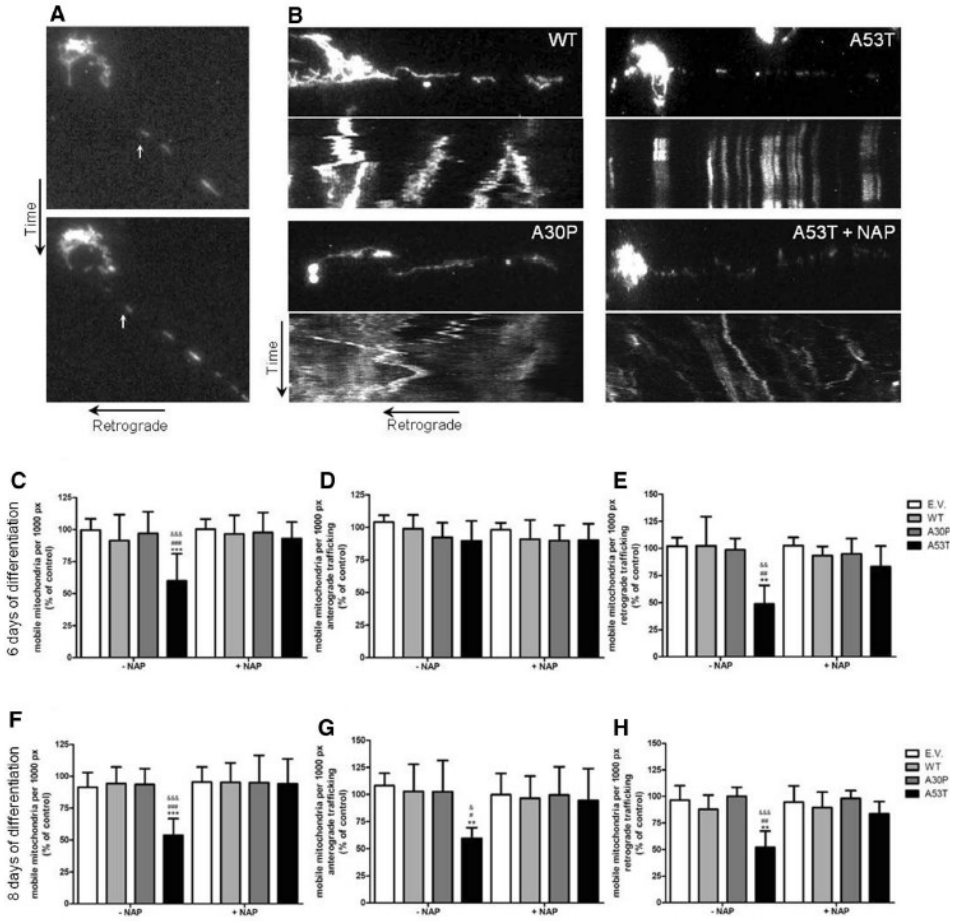

Figure 4. Mitochondria mobility analysis in SH-SY5Y. *(A)Time-lapse recordings show the retrograde movements of mitochondria in the neurite-like extension of a SH-SY5Y cell after 8 days of differentiation. (B) Kymographs represent mitochondria movement in neurons derived from SH-SY5Y cells after 6 days of differentiation expressing either wild-type, A30P or A53T α-synuclein (in the absence and presence of NAP). Analysis of movement reveals that trafficking is decreased at 6 and 8 days of differentiation (C and F respectively). Separate analysis of retrograde and anterograde trafficking shows unaltered anterograde trafficking but decreased retrograde trafficking at 6 days of differentiation (D and E); at 8 days of differentiation both anterograde and retrograde trafficking appears to be reduced (G and H, respectively). Neurons treated with NAP at 5nM for 48h show a rescued mitochondria trafficking at 6 and*

*8 days of differentiation (C, E, F, G and H). Data of moving mitochondria per 1,000 pixels are expressed as percent relative to control (E.V.) ± SD. Two-way ANOVA following Bonferroni post- test were the statistical tests employed *p ≤ 0.05 compared to control. # p ≤ 0.05 compared to cells expressing WT. & p ≤ 0.05, compared to cells expressing A30P α-synuclein. Data are expressed as mean of 3 independent experiments.*

Effect of NAP on mitochondrial trafficking

To examine the mechanisms by which the A53T α-synuclein induced impairment of mitochondrial trafficking in the neuronally differentiated SH-SY5Y cells, we treated the SH-SY5Y cell cultures with NAP since it has been shown to restore microtubule integrity (Gomez 2007; Estevez et a;, 2014). Adding NAP, indeed, appeared to completely restore retrograde as well as anterograde mitochondria trafficking in the A53T α-synuclein expressing SH-SY5Y derived cells (Fig. 4). Although both motor proteins, dynein and kinesin, have clear structural distinctions and move across the microtubule surface with different speed, step sizes and in opposite directions, apparently the A53T α-synuclein-induced microtubules destruction, restorable by NAP, affects the interaction between the motor proteins and the microtubules in a similar mode.

Effect of NAP on mitochondrial membrane potential and morphology

Impairment of mitochondrial dynamics due to the overexpression of α-synuclein or the expression of its mutants A30P and A53T may involve an increase in the production ROS and a disruption of the mitochondrial membrane potential.

We found a significant increase in ROS levels in the α-synuclein expressing cells in comparison to the controls, with the highest level in the A53T mutant (Fig. 5A and C). Adding NAP to the culture, completely annihilated the ROS increase observed in all the α-synuclein expressing cell lines (Fig. 5B and C).

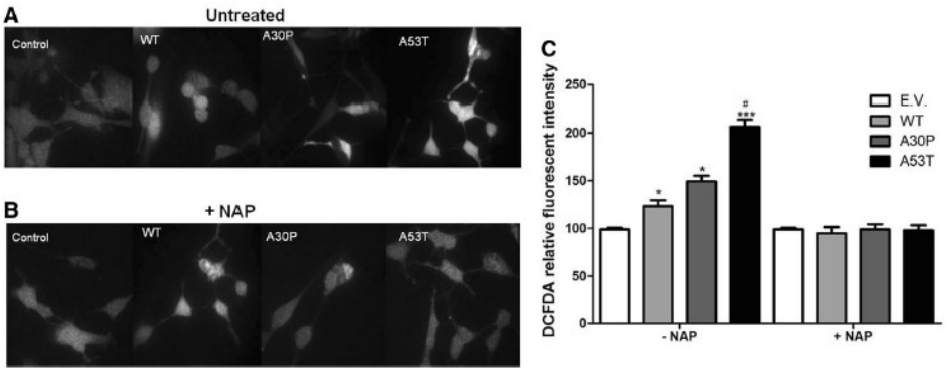

Figure 5. ROS production. *Photomicrographs show neurons incubated with green fluorescent probe DCFDA untreated (A) or treated with NAP (B). Differentiated SH-SY5Y cells at 8DIV expressing WT, A30P or A53T α-synuclein or controls (E.V.=empty vector) were incubated with CM-H_2DCFDA, a fluorescent ROS detector, untreated (A) or treated with NAP (B). Fluorescence intensity measurements (C) show significantly higher levels of ROS compared to control (E.V.); treatment with NAP restored levels of ROS to basal levels of control cells. Data are expressed as percentage of control (E.V.) ± SD. Two-way ANOVA following Bonferroni post- test was the statistical test employed *p ≤ 0.05; **p ≤ 0.01; ***p ≤ 0.001 compared to control. # p ≤0.05 compared to cells expressing WT. Data are expressed as mean of 3 independent experiments.*

Neuronal cells transfected with pDsRed2-Mito or those fixed and stained for TOM20 showed the same pattern of mitochondria morphology when expressing WT or A30P alpha-synuclein compared to control (transfected with empty vector). About 65% of neurons expressing A53T alpha-synuclein showed small spherical mitochondria clusters. After NAP treatment, only 20% of DA neurons expressing A53T alpha-synuclein showed fragmented mitochondria (Fig.6).

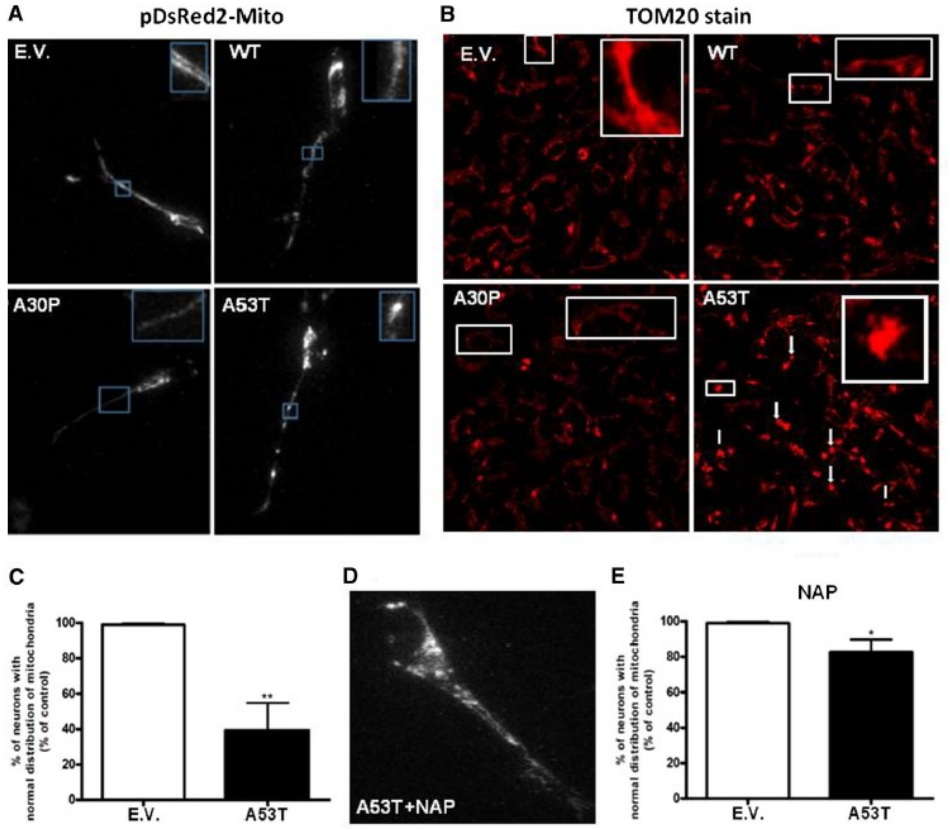

Figure 6: Mitochondria distribution and connectivity. *Photomicrographs illustrate mitochondria distribution and connectivity in neurons transfected with pDsRed2-Mito (63x objective) (**A**) or in neurons stained for mitochondria using TOM20 antibody (20x objective) (**B**). Quantification of neurons with normal mitochondria distribution reveals a significant decrease after expression of A53T α-synuclein (**C**). Treatment with NAP increases the amount of neurons with normal mitochondria distribution and connectivity to 70% (**D** and **E**). Data are expressed as percent relative to control (EV). *p<0.05 and **p<0.01 compared with EV according to Student's T-test. n = 5. Experiments were repeated 3 times.*

Discussion

Our studies show that, in contrast to wild-type and A30P α-synuclein, A53T α-synuclein significantly inhibited mitochondrial trafficking in the SH-SY5Y cell model for Parkinson's disease. Retrograde trafficking appears to be the first to be disturbed, followed in a later stage by anterograde trafficking. Accordingly, A53T α-synuclein also caused the highest increase in ROS production in these apparently demobilized and fragmented mitochondria in comparison to wild-type or A30P α-synuclein. Treatment with the active peptide (NAP) of activity-dependent neuroprotective protein (ADNP) completely annihilated the adverse effects of A53T on mitochondrial dynamics.

Our findings regarding the effect of A53T α-synuclein on mitochondrial trafficking not only confirm but also extend previous data [33, 34] since we also studied the time-frame of mitochondria trafficking disturbance: we wanted to determine which type of trafficking was disturbed first, anterograde or retrograde. Impairment of anterograde or retrograde trafficking can lead to different injuries in organelles in neurons. In our previous studies [24, 26], we revealed that the expression of proteins involved in anterograde or retrograde trafficking was differentially affected. It has been reported that disrupted anterograde mitochondria trafficking leads to fragmentation of mitochondria, abnormal mitochondria distribution and biogenesis, depletion of ATP and high ROS levels, resulting in cell death [38], while disrupted retrograde trafficking leads to ageing and swollen mitochondria, depletion of ATP, higher ROS levels and cell death [39]. Although the outcome (cell death) is the same, determining the direction of trafficking that is impaired first enables elucidation of the actual mechanisms responsible for neuronal death; it may lead to a more specific therapeutical approach to prevent the phenotype of the disease. In the present study we showed that A53T first impairs retrograde trafficking in neurons derived from the SHSY-5Y cells. In addition we showed that NAP is able to recover mitochondria trafficking.

The prominent effect on mitochondrial trafficking of A53T α-synuclein in comparison to A30P and wild-type α-synuclein most likely reflects the fact that A53T α-synuclein is more prone to oligomer or aggregate formation. It has been shown that the interaction of wild type α-synuclein and α-synuclein variants with molecular motors, tubulin, and the microtubules-associated proteins, MAP2 and Tau, is stronger for oligomers than for monomers (Prots et al., 2013). There appear to be differential effects between seeds and oligomers on (Tau-promoted) microtubules assembly and on the microtubules gliding velocity across kinesin-coated surfaces (Prots et al., 2013). Due to the fact that NAP, a protein known to repair microtubules integrity, restores the A53T α-synuclein-induced impairment of mitochondrial trafficking, may point to a disruption of microtubules assembly by A53T α-synuclein disturbing the interplay between microtubules and kinesin (Prots et al., 2013). The earliest effects of A53T α-synuclein was observed in the retrograde dynein-driven trafficking of mitochondria, indicating that also the dynein-microtubules interplay may be disturbed. The reason that retrograde mitochondrial trafficking is the first to be affected may be related to the lower velocity of retrograde transport in which even small disturbances leads to an actual stop in trafficking. Obviously, the machinery underlying mitochondrial trafficking along the microtubules in axons concerns a complex structure consisting, besides of kinesin and dynein, of Miro (also known as RhoT1/2) and Milton (for a review see Schwarz, 2013). Interactions between oligomers/aggregates of α-synuclein and Miro and Milton are as yet unknown.

Although the best known action of NAP is upon microtubule stabilization, this peptide has also been reported to affect autophagy [40] and oxidative stress [41, 42]. In fact, we observed a decrease in ROS content after NAP treatment, which may be either the cause or the consequence of altered mitochondria trafficking.

A wide variety of studies have shown that changes in mitochondrial trafficking are the earliest events to occur in cell models for Parkinson's

disease with abnormal α-synuclein expression [43-47]. The stressed, demobilized, mitochondria start to produce high levels of ROS, subsequently leading to other cytopathological processes. The annihilating effect of NAP on the ROS levels in our cell cultures expressing α-synuclein variants, must be ascribed to the recovery of the mitochondrial motility by NAP [31].

Summarizing, we propose that A53T α-synuclein leads to impairment of trafficking in SH-SY5Y cells, most likely by a disturbance of microtubule integrity. This in turn leads to impairment of mitochondrial turnover, particularly in distal regions of the cell. NAP treatment rescues mitochondria trafficking and so proper mitochondrial function and turnover. After 8 days of differentiation of the SH-SY5Y cells, we observed aggregates only in neurons expressing A53T alpha-synuclein. As mentioned above, time to form oligomers of alpha-synuclein is dependent of its type, where A53T alpha-synuclein oligomerizes easier and faster than A30P alpha-synuclein, which in turn oligomerizes easier and faster than WT alpha-synuclein. Moreover, not only the levels of oligomers influence cellular damage, but also the type of oligomer is important for the type and amount of damage in neurons [48]. In view of this, our findings suggest that we have more oligomers of A53T alpha-synuclein and that they are more toxic than oligomers of A30P or WT alpha-synuclein. The increase in ROS production we observed may be related with lowered mitochondrial integrity at distal sites. We have shown that these effects can be rescued by using NAP, negating the effect of α-synuclein expression and leading to increased mitochondrial turnover.

Our data implies mitochondrial trafficking as an important mechanism relating mitochondrial damage to protein occlusions observed in early Parkinson's disease. Early impairment of retrograde transport would lead to accumulation of damaged mitochondria near the axon terminal, which has been proposed as an early event in clinical cases of Parkinson's disease [49].

Acknowledgements

This study was supported by research grants from Fundacao de Amparo a Pesquisa do Estado de Sao Paulo (FAPESP) (2012/15495-2; 2013/08028-1), and CNPq (Conselho Nacional de desenvolvimento Cientifico e Tecnologico (401670/2013-9; 471999/2013-0). T.Q.M. received fellowships from CAPES (38794040893) and CNPq (240703/2012-0).

References

1. Tanner CM. Occupational and environmental causes of parkinsonism. **Occup Med**. 1992;7:503-513.
2. Siderowf A, Stern M. Update on Parkinson disease. **Ann Intern Med**. 2003;138:651-658.
3. Gruden MA, Sewell RD, Yanamandra K et al. Immunoprotection against toxic biomarkers is retained during Parkinson's disease progression. **J Neuroimmunol**. 2011;233:221-227.
4. Qian JJ, Cheng YB, Yang YP et al. Differential effects of overexpression of wild-type and mutant human alpha-synuclein on MPP+-induced neurotoxicity in PC12 cells. **Neurosci Lett**. 2008;435:142-146.
5. Simcox EM, Reeve A, Turnbull D. Monitoring mitochondrial dynamics and complex I dysfunction in neurons: implications for Parkinson's disease. **Biochem Soc Trans**. 2013;41:1618-1624.
6. Chartier-Harlin MC, Kachergus J, Roumier C et al. Alpha-synuclein locus duplication as a cause of familial Parkinson's disease. **Lancet**. 2004;364:1167-1169.
7. Kruger R, Kuhn W, Muller T et al. Ala30Pro mutation in the gene encoding alpha-synuclein in Parkinson's disease. **Nat Genet**. 1998;18:106-108.
8. Polymeropoulos MH, Lavedan C, Leroy E et al. Mutation in the alpha-synuclein gene identified in families with Parkinson's disease. **Science**. 1997;276:2045-2047.
9. Singleton AB, Farrer M, Johnson J et al. alpha-Synuclein locus triplication causes Parkinson's disease. **Science**. 2003;302:841.
10. Edwards TL, Scott WK, Almonte C et al. Genome-wide association study confirms SNPs in SNCA and the MAPT region as common risk factors for Parkinson disease. **Ann Hum Genet**. 2010;74:97-109.

11. Lill CM, Roehr JT, McQueen MB et al. Comprehensive research synopsis and systematic meta-analyses in Parkinson's disease genetics: The PDGene database. **PLoS Genet**. 2012;8:e1002548.
12. Nalls MA, Pankratz N, Lill CM et al. Large-scale meta-analysis of genome-wide association data identifies six new risk loci for Parkinson's disease. **Nat Genet**. 2014;46:989-993.
13. Victoria GS, Zurzolo C. Trafficking and degradation pathways in pathogenic conversion of prions and prion-like proteins in neurodegenerative diseases. **Virus Res**. 2015;207:146-154.
14. Winslow AR, Chen CW, Corrochano S et al. alpha-Synuclein impairs macroautophagy: implications for Parkinson's disease. **J Cell Biol**. 2010;190:1023-1037.
15. Perfeito R, Lazaro DF, Outeiro TF et al. Linking alpha-synuclein phosphorylation to reactive oxygen species formation and mitochondrial dysfunction in SH-SY5Y cells. **Mol Cell Neurosci**. 2014;62:51-59.
16. Wang Y, Nartiss Y, Steipe B et al. ROS-induced mitochondrial depolarization initiates PARK2/PARKIN-dependent mitochondrial degradation by autophagy. **Autophagy**. 2012;8:1462-1476.
17. Arnold B, Cassady SJ, VanLaar VS et al. Integrating multiple aspects of mitochondrial dynamics in neurons: age-related differences and dynamic changes in a chronic rotenone model. **Neurobiol Dis**. 2011;41:189-200.
18. Hunn BH, Cragg SJ, Bolam JP et al. Impaired intracellular trafficking defines early Parkinson's disease. **Trends Neurosci**. 2015;38:178-188.
19. Amiri M, Hollenbeck PJ. Mitochondrial biogenesis in the axons of vertebrate peripheral neurons. **Dev Neurobiol**. 2008;68:1348-1361.
20. Cai Q, Gerwin C, Sheng ZH. Syntabulin-mediated anterograde transport of mitochondria along neuronal processes. **J Cell Biol**. 2005;170:959-969.
21. Van Laar VS, Berman SB. Mitochondrial dynamics in Parkinson's disease. **Exp Neurol**. 2009;218:247-256.
22. Celardo I, Martins LM, Gandhi S. Unravelling mitochondrial pathways to Parkinson's disease. **Br J Pharmacol**. 2014;171:1943-1957.
23. Roy B, Jackson GR. Interactions between Tau and alpha-synuclein augment neurotoxicity in a Drosophila model of Parkinson's disease. **Hum Mol Genet**. 2014;23:3008-3023.
24. Melo TQ, D'Unhao A M, Martins SA et al. Rotenone-dependent changes of anterograde motor protein expression and mitochondrial

mobility in brain areas related to neurodegenerative diseases. **Cell Mol Neurobiol**. 2013;33:327-335.
25. Chu Y, Morfini GA, Langhamer LB et al. Alterations in axonal transport motor proteins in sporadic and experimental Parkinson's disease. **Brain**. 2012;135:2058-2073.
26. Chaves RS, Melo TQ, D'Unhao AM et al. Dynein c1h1, dynactin and syntaphilin expression in brain areas related to neurodegenerative diseases following exposure to rotenone. **Acta Neurobiol Exp (Wars)**. 2013;73:541-556.
27. Credle JJ, George JL, Wills J et al. GSK-3beta dysregulation contributes to parkinson's-like pathophysiology with associated region-specific phosphorylation and accumulation of tau and alpha-synuclein. **Cell Death Differ**. 2015;22:838-851.
28. Magdalinou NK, Paterson RW, Schott JM et al. A panel of nine cerebrospinal fluid biomarkers may identify patients with atypical parkinsonian syndromes. **J Neurol Neurosurg Psychiatry**. 2015;86:1240-1247.
29. Wade-Martins R. Genetics: The MAPT locus-a genetic paradigm in disease susceptibility. **Nat Rev Neurol**. 2012;8:477-478.
30. Magen I, Ostritsky R, Richter F et al. Intranasal NAP (davunetide) decreases tau hyperphosphorylation and moderately improves behavioral deficits in mice overexpressing alpha-synuclein. **Pharmacol Res Perspect**. 2014;2:e00065.
31. Esteves AR, Gozes I, Cardoso SM. The rescue of microtubule-dependent traffic recovers mitochondrial function in Parkinson's disease. **Biochim Biophys Acta**. 2014;1842:7-21.
32. Giasson BI, Duda JE, Quinn SM et al. Neuronal alpha-synucleinopathy with severe movement disorder in mice expressing A53T human alpha-synuclein. **Neuron**. 2002;34:521-533.
33. Xie W, Chung KK. Alpha-synuclein impairs normal dynamics of mitochondria in cell and animal models of Parkinson's disease. **J Neurochem**. 2012;122:404-414.
34. Li L, Nadanaciva S, Berger Z et al. Human A53T alpha-synuclein causes reversible deficits in mitochondrial function and dynamics in primary mouse cortical neurons. **PLoS One**. 2013;8:e85815.
35. Bassan M, Zamostiano R, Davidson A et al. Complete sequence of a novel protein containing a femtomolar-activity-dependent neuroprotective peptide. **J Neurochem**. 1999;72:1283-1293.
36. Gozes I. Activity-dependent neuroprotective protein: from gene to drug candidate. **Pharmacol Ther**. 2007;114:146-154.

37. Zamostiano R, Pinhasov A, Gelber E et al. Cloning and characterization of the human activity-dependent neuroprotective protein. **J Biol Chem**. 2001;276:708-714.
38. Matenia D, Hempp C, Timm T et al. Microtubule affinity-regulating kinase 2 (MARK2) turns on phosphatase and tensin homolog (PTEN)-induced kinase 1 (PINK1) at Thr-313, a mutation site in Parkinson disease: effects on mitochondrial transport. **J Biol Chem**. 2012;287:8174-8186.
39. Morris RL, Hollenbeck PJ. The regulation of bidirectional mitochondrial transport is coordinated with axonal outgrowth. **J Cell Sci**. 1993;104 (Pt 3):917-927.
40. Gozes I. The cytoskeleton as a drug target for neuroprotection: the case of the autism- mutated ADNP. **Biol Chem**. 2016;397:177-184.
41. Sharma NK, Sethy NK, Meena RN et al. Activity-dependent neuroprotective protein (ADNP)-derived peptide (NAP) ameliorates hypobaric hypoxia induced oxidative stress in rat brain. **Peptides**. 2011;32:1217-1224.
42. Greggio S, de Paula S, de Oliveira IM et al. NAP prevents acute cerebral oxidative stress and protects against long-term brain injury and cognitive impairment in a model of neonatal hypoxia-ischemia. **Neurobiol Dis**. 2011;44:152-159.
43. Arduino DM, Esteves AR, Swerdlow RH et al. A cybrid cell model for the assessment of the link between mitochondrial deficits and sporadic Parkinson's disease. **Methods Mol Biol**. 2015;1265:415-424.
44. Coskun P, Wyrembak J, Schriner SE et al. A mitochondrial etiology of Alzheimer and Parkinson disease. **Biochim Biophys Acta**. 2012;1820:553-564.
45. Franco-Iborra S, Vila M, Perier C. The Parkinson Disease Mitochondrial Hypothesis: Where Are We at? **Neuroscientist**. 2016;22:266-277.
46. Keogh MJ, Chinnery PF. Mitochondrial DNA mutations in neurodegeneration. **Biochim Biophys Acta**. 2015;1847:1401-1411.
47. Prots I, Veber V, Brey S et al. alpha-Synuclein oligomers impair neuronal microtubule-kinesin interplay. **J Biol Chem**. 2013;288:21742-21754.
48. Stefanovic AN, Lindhoud S, Semerdzhiev SA et al. Oligomers of Parkinson's Disease-Related alpha-Synuclein Mutants Have Similar Structures but Distinctive Membrane Permeabilization Properties. **Biochemistry**. 2015;54:3142-3150.
49. Cheng A, Hou Y, Mattson MP. Mitochondria and neuroplasticity. **ASN Neuro**. 2010;2:e00045.

Chapter 3

Using metabolic preference for the highly efficient generation of pure neuronal populations from human induced pluripotent stem cells

Neuronal selection using a lactate switch

Koen C. van Zomeren, Susanne M. Kooistra, Hilmar R.J. van Weering, Rob Bakels, Erik Boddeke and Sjef Copray

Department of Neuroscience, University Medical Centre Groningen, University of Groningen, Groningen, The Netherlands

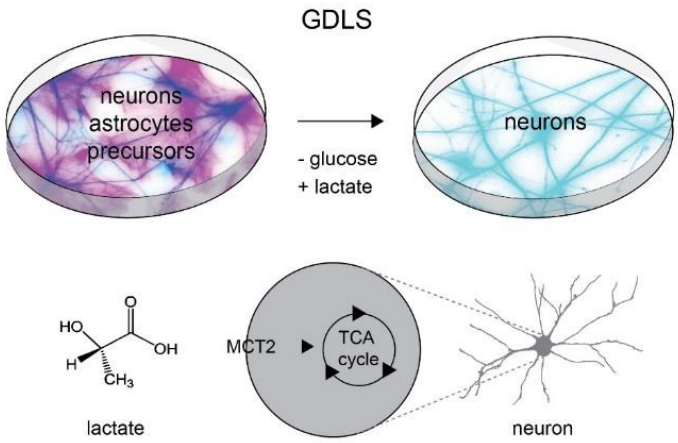

Graphical abstract

Glucose deprivation and lactate supplementation (GDLS) treatment of differentiating hiPSCs results in highly pure (>90%) neuronal cultures. Monocarboxylate transporter 2 is required for the selective survival of neurons. GDLS provides a low-cost, robust method for generating pure neuronal cultures.

Submitted

Abstract

Differentiated human induced pluripotent stem cells (hiPSCs) hold great promise as a source for autologous cells for cell replacement therapies and disease modeling. While the initial yield of differentiated cells can be high, cultures are often contaminated with a variety of unwanted cellular phenotypes. Moreover, current methods to obtain pure populations of specific differentiated cell types are laborious, expensive and often difficult to reproduce. We present an efficient method to purify hiPSC-derived neuronal cultures utilizing their metabolic capacity through supplying selective metabolic substrates based on glucose deprivation and lactate supplementation (GDLS). hiPSC-derived neurons that were purified by GLDS show electrophysiological activity, similar to unpurified hiPSC-derived neurons, and can be cultured for a prolonged duration. The GDLS purification procedure is equally effective for patient and control iPSC-derived neurons. This brief, simple and cost-effective method to obtain pure hiPSC-derived neuronal cultures creates new opportunities for hiPSC-associated neuronal disease modeling.

Introduction

Human induced pluripotent stem cells (hiPSCs) offer an advanced tool for disease modelling, drug screening and cell replacement therapies (1, 2). Unlimited self-renewal and the potential to differentiate into cells of all three germ layers provide an unprecedented source for otherwise unobtainable autologous cells that can be used for disease modeling or transplantation purposes. However, hiPSC-based generation of specific cellular populations with high efficiency and purity has proven to be a major challenge for a number of lineages, including the dopaminergic neuronal lineage (3, 4).

hiPSCs are frequently used to generate neuronal subtypes to model neurodegenerative disorders and are currently considered for cell transplantation as regenerative therapy. Parkinson's disease (PD) is one of the most obvious candidates for such a cell replacement therapy, since early neuronal pathology is largely confined to the nigrostriatal pathway, and characterized by loss of dopaminergic (DA) neurons in the substantia nigra pars compacta (5). Moreover, ample experience with cell transplantation approaches in PD patients using abortion-derived fetal DA neurons has already demonstrated its feasibility and therapeutic efficacy in the 80's and 90's (6).

A major bottleneck in stem cell-based replacement therapy is the impurity of the DA cell graft. Apart from contaminating, undifferentiated and possibly teratogenic iPSCs, other neuronal and in particular non-neuronal cell types may still be present, interfering with therapeutic outcome. Current strategies to eliminate or decrease unwanted populations of cells include laborious and harmful sorting techniques (7-9), application of mitosis-inhibiting chemicals like mitomycin C (10) or the use of neuronal cells at early time-points (<40 days in vitro (DIV)) (11-13). Harmful elimination and purification steps are considered highly undesirable in current procedures for replacement strategies or disease modeling. Furthermore, use of less mature neuronal cells is questionable given the nature of most late-onset neuronal disorders studied with iPSCs.

Apart from this, estimation of differentiation efficiency at early time points can lead to an overestimation of neuronal content at later time points, since contaminating populations often proliferate.

To improve the outcome of differentiation procedures, we implemented a novel strategy to purify iPSC-derived neuronal populations based on their metabolic properties. Replacing glucose and using lactate as a metabolic substrate effectively annihilates the presence of glial- and neuronal precursor populations, which are glucose-dependent, in neuronal differentiated cell cultures. In addition to presenting an effective tool for neuronal purification, our method also provides further evidence for the brain lactate shuttle hypothesis, originally proposed over 20 years ago (14). This concept has gained renewed attention through the first evidence for this shuttle in vivo (15). In the central nervous system, astrocytes and oligodendrocytes produce lactate, which is exported via the low affinity monocarboxylate transporter (MCT) 4 and/or MCT1, to be taken up by the high affinity MCT2 transporter expressed by neurons (16). The neuronal lactate shuttle hypothesis states that neurons can take up lactate in case of high energy demand, such as during stroke and even brain development (15, 17-19). In contrast, the primary metabolic pathways in pluripotent stem cells are dependent on glucose and glycolysis (20).

We hypothesized that lactate shuttling is active in hiPSCs-derived neurons and can be exploited in combination with glucose deprivation to selectively sustain neuronal populations. In contrast, progenitor, glial and undifferentiated counterparts are glucose-dependent. In this study, we present a method to derive functional neuronal populations from iPSCs with high purity by combining existing iPSC differentiation protocols with glucose deprivation and lactate supplementation (GDLS).

GDLS-treated neurons in our study show mature action potentials, spontaneous neuronal activity and express mature neuronal markers.

Moreover, we have cultured these neurons for prolonged periods, up to 90 DIV, which is a requirement for proper disease modelling.

Materials and methods

Cell culture

Fibroblast cell lines from Parkinson patients were obtained from Corriel biorepository (ND27760, ND40996). Healthy donor fibroblast lines were acquired from the UMCG Department of Dermatology. Generation of iPSCs was done following the protocol and using episomal vectors from Okita et al. (2011). Briefly, to generate iPSCs, one million fibroblasts were nucleofected with 0.85 µg pCXLE-hMLN, 0.85 µg pCXLE-hOCT3/4 and 1.3 µg pCXLE-hSK (Addgene #27079, #27076, #27078). Clones were checked for expression of pluripotency factors (OCT3/4, SOX2, KLF4, TRA1-60, TRA-1-81, live alkaline phosphatase) and karyotype was assessed using metaphase spreads. Differentiation potential was assessed by spontaneous embryoid body (EB) differentiation, using antibodies for ectoderm (TUJ1), endoderm (GATA4) and mesoderm (DESMIN). H9 ESCs were used in collaboration with the Department of Experimental Cardiology, UMCG. Cells were maintained on Geltrex® coated plates in Essential 8™ medium (Thermo Fisher), and passaged weekly using ReLeSR™ (Stemcell Technologies). All cells were used for experiments between passage 20 and 50, and kept in a humidified incubator at 37°C with 5%CO_2.

Neuronal differentiation

For differentiation, a slightly adapted protocol from Kriks et al. was followed (21). Briefly, cells were grown to 70% confluency, and medium was changed to 50% KSR and 50% DMEM/F12. Over the course of 7 days, medium was changed to DMEM/F12 supplemented with N1 (Sigma). The following small molecules and proteins were added; 10 µM SB-431542 (Stemcell Technologies) from day 1-5, 100nM LDN-193189

(Stemcell Techologies) from day 1-11, 3 μM Purmorphamine (Stemcell Techologies) from day 3-7, 500 nM Smoothened agonist from day 3-7, 100 ng/ml SHH (Peprotech) from day 3-8, 50 ng/ml FGF8 (Peprotech) from day 3-8 and 2 μM CHIR99021 (Stemcell Technologies) from day 5-13. Terminal neuronal induction towards a dopaminergic ventral midbrain phenotype was started at day 12 by switching to Neurobasal A™ (NBA) medium supplemented with SM1-Vit.A 50x (Stemcell Techologies), N1 250x (Sigma), BDNF (20 ng/ml, Peprotech), Ascorbic Acid (200 μM, Sigma), GDNF (20 ng/ml, Peprotech), dibutyryl cAMP (0.5 mM, Sigma), DAPT (10 μM, Stemcell Technologies), and TGF-β3 (1 ng/ml, Peprotech) (BAGCDT). Eighteen to twenty days after the start of differentiation cells were dissociated using Accutase (Sigma), strained with a 45μM cell strainer to remove cell debris, and plated on Geltrex® coated tissue culture treated plates at a density of roughly 80.000 cells/cm^2.

For motor neuron differentiation a modified protocol was used (S2A Fig). Cells were grown in similar conditions as described above, with addition of 10 μM SB-431542 (Stemcell Technologies) from day 1-5, 100nM LDN-193189 (Stemcell Techologies) from day 1-11, 3 μM Purmorphamine (Stemcell Techologies) from day 3-7, 500 nM Smoothened agonist from day 3-7, 100 ng/ml SHH (Peprotech) from day 3-8, 10 μM all-trans retinoic acid (RA; Peprotech) from day 5-20 and 2 μM CHIR99021 (Stemcell Technologies) from day 5-13.

Glucose deprivation and lactate supplementation (GDLS)

GDLS was initiated between 26 days and 36 days of differentiation, and was carried out for a period of 4-6 days based on visual inspection of the plate. NBA medium without glucose and sodium pyruvate supplemented with BAGCDT, SM1 50x and N1 250x, was added to the wells and supplemented with sodium DL-lactate (Sigma, L1375) to a final concentration of 5 mM. Cells were inspected daily to assess the GDLS based selection, and media was changed every other day. After cessation

of GDLS treatment, cells were recovered in glucose supplemented (25 mM) NBA and used for subsequent analysis.

Cell imaging

Phase contrast imaging was performed on a Leica AF-6000 microscope, using a 20x objective (PL FLUOTAR 20x/NA 0.4, Dry). Phase contrast images were taken at fixed positions in each well, to prevent biased imaging.

Large-scale tile scan imaging was performed using Tissuegnostics TissueFaxs setup, using a 10x phase contrast Zeiss-objective (Plan-Neofluar 10x/NA 0.3, Dry). Fully automated tile scans were performed in 6-well plates, and stitching was done using TissueFaxs viewer software (v3.5).

Calcium imaging recordings

Cells were replated at 80.000 cells/cm^2 on Geltrex® coated Nunc™ Lab-Tek™ II chamber slides™. Medium was switched to BrainPhys™ medium (Stemcell Technologies) plus growth factors to electrically mature neurons 14 DIV before imaging. Cells were incubated with 0.5 µM Fluo-AM (Thermo Fisher, Cat No. F14217) and placed inside an imaging chamber at 37°C with 5% CO2 and 95% humidity without washing. Calcium imaging movies were recorded using the Deltavision Elite live cell imaging system (GE Healthcare) equipped with PLAPON 60x oil, NA 1.42, WD 0.15 mm (Olympus) and a 15-bit EDGE/sCMOS camera (PCO) with GFP live filter wheel settings. At least 5 movies ranging from 1 min to 2 min intervals were recoded for selected cells, with timeframes ranging from 0.1 s to 0.5 s at 3.2% illumination intensity. Time series analysis was done using ImageJ (1.49s), by plotting y-axis profiles for both whole image analysis and regions of interest (ROIs). Neuronal calcium events were defined as a sharp transient increase in fluorescence intensity (Fluo-4 AM, dF/F >5%, fast rise, slower decay).

Electrophysiological recordings

Selected and non-selected cells were plated on Geltrex® coated coverslips at 45 DIV, and electrically matured in supplemented BrainPhys™ medium. At 60 DIV, coverslips were placed in a measuring chamber attached to an inverted microscope (Axioskop 2 FS, Zeiss) with a 40X water-immersion objective (NA 0.8, W ACHROPLAN). Membrane currents and voltages were measured using an Axopatch 200 B patch clamp amplifier (Molecular Devices) in whole-cell mode. Pipettes were pulled from GC120F-10 borosilicate glass (Harvard Apparatus, Holliston, MA) and filled with a solution containing 140 mM KCl, 10 mM Hepes, 1 mM MgCl2, 10 mM EGTA, 1 mM $CaCl_2$ and 2 mM Na_2ATP (280–290 mOsm, pH 7.4). Bathing solution contained 140 mM NaCl, 4 mM KCl, 1 mM $MgCl_2$, 2 mM $CaCl_2$, 1.2 mM HEPES and 10 mM glucose (mOsm 330, pH 7.4). Membrane currents were recorded at room temperature (20–22°C) with the amplifier in whole cell voltage clamp mode. Recording quality was continuously assessed by monitoring resistance and leak current. Initial pipette resistance was between 4 and 8 MΩ, with series resistance in samples averaging 50 MΩ. Currents were low-pass filtered at 5 kHz and sampled at 10 kHz using a Digidata 1320 AD converter (Molecular Devices). Currents were evoked by a voltage protocol, from -70 mV to +30 mV in 10 mV increments. After measuring membrane currents, the amplifier was switched to current clamp mode. Following measurement of the resting potential, the membrane potential was adjusted to -60 mV using a steady injected current through the patch pipette. Action potentials were evoked by depolarizing current pulses (50 ms duration in order to analyze single spikes, and 500 ms pulses to induce repetitive firing. Voltage clamp step protocols were generated and data were analyzed using Pclamp software (Molecular Devices).

Immunocytochemistry

Neuronal cultures on glass coverslips or 6-well plates were fixed in paraformaldehyde 4% for 15 min at room temperature. Samples were

permeabilized and blocked with PBS containing 0.1% Triton, 1% BSA and 5% normal goat serum for ~60 min at RT. Samples were incubated with primary antibodies overnight at 6°C, then washed 3 times with PBS and incubated with a fluorescent conjugated secondary antibody and Hoechst 33258 (Sigma, 14530). Mowiol® 4-88 (Sigma) was used as mounting medium to attach coverglasses to the coverslip. Samples were stored at 4°C until further analysis.

Fluorescent imaging and analysis

Single fluorescent images were acquired using a Leica AF-6000 fluorescent microscope, using a PL FLUOTAR 20x/NA 0,4, Dry lens. Images were analyzed using the ImageJ cell counter plugin.

Large-scale tile scan imaging was performed using Tissuegnostics TissueFaxs equipment, with a 10x phase contrast Zeiss-objective (Plan-Neofluar 10x/NA 0.3, Dry). Fully automated tile scans were performed in 6-well plates, and stitching was done using TissueFaxs viewer (v3.5) software. Analysis with ImageJ was performed on complete tile scans, assessing the total surface of signal from each fluorophore.

Antibodies

The following primary antibodies were used: Alkaline Phosphatase Live Stain (Thermo Fischer, A14353), βIII-Tubulin (mouse, 1:1000, Abcam, ab7751), DESMIN (mouse, 1:1000, DAKO, M0760), GATA4 (mouse, 1:1000, Santa Cruz Biotechnology, sc25310) Glial fibrillary acidic protein (rabbit, 1:1000, Dako, Z0334), NANOG (rabbit, 1:500, Abcam, ab80892), OCT3/4 (rabbit, 1:500, Santa Cruz Biotechnology, sc-9081), SOX2 (mouse, 1:500, Cell Signaling, #4900S), SSEA4 (mouse, 1:500, Hybridoma Bank, MC-813-70), TRA1-81 (mouse, 1:500, Santa Cruz Biotechnology, sc-21706), Tyrosine hydroxylase (rabbit, Abcam, AB152), Tyrosine hydroxylase (mouse, 1:1000, Immunostar, 22941). The following secondary fluorescently conjugated antibodies were used at 1:500 dilution: Goat anti-mouse Cy3 (Jackson Immuno Research, 115-165-

003), goat-anti-rabbit-DyLight 488 (Thermo Fisher, 35552), donkey anti-mouse-AF488 (Mol Probes, Thermo Fisher, A21202), donkey anti-rabbit Cy3 (Jackson Immuno Research, 711-165-152).

Quantitative Real-Time PCR

Total RNA was extracted with an RNeasy Mini kit (Qiagen) and quantitative RT–PCR reaction was performed using the maxima SYBR Green/ROX master mix (Thermo Scientidic). CDNA was reverse transcribed from 1 µg of RNA using M-MLV Reverse Transcriptase (Thermo-Scientific). Primers were acquired from Biolegio and reactions were run on a Roche Lightcycler® 480 and analyzed with accessory software (v1.5). Expression levels were normalized to endogenous *HMBS* levels, and fold-change in gene expression was calculated using the $2^{\Delta\Delta CT}$ method.

The following primers were used. *FOXA2* (NM-153675, forward; GGAGCAGCTACTATGCAGAG, reverse; CTCATGTACGTGTTCATGCC), *GIRK2* (NM_002240, forward; GCCAGGAAAAGCACAAAGAA, reverse; CTTTCGACGTCCTGATCCAT), *HMBS* (NM-001024382.1, forward; TGCCAGAGAAGAGTGTGGT, reverse; CCGAATACTCCTGAACTCC), *LDHA* (NM_005566, forward; GGCCTGTGCCATCAGTATCT, reverse; GGAGATCCATCATCTCTCCC), *LMX1A* (NM-177398, forward; GACTACGAGAAGCTGTTTGCT, reverse; GCAGCTCAGGTGGTATACAC), *MCT2* (NM_004731, forward; CAACACCATTCCAAGACAGC, reverse; TGGCTGTTATGTACGCAGGA), *NURR1* (NM-006168, forward; ATTAGCATACAGGTCCAACCC, reverse; ACAATGGAATCAATCCATTCCC), *SNCA* (NM-000345, forward; AAGAGGGTGTTCTCTATGTAGGC, reverse; GCTCCTCCAACATTTGTCACTT), *SOX2* (NM-003106, forward; CACAACTCGGAGATCAGCAA, reverse; CGGGGCCGGTATTTATAATC), *TH* (NM-199292, forward; GAGATCGCCTTCCAGTACAG, reverse; TGGTGTAGACCTCCTTCCAG), *TUJ1* (NM_00107.4, forward; GGCCTCTTCTCACAAGTACG, reverse; GAAGAGATGTCCAAAGGCCC).

Statistical analysis

All statistical tests were performed using Sigmaplot 13.0. Statistical significance was determined with the nonparametric Mann–Whitney *U* test. A p value < 0.05 was considered significant. Data are presented as minimum to maximum whisker box plots or dot plots.

Results

GDLS is compatible with neuronal differentiation protocols and results in highly pure neuronal cultures

To explore the validity of the hypothesis that lactate can selectively sustain neurons in vitro, we applied GDLS to a dual SMAD inhibition based protocol (22) combined with a protocol inducing dopaminergic patterning *(21)*. While GDLS works on all dual SMAD inhibition based protocols, we have chosen to implement our procedure on the dopaminergic differentiation protocol, since this enables us to determine the relative sensitivity of a neuronal subtype (i.e. DA neurons) to GDLS.

In dual SMAD inhibition based DA differentiation, cells are first differentiated to neural floor plate precursor cells, followed by more terminal neuronal induction towards a dopaminergic ventral midbrain phenotype (Fig 1A). The maturation of functional neurons capable of generating action potentials can take up to 60 DIV, and markers for mature dopaminergic cells such as GIRK2 appear between 60 and 90 DIV.

To implement GDLS, we first passaged differentiated cell cultures after 18 DIV. Subsequently, between 26 DIV and 36 DIV, cells were fully deprived of glucose and simultaneously supplied with lactate (5mM) for 4-6 days. Medium was changed back to glucose-containing (25mM) medium based on visual inspection of the absence of contaminating cells in the culture. Finally, cells were allowed to recover for a minimum of six days in glucose containing medium before passaging or subsequent analysis.

Gross morphological analysis indicates that GDLS treatment of differentiated hiPSC cultures results in more uniform cell cultures, where the majority of cells have a neuronal morphology with small soma and large processes (Fig 1B). The advantageous effect of GDLS on the purity of the culture is independent of disease background, as both control and familial PD patient iPSC lines showed a similar response to GDLS. Images represent randomly selected excerpts from large tile scan stitches (>2.5 cm^2 surface) taken at 45 DIV. PD patient lines used carry mutations in the *SNCA* gene leading to familial PD. PD4 contains a triplication of the *SNCA* genomic region and PD1 contains the *SNCA* gene G209A mutation causing an A53T mutation in the α-synuclein protein.

Figure 1C illustrates immunofluorescent analysis of βIII tubulin (TUJ1, green), tyrosine hydroxylase (TH, red) and nuclei (Hoechst, blue) of GDLS-treated and non-treated cultures of the PD4 iPSC line at 60DIV (bars 50 μm). In comparison to previous protocols (3, 10, 11, 23, 24), GDLS almost annihilates the presence of non-neuronal cell types and drastically increases the relative proportion of neurons (34.2% of TUJ1 positive cells in control against 93.3% in GDLS-treated, Fig 1C, D). Consequently, the fraction of dopaminergic neurons within the total cell population is increased (8.3% vs. 27.3% TH positive cells). However, within the population of neuronal cells, the relative contribution of dopaminergic neurons is maintained (22.4% vs. 29.4%, Fig 1D), indicating that the subpopulation of dopaminergic neurons is not more or less sensitive to GDLS than the other neuronal cell types present. iPSCs were routinely characterized via standardized procedures (S1 Fig). To show GDLS can be widely implemented and is functional in the generation of different neuronal lineages, we applied the same approach to motor neurons differentiated from hiPS cells. This is illustrated in figure S2, where we show motor neurons can be successfully purified, and are electrically active using Ca^{2+} imaging.

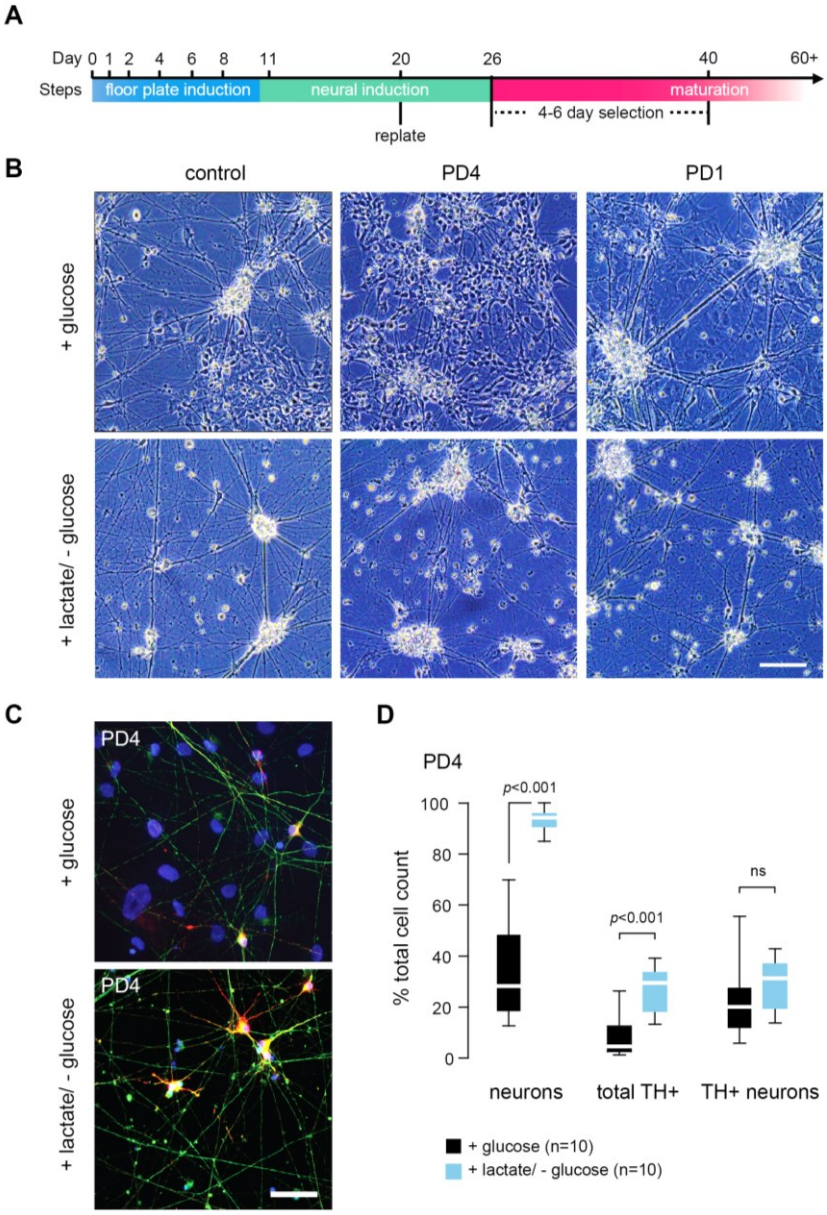

Figure 1. Glucose deprivation and lactate supplementation (GDLS) can be combined with dual SMAD inhibition. (A) *Schematic representation of the applied protocol for the differentiation and GDLS-treatment of hiPSCs.* ***(B)*** *Randomly selected phase contrast images of whole-well tile scan image of two*

PD patient lines and a control line. Selection was initiated at 30 DIV, and images were taken at 45 DIV (bars 100 µm). ***(C)*** *Fluorescent microscopy images for TUJ1 (green), TH (red) and Hoechst (blue) at 60DIV (bars 50 µm).* ***(D)*** *Quantifications of GDLS-treated (n=10) and control (n=10) cultures. Box plots (min to max) represent the percentage of neurons, percentage of TH-positive cells and percentage of TH-positive neurons.*

Purified neuronal cultures are electrophysiologically active

To assess the functional maturity of the neuronal cells obtained following GDLS, their electrical activity was measured at 60 DIV. Six days after GDLS treatment cells were replated on Geltrex® coated Labtek II chamber slides or coverslips. In addition, they were grown in BrainPhys™ medium plus growth factors for two weeks to electrically mature neuronal cells. Whole cell patch clamp recordings were performed on neurons derived from both control and PD1 patient iPS lines. Successful neuronal differentiation in patched samples was confirmed by subsequent staining for neuronal (TUJ1, red) and dopaminergic (TH, green) cells (Fig 2A).

A typical patch clamp recording experiment (current clamp mode) is depicted in Figure 2B, showing repetitive action potentials of both control (black) and PD1 patient-derived (blue) neurons. No differences were observed between GDLS-treated and -untreated neurons. Moreover, of 30 analyzed cells in three separate experiments in two iPS cell lines, all recorded cells were electrically active. Evoking repetitive action potentials with a 500 ms depolarizing current pulse resulted in an average of 5 spikes, with the amplitudes of the first spikes in a series averaging greater than 70 mV (Fig 2C). No differences in amplitudes of voltage-activated currents were observed between control (black) and PD1 patient (blue) iPSC neurons when recorded in voltage clamp mode (Fig 2D).

Calcium imaging experiments demonstrated that GDLS neurons display spontaneous firing activity, and are able to fire in synchrony (Fig 2E-G). Images containing multiple cells were analyzed over time as a

whole image, and individual cells were analyzed separately using a region of interest (ROI1/2, Fig 2E).

Neurons have the tendency to fire in synchrony, as evidenced by the same activity patterns in ROI1 and ROI2 (Fig 2G), and the overall trend observed in whole image analysis (Fig 2F). This indicates the formation of neuronal networks that are performing synchronous bursting, a hallmark of early neuronal plasticity (25, 26). Network activity patterns were observed in all recorded cultures, and showed synchronous bursting at rates of 2-3 field activations per minute, indicating neurons are able to electrically mature following GDLS treatment.

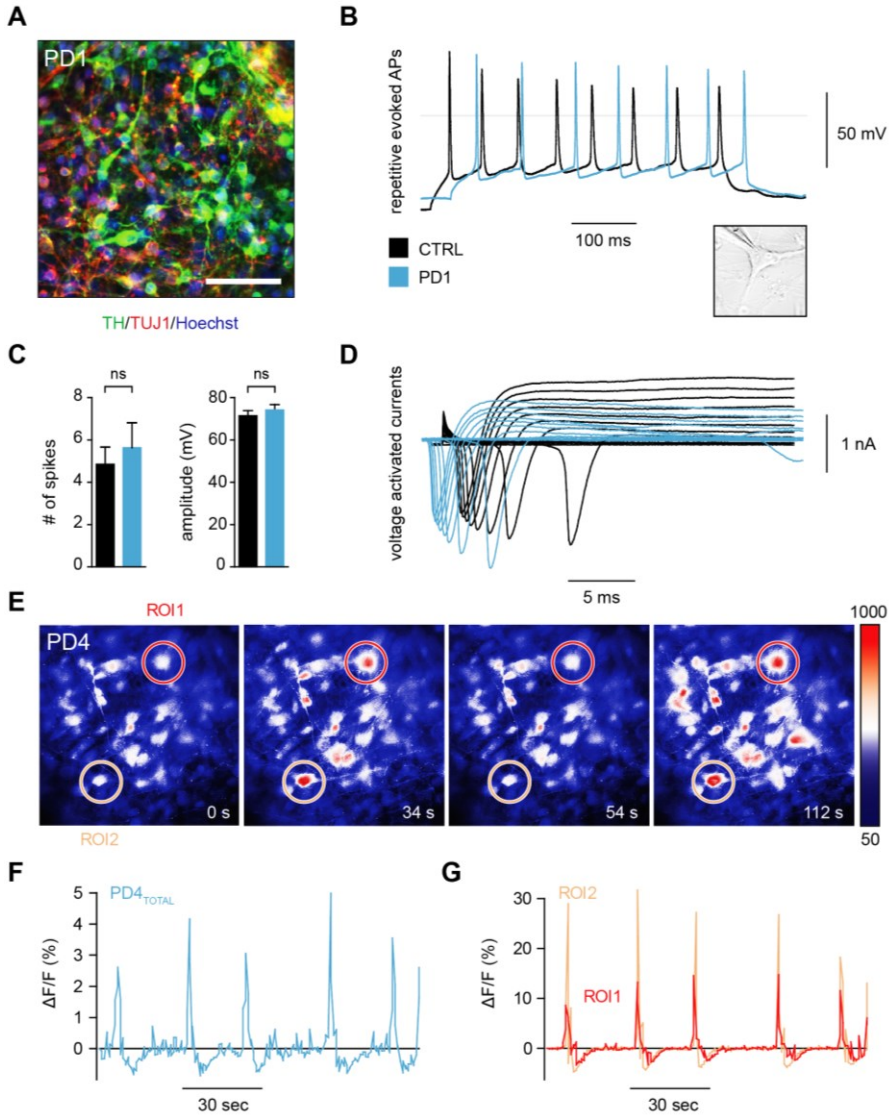

Figure 2. Neurons from patients and controls generate action potentials and perform synchronous bursting. ***(A)*** *Staining of patched samples at 60DIV using TH (green), TUJ1 (red) and Hoechst (blue) (bars 50 µm).* ***(B)*** *A representative repetitive evoked action potential recording of GDLS neurons.* ***(C)*** *Average spike amplitude was greater than 70 mV and neurons generated 5 action potentials on average. No differences were observed between neurons derived from patients and controls.* ***(D)*** *Representative voltage clamp recordings of GDLS*

*neurons in response to depolarizing voltage steps. In images **(B)**, **(C)** and **(D)** black represents a control line while blue represents a PD1 patient line. **(E)** Calcium imaging sequence of GDLS neurons showing spontaneous activity. **(F)** Calcium imaging analysis ($\Delta F/F_0$) of whole image and interspaced **(G)** neurons (ROI1/ROI2) demonstrates synchronous firing.*

GDLS-treated cultures have a greatly reduced astrocytic footprint and are enriched for the expression of neuronal marker genes

Since astrocytes are common contaminants in neuronal cultures derived from pluripotent stem cells we analyzed the occurrence of these cells in GDLS treated cultures. Immunocytochemical analysis of glial fibrillary acidic protein (GFAP) positive cells shows that GDLS treatment results in cultures that are almost completely devoid of astrocyte contamination (Fig 3A). Furthermore, the extent of the dopaminergic neuronal marker TH was not significantly altered upon GDLS treatment. Nuclear staining by Hoechst indicated a pronounced reduction in the total number of nuclei, suggesting that GDLS-treated cells have entered a post-mitotic phase and/or many non-neuronal cells have gone in apoptosis.

Total fluorescence was assessed in large tile scan stitches (n=5 per group) with a surface over 2.5 cm^2 (Fig 3C). An example of a complete tile scan stitch is presented in Figure 3B, showing both the size of the analyzed images and the homogenous cellular distribution, assuring that an imaging bias in the quantification is unlikely to occur.

GDLS results in a significant reduction in GFAP fluorescence, combined with a significant reduction in Hoechst fluorescence at all conditions (Fig 3C). TH content was not significantly altered between control and GDLS-treated conditions. An example of total fluorescence analysis is depicted in Figure S3.

In order to confirm the relative increase in neuronal cells in GDLS cultures, we determined mRNA expression levels of neuronal markers (Fig 3D). We observed enrichment for the general neuronal marker *TUJ1*. Expression of ventral midbrain dopaminergic markers *GIRK2*, *PITX3*, *OTX2* and *TH* also showed a robust enrichment when compared to untreated control

cells. Expression of the neuronal precursor and pluripotency marker *SOX2* shows reduced expression, indicating the loss of precursor cells and undifferentiated cells. In addition, the relative expression of the lactate transporter *MCT2* and lactate converting enzyme *LDHA* was increased. Summarizing, our data show the specific enrichment for neuronal populations after GDLS treatment, without having a deleterious effect on specific neuronal subtypes.

Inhibition of the MCT2 lactate transporter blocks selection

The brain lactate shuttle is thought to function through the MCT2 transporter protein (16). To confirm involvement of MCT2 and reveal the underlying mechanism of neuronal selection in our culture system, we used the MCT2 inhibitor alpha-cyano-4-hydroxycinnamic acid (4-CIN). Figure 4A shows a schematic overview of the experiment, wherein 100 µM of 4-CIN blocks the function of MCT2, while having a minor effect on the function of MCT1 and 4 (27).

Glucose-deprivation of cultures results in overall cell death, while GDLS-treated cells showed preferential survival of neuronal cells (Fig 4C-D). When 4-CIN was added during the GDLS procedure, cells were unable to take up lactate from the culture medium, leading to cell death at a similar rate as the glucose-deprived condition (Fig 4C-E). 4-CIN had no effect on cells supplemented with glucose, indicating that there was no direct toxic effect of 4-CIN (Fig 4B), while under GDLS conditions purification of neuronal populations was achieved (Fig 4D). Additional images of time courses of these experiments are presented in Figure S4, showing different time points of the experiment.

In summary, these data show that differentiated neuronal cells are capable of using lactate as a source of energy, in contrast to undifferentiated and glial cell types. Furthermore, these results confirm that the supplemented lactate is taken up through the MCT2 pathway.

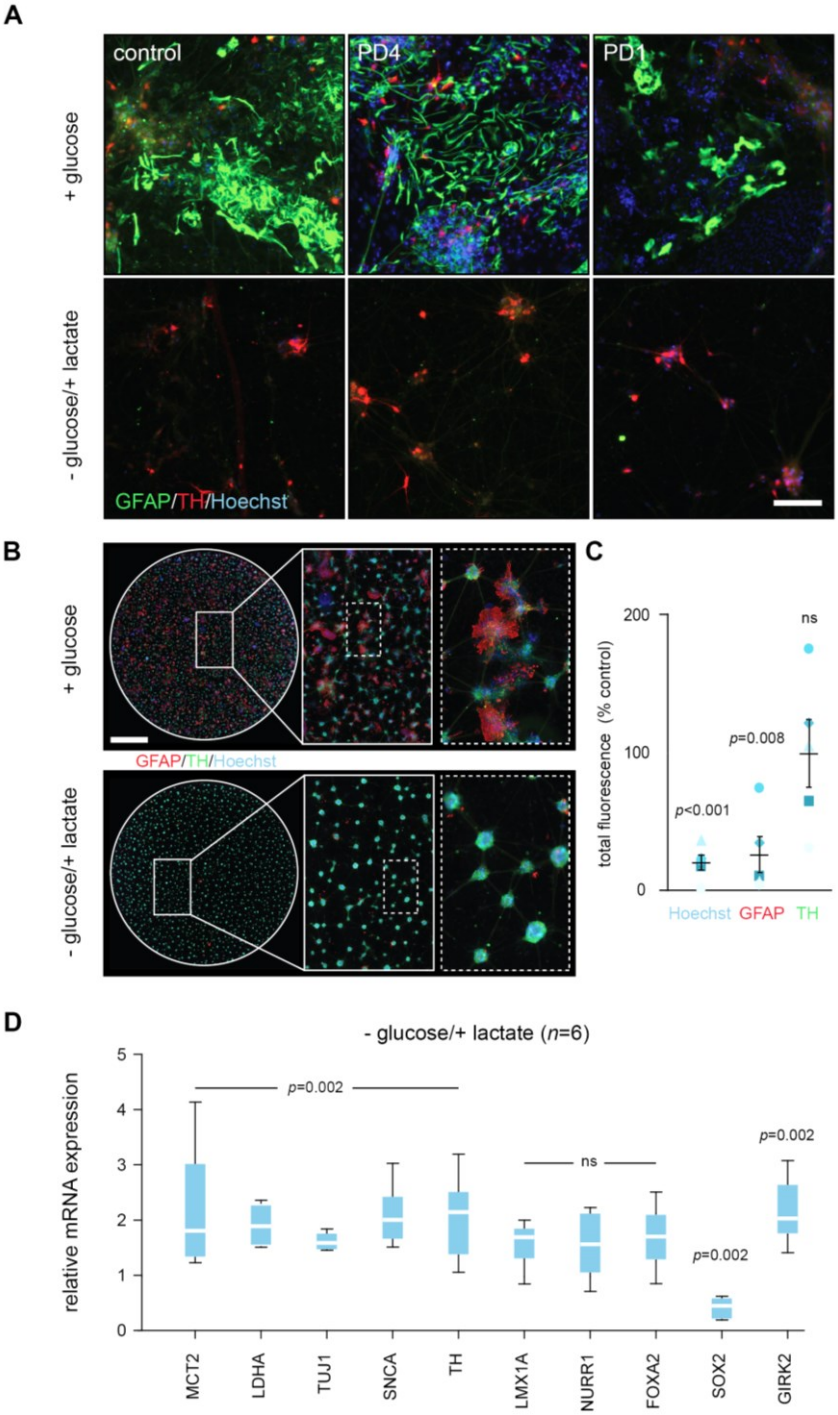
A
control
PD4
PD1
+ glucose
- glucose/+ lactate
GFAP/TH/Hoechst
B
+ glucose
- glucose/+ lactate
GFAP/TH/Hoechst
C
total fluorescence (% control)
200
100
0
ns
p=0.008
p<0.001
Hoechst
GFAP
TH
D
- glucose/+ lactate (n=6)
relative mRNA expression
5
4
3
2
1
0
p=0.002
ns
p=0.002
p=0.002
MCT2
LDHA
TUJ1
SNCA
TH
LMX1A
NURR1
FOXA2
SOX2
GIRK2

Figure 3. GDLS cultures demonstrate enrichment for neuronal markers and reduced expression of non-neuronal markers. (A) *Immunofluorescent images for Hoechst (blue), GFAP (green) and TH (red) of healthy and PD cell lines. Images are random excerpt of large scale tile scan stitches (>2,5 cm²) (bars 50 µm).* ***(B)*** *Large scale fluorescence surface analysis of Hoechst, GFAP, and TH (bars 200µm). Analysis was done using large tile scan images (>2,5 cm²), as depicted in* ***(C)****.* ***(D)*** *Expression analysis of neuronal and dopaminergic markers (TUJ1, SNCA, TH, LMX1A, NURR1 and GIRK2) in GDLS treated cultures, and the pluripotency and neuronal precursor marker SOX2. MCT2 and LDHA expression are upregulated in GDLS-treated cells. Non-treated cultures were used as reference value.*

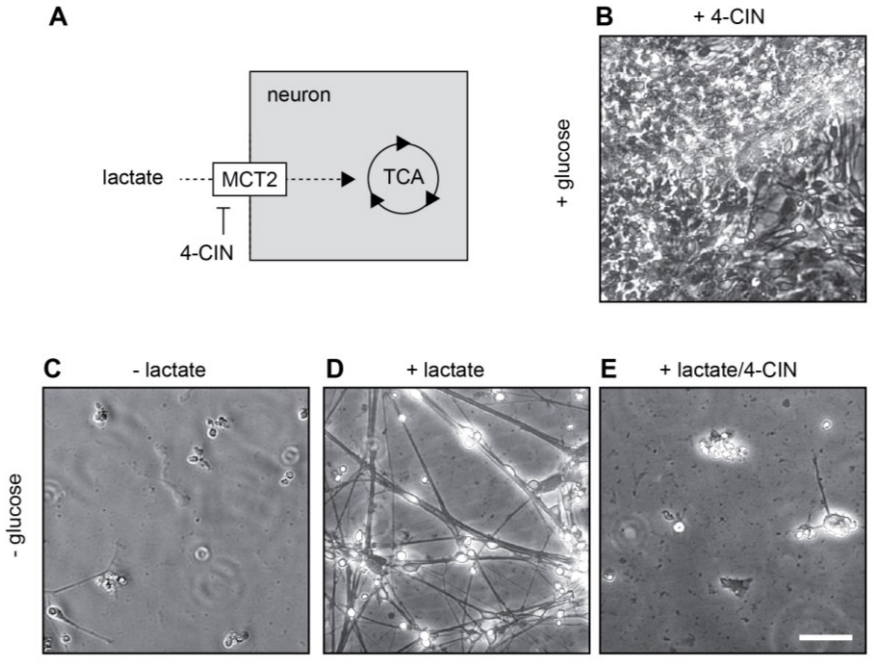

Figure 4. MCT-2 mediates GDLS neuronal selection. (A) *Schematic overview of the mechanism underlying 4-CIN inhibition.* ***(B-E)*** *Representative phase contrast images of control cells treated with glucose and 4-CIN* ***(B)*** *glucose and lactate deprivation* ***(C)*** *GDLS* ***(D)*** *and GDLS in combination with 4-CIN* ***(E)****.(bars 50 µm)*

Discussion and conclusion

The introduction of an effective, non-laborious and inexpensive protocol to purify hiPSC-derived neuronal cultures will provide the opportunity to perform complex experiments on these neurons, and use more pure cultures for disease modelling. Various protocols produce relatively pure neuronal cultures from human ESCs, but application of these protocols on hiPSCs often results in contamination with unwanted cell populations and proliferating cells. This hampers the use of long-term neuronal cultures, since contaminating proliferative cells will eventually overgrow neuronal cells. For this reason, many experiments are performed below 40 DIV (3), while more functional neurons arise around 60 DIV (28). At such early differentiation and maturation stages, late onset disease effects might not be measurable. Furthermore, early determination of differentiation efficiency lead to optimistic estimates of differentiation yields since proliferating cells progressively contaminate the neuronal cultures. While several articles have claimed high differentiation yields, it may prove difficult to replicate these results, due to subtle differences in culturing methods and the intrinsic variance in differentiation potential between iPSC lines (29).

Providing a cost-efficient and robust method to purify neuronal populations will make comparable high neuronal differentiation yields more accessible, and improve the outcome of many iPSC studies. Previously, cardiomyocytes have been purified from human ES cells by metabolic selection (30). Importantly, the selection approach efficiently used for pure cardiomyocytes, led to cell death in fetal mouse neuronal cells. Our results demonstrate that an adapted metabolic selection procedure on hiPSCs results in highly pure and viable neuronal cell cultures. These differences are likely attributable to media composition, since the absence of neurotrophic factors can lead to premature neuronal cell death.

We demonstrate that the GDLS selection procedure utilizes the MCT2 transporter and is based on the widely accepted concept of lactate

shuttling (14, 15, 17, 31). In this light, our data adds further evidence to the importance of lactate metabolism in neuroenergetics. This supports a view of lactate providing a beneficial effect, opposed to the classical view of lactate being associated with an allostatic load in the brain (31).
In summary, we have developed a method that makes the generation of pure neuronal cultures highly accessible. Importantly, GDLS does not negatively affect neuronal characteristics and greatly increases the relative amount of neuronal cells obtained from iPSC differentiation procedures.

Acknowledgements

We would like to thank Prof. Dr. Jon Laman for critical reading of the manuscript and Martijn Hoes from the Department of Experimental Cardiology (UMCG) for providing critical feedback during the experimental procedures.

References

1. Avior Y, Sagi I, Benvenisty N. Pluripotent stem cells in disease modelling and drug discovery. Nature reviews Molecular cell biology. 2016;17(3):170-82.
2. Goldman SA. Stem and Progenitor Cell-Based Therapy of the Central Nervous System: Hopes, Hype, and Wishful Thinking. Cell stem cell. 2016;18(2):174-88.
3. Torrent R, De Angelis Rigotti F, Dell'Era P, Memo M, Raya A, Consiglio A. Using iPS Cells toward the Understanding of Parkinson's Disease. Journal of clinical medicine. 2015;4(4):548-66.
4. Marx V. Stem cells: a dish of neurons. Nature methods. 2016;13(8):617-22.
5. Braak H, Del Tredici K, Rub U, de Vos RA, Jansen Steur EN, Braak E. Staging of brain pathology related to sporadic Parkinson's disease. Neurobiology of aging. 2003;24(2):197-211.
6. Freed CR, Breeze RE, Rosenberg NL, Schneck SA, Wells TH, Barrett JN, et al. Transplantation of human fetal dopamine cells for Parkinson's disease. Results at 1 year. Archives of neurology. 1990;47(5):505-12.

7. Woodard CM, Campos BA, Kuo SH, Nirenberg MJ, Nestor MW, Zimmer M, et al. iPSC-derived dopamine neurons reveal differences between monozygotic twins discordant for Parkinson's disease. Cell reports. 2014;9(4):1173-82.
8. Schondorf DC, Aureli M, McAllister FE, Hindley CJ, Mayer F, Schmid B, et al. iPSC-derived neurons from GBA1-associated Parkinson's disease patients show autophagic defects and impaired calcium homeostasis. Nature communications. 2014;5:4028.
9. Doi D, Samata B, Katsukawa M, Kikuchi T, Morizane A, Ono Y, et al. Isolation of human induced pluripotent stem cell-derived dopaminergic progenitors by cell sorting for successful transplantation. Stem cell reports. 2014;2(3):337-50.
10. Miller JD, Ganat YM, Kishinevsky S, Bowman RL, Liu B, Tu EY, et al. Human iPSC-based modeling of late-onset disease via progerin-induced aging. Cell stem cell. 2013;13(6):691-705.
11. Reinhardt P, Schmid B, Burbulla LF, Schondorf DC, Wagner L, Glatza M, et al. Genetic correction of a LRRK2 mutation in human iPSCs links parkinsonian neurodegeneration to ERK-dependent changes in gene expression. Cell stem cell. 2013;12(3):354-67.
12. Devine MJ, Ryten M, Vodicka P, Thomson AJ, Burdon T, Houlden H, et al. Parkinson's disease induced pluripotent stem cells with triplication of the alpha-synuclein locus. Nature communications. 2011;2:440.
13. Mazzulli JR, Xu YH, Sun Y, Knight AL, McLean PJ, Caldwell GA, et al. Gaucher disease glucocerebrosidase and alpha-synuclein form a bidirectional pathogenic loop in synucleinopathies. Cell. 2011;146(1):37-52.
14. Pellerin L, Magistretti PJ. Glutamate uptake into astrocytes stimulates aerobic glycolysis: a mechanism coupling neuronal activity to glucose utilization. Proceedings of the National Academy of Sciences of the United States of America. 1994;91(22):10625-9.
15. Machler P, Wyss MT, Elsayed M, Stobart J, Gutierrez R, von Faber-Castell A, et al. In Vivo Evidence for a Lactate Gradient from Astrocytes to Neurons. Cell metabolism. 2016;23(1):94-102.
16. Halestrap AP. The monocarboxylate transporter family--Structure and functional characterization. IUBMB life. 2012;64(1):1-9.
17. Hu Y, Wilson GS. A temporary local energy pool coupled to neuronal activity: fluctuations of extracellular lactate levels in rat brain monitored with rapid-response enzyme-based sensor. Journal of neurochemistry. 1997;69(4):1484-90.

18. Lee Y, Morrison BM, Li Y, Lengacher S, Farah MH, Hoffman PN, et al. Oligodendroglia metabolically support axons and contribute to neurodegeneration. Nature. 2012;487(7408):443-8.
19. Goyal MS, Hawrylycz M, Miller JA, Snyder AZ, Raichle ME. Aerobic glycolysis in the human brain is associated with development and neotenous gene expression. Cell metabolism. 2014;19(1):49-57.
20. Moussaieff A, Rouleau M, Kitsberg D, Cohen M, Levy G, Barasch D, et al. Glycolysis-mediated changes in acetyl-CoA and histone acetylation control the early differentiation of embryonic stem cells. Cell metabolism. 2015;21(3):392-402.
21. Kriks S, Shim JW, Piao J, Ganat YM, Wakeman DR, Xie Z, et al. Dopamine neurons derived from human ES cells efficiently engraft in animal models of Parkinson's disease. Nature. 2011;480(7378):547-51.
22. Chambers SM, Fasano CA, Papapetrou EP, Tomishima M, Sadelain M, Studer L. Highly efficient neural conversion of human ES and iPS cells by dual inhibition of SMAD signaling. Nature biotechnology. 2009;27(3):275-80.
23. Byers B, Cord B, Nguyen HN, Schule B, Fenno L, Lee PC, et al. SNCA triplication Parkinson's patient's iPSC-derived DA neurons accumulate alpha-synuclein and are susceptible to oxidative stress. PloS one. 2011;6(11):e26159.
24. Jiang H, Ren Y, Yuen EY, Zhong P, Ghaedi M, Hu Z, et al. Parkin controls dopamine utilization in human midbrain dopaminergic neurons derived from induced pluripotent stem cells. Nature communications. 2012;3:668.
25. Stephens CL, Toda H, Palmer TD, DeMarse TB, Ormerod BK. Adult neural progenitor cells reactivate superbursting in mature neural networks. Experimental neurology. 2012;234(1):20-30.
26. Wagenaar DA, Nadasdy Z, Potter SM. Persistent dynamic attractors in activity patterns of cultured neuronal networks. Physical review E, Statistical, nonlinear, and soft matter physics. 2006;73(5 Pt 1):051907.
27. Erlichman JS, Hewitt A, Damon TL, Hart M, Kurascz J, Li A, et al. Inhibition of monocarboxylate transporter 2 in the retrotrapezoid nucleus in rats: a test of the astrocyte-neuron lactate-shuttle hypothesis. The Journal of neuroscience : the official journal of the Society for Neuroscience. 2008;28(19):4888-96.
28. Pre D, Nestor MW, Sproul AA, Jacob S, Koppensteiner P, Chinchalongporn V, et al. A time course analysis of the electrophysiological properties of neurons differentiated from human induced pluripotent stem cells (iPSCs). PloS one. 2014;9(7):e103418.

29. Hu BY, Weick JP, Yu J, Ma LX, Zhang XQ, Thomson JA, et al. Neural differentiation of human induced pluripotent stem cells follows developmental principles but with variable potency. Proceedings of the National Academy of Sciences of the United States of America. 2010;107(9):4335-40.
30. Tohyama S, Hattori F, Sano M, Hishiki T, Nagahata Y, Matsuura T, et al. Distinct metabolic flow enables large-scale purification of mouse and human pluripotent stem cell-derived cardiomyocytes. Cell stem cell. 2013;12(1):127-37.
31. Mason S. Lactate Shuttles in Neuroenergetics-Homeostasis, Allostasis and Beyond. Frontiers in neuroscience. 2017;11:43.

Supplemental figures

S1 Fig.pdf vZomeren et al, 2017

Figure S1. Characterization of iPSC lines, related to Figure 1
(A) Phase contrast image of feeder free iPSC culture. (B) iPSC culture stained with Live Alkaline Phosphatase staining (Thermo Scientific). (C) Embryoid body formation. (D-F) iPSC immunocytochemistry for various pluripotency markers. (D) Staining for OCT4 (green), SOX2 (red) and Hoechst (blue). (E) Staining for NANOG (green), SSEA4 (red) and Hoechst (blue) (F) Staining for TRA1-81 (red) and Hoechst (blue) (G-I) Embryoid body immunocytochemistry for DESMIN (red) and Hoechst (blue) (G), TUJ1 (green) and Hoechst (blue) (I) and GATA4 (red) and Hoechst (blue) (J). Scalebar is 50μm

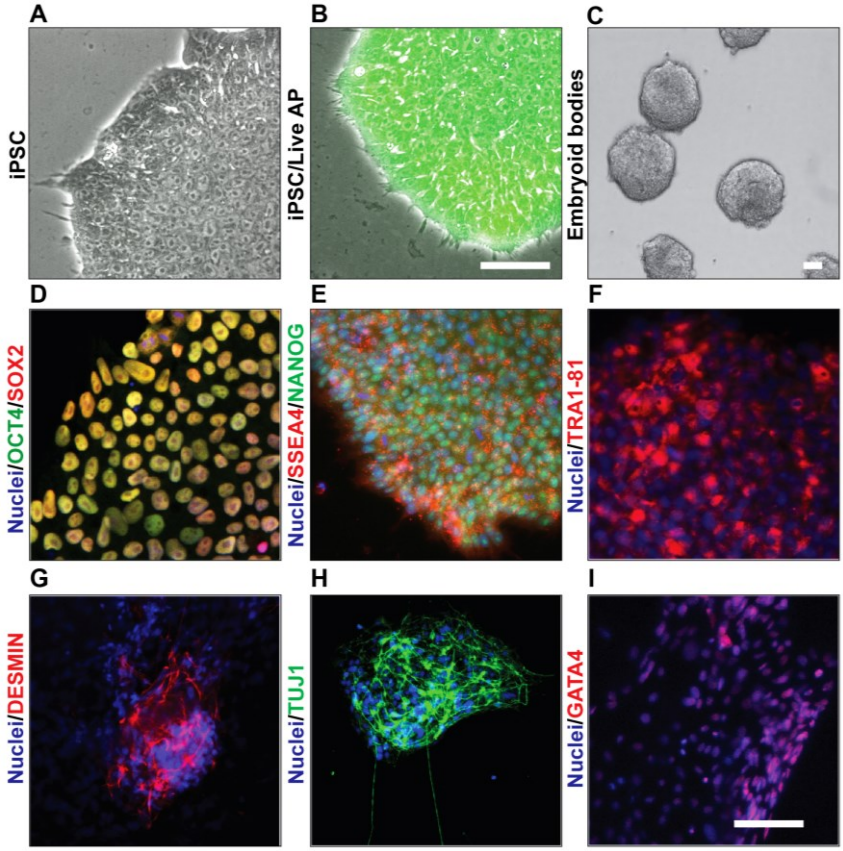

S2 Fig.pdf vZomeren et al, 2017

Figure S2. Motor neuron (MN) differentiation based on dual SMAD inhibition, related to Figure 1. (A) Applied protocol for the differentiation of MN and GDLS-treatment of hiPSCs. (B) Non-treated and GDLS treated MN cultures at 30DIV. (C) Staining of MN at 45DIV using ChAT (green), TUJ1 (red) and Hoechst (blue). (D) MN cultures incubated with 0.5 µM Fluo-AM at 45DIV (E) Calcium imaging analysis (ΔF/F0) of whole image. (F) Corresponding images to time points 20s, 47s, 81s and 82s in calcium imaging analysis. All experiments were performed with a control iPSC line Scalebar represents 100µm in all images.

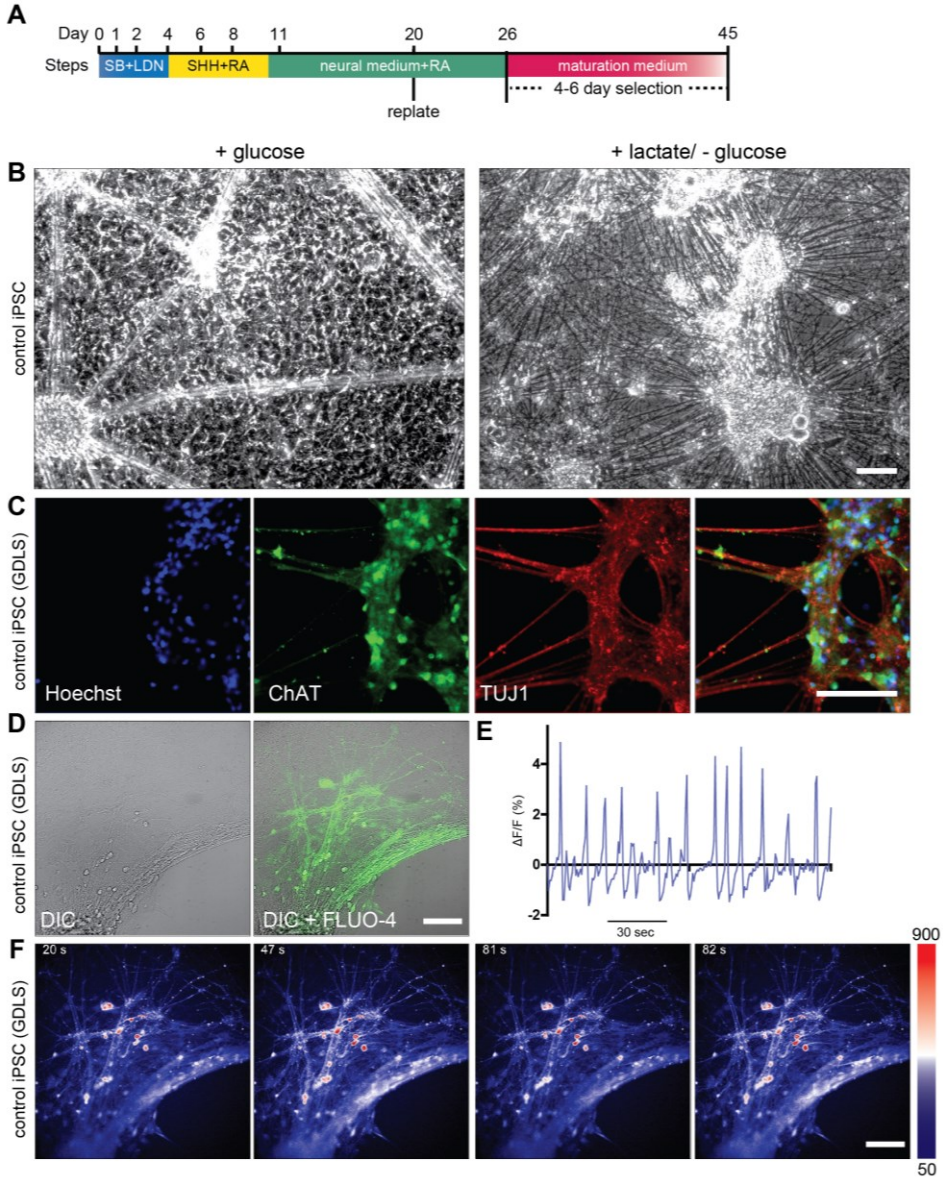

S3 Fig.pdf vZomeren et al, 2017

Figure S3. Analysis of immunofluorescent surface, related to Figure 3
Fluorescent images show an example of the assessment of fluorescence surface analysis for Hoechst (blue), GFAP (red) and TH (green) in both control and GDLS treated condition. Similar thresholding was used, and black and white images used for quantification are shown. Total surface of these analysis image was >6 cm2.

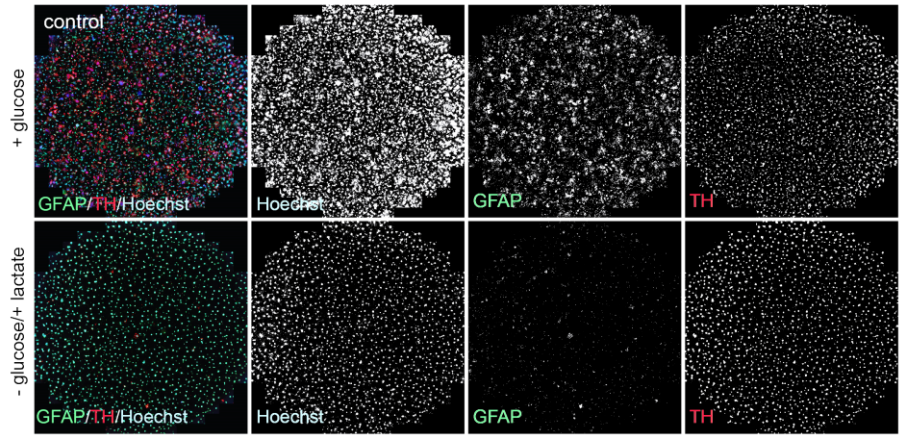

S4 Fig.pdf vZomeren et al, 2017

Figure S4. MCT2 inhibition over different time points, related to Figure 4
In a time dependent series of Figure 4, cells are followed over a period of 4 days, with a glucose (25mM) recovery phase at day 5 and 6. (A) Illustrates glucose (25mM) containing medium supplemented with 100 µM 4-CIN. (B) Shows glucose deprived cells without additional lactate supplementation. (C) GDLS treated cultures show preferential survival of neuronal cells, which is blocked if 4-CIN is added to the medium (D).

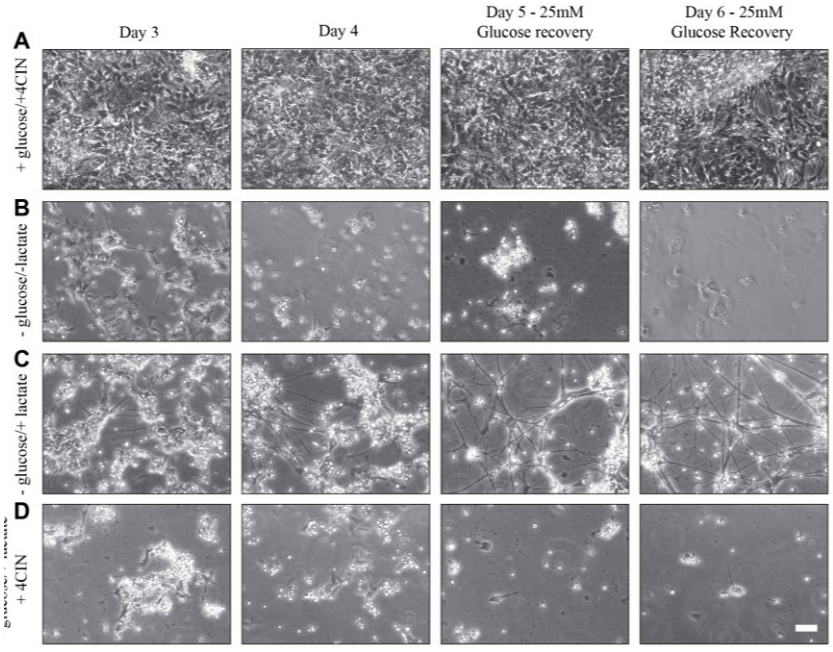

Chapter 4

Mitochondrial trafficking impairment in dopaminergic neurons from Parkinson patient-derived iPS cells

Zomeren, K.C. van[a], Melo, T.Q.[ab]; Ferrari, M.F.R.[b]; Boddeke, H.W.G.M.[a] and Copray, J.C.V.M.[a]

a) Department of Neuroscience, section Medical Physiology, University Medical Center Groningen, Antonius Deusinglaan 1, 9713 AV, Groningen, The Netherlands.

b) Department of Genetics and Evolutionary Biology, Institute for Biosciences, University of Sao Paulo, Sao Paulo, Brazil.

Submitted

Abstract

While it is widely recognized that Parkinson's disease (PD) is accompanied by mitochondrial dysfunction in dopaminergic (DA) neurons, the etiology of the disease remains elusive. Discovery of the implication of α-synuclein as the main constituent of Lewy bodies has driven research in the last decade, but the nature of the relationship between α-synuclein and mitochondrial dysfunction has not yet been elucidated. In this study, we use a patient-derived stem cell model of PD, comparing control cells with patient cells containing a triplication of or a mutation (A53T) in the SNCA gene. Using a long-term (90 days) culture approach, we analysed mitochondrial trafficking in cultured dopaminergic neurons. We demonstrated that mitochondrial trafficking is impaired in PD neurons when compared to control neurons, and mitochondria are frequently fragmented in patient-derived DA neurons. These results indicate that endogenous expression of α-synuclein in PD patient iPS-derived dopaminergic neurons results in mitochondrial pathology. Our results suggest that mitochondrial fragmentation and impaired trafficking are early events that contribute to mitochondrial dysfunction in PD.

Highlights:

- Mitochondrial trafficking is impaired in PD patient dopaminergic neurons
- PD mitochondria demonstrate fragmentation
- Alterations in mitochondrial trafficking might precede PD pathology

Introduction

Parkinson's disease (PD) is the world's most common movement disorder and is characterized by rigidity, slowness of movement and resting tremors. The pathophysiological hallmark of PD is the occurrence of inclusion bodies in the brain named Lewy bodies. These cellular inclusions consist of abnormal protein aggregates and their occurrence is correlated to disease progression. Neuronal degeneration is most striking in the substantia nigra pars compacta in the ventral midbrain and dopaminergic (DA) cell death in this area is thought to contribute to most of the observed symptoms.

While research has been conducted for many years, the etiology of the disease remains poorly understood and treatment of PD merely addresses the symptoms. Experimental studies with substances that have been implied in causing specific dopaminergic degeneration, such as MPTP and pesticides like rotenone have elucidated at least part of the observed cell pathology, thus linking mitochondrial dysfunction to disease progression [1, 2]. The discovery in 1997 of a dominant genetic form of PD [3], linked to the SNCA gene, implicates α-synuclein in cell pathogenesis. As one of the major components in Lewy bodies, it has been shown that monomeric and oligomeric forms of α-synuclein are able to spread in a prion-like manner, leading to spreading of disease pathology [4, 5]. The link between α-synuclein and mitochondrial dysfunction remains poorly understood, and studies ranging from linking α-synuclein to mitochondrial permeability transition pore regulation [6] to ER membrane stress have been performed [7].

Most current understanding of cell pathogenesis in PD has been acquired through cell-models, genetics, animal studies and post mortem patient material. While these studies provided important insights in various cell pathological aspects, these approaches have their limitations. The scientific revolution of induced pluripotent stem cells (iPSCs) has led to the possibility of generating previously unobtainable cell populations

from PD patients [8]. Specifically, the generation of ventral midbrain dopaminergic neurons via iPSCs is bound to yield new understanding of PD and has already produced exciting new leads.

The link between mitochondrial dysfunction and α-synuclein has been further elucidated by assessing the vulnerability of PD iPSC-derived DA neurons to environmental toxins, showing a preferential vulnerability to maneb, paraquat and rotenone [9]. However, without using environmental toxins, hiPSC-derived DA neurons in culture conditions reveal little pathology, and have to be cultured for extended periods of time to observe pathological defects [10].

It is hypothesized that early events in the synuclein cascade might compromise intracellular trafficking, leading to altered mitochondrial dynamics and development of early mitochondrial pathology [11, 12]. While there is evidence that points in this direction, data from iPSC-derived DA neurons, with long axonal processes have not yet been presented.

In this study, we have used dermal fibroblast-derived iPSCs from 2 autosomal dominant familial PD patients and a healthy gender and age-matched control to generate DA neurons. Our PD4 iPSC lines have a triplication of the SNCA locus (Parkinson Disease 4), and our PD1 iPSC lines have a reported mutation in the SNCA gene causing the missense variant A53T α-synuclein (Parkinson Disease 1). We show that (mutated) α-synuclein impairs mitochondrial trafficking in PD patient-derived iPSC-DA neurons cultured for 90 days in comparison to iPSC-DA neurons from healthy controls. Our findings provide evidence for a link between α-synuclein and early mitochondrial pathology in PD.

Materials and methods

Generation of hiPSCs

Human iPSCs were generated using a slightly modified protocol of Okita et al. (2011). Briefly, one million cells were nucleofected using an Amaxa nucleofector 1 using 0.85 µg pCXLE-hMLN, 0.85 µg pCXLE-

hOCT3/4 and 1.3 µg pCXLE-hSK (Addgene #27079, #27076, #27078). Individual clones were picked and expanded, and checked for expression of pluripotency factors on regular basis (OCT3/4, SOX2, TRA1-60, NANOG, live alkaline phosphatase). Embryoid bodies (EBs) were allowed to spontaneously differentiate in order to assess the pluripotent differentiation potential, followed by immunostaining for ectoderm (TUJ1), endoderm (GATA4) and mesoderm (DESMIN) (See supplemental figure S1). Geltrex® coated plates and Essential 8™ medium (Thermo Fisher) were used to maintain cells, while passaging was done using ReLeSR™ (Stemcell Technologies). All cells were maintained in a humidified incubator at 37°C with 5%CO_2 and used for experiments between passage 25 and 35.

Dopaminergic differentiation

Dopaminergic differentiation was achieved using a slightly adapted protocol from Kriks et al. [13]. Briefly, cells were maintained to over 50% confluency after which medium was changed to 50% DMEM/F12 and 50% KSR medium (containing KnockOut™ DMEM and 15% KnockOut™ Serum Replacement, Thermo Fisher). Medium composition was gradually shifted to DMEM/F12 supplemented with N1 (Sigma) over 7 days, while the following small molecules were added; 10 µM SB-431542 (Stemcell Technologies, day 1-5), 100nM LDN-193189 (Stemcell Technologies, day 1-11), 3 µM Purmorphamine (Stemcell Technologies, day 3-7), 500 nM Smoothened agonist (Stemcell Technologies, day 3-7), 100 ng/ml SHH (Peprotech, day 3-8), 50 ng/ml FGF8 (Peprotech, day 3-8) and 2 µM CHIR99021 (Stemcell Technologies, day 5-13). At day 12, the medium was switched to Neurobasal A™ (NBA) medium (supplemented with SM1-Vit.A 50x (Stemcell Technologies), N1 250x (Sigma), BDNF (20 ng/ml, Peprotech), Ascorbic Acid (200 µM, Sigma), GDNF (20 ng/ml, Peprotech), dibutyryl cAMP (0.5 mM, Sigma), DAPT (10 µM, Stemcell Technologies), TGF-β3 (1 ng/ml, Peprotech) (BAGCDT) and 0,1% Pen/Strep (Lonza)) to start

terminal neuronal induction. At day 20 of differentiation, cells were dissociated with Accutase (Sigma) and plated on Geltrex® coated tissue culture treated plates. To purify cultures, cultures were exposed to glucose deprivation and lactate (5mM) supplementation (GDLS) at 26DIV for 6 days (manuscript submitted). The resulting purified cultures were recovered in NBA for 6 days, dissociated with Accutase and passaged to either Geltrex® coated Nunc™ Lab-Tek™ II chamber slides™ or to Geltrex® coated borosilicate glass coverslips. Cells were maintained to 60 DIV, after which medium was changed to supplemented NBA without Pen/Strep until 90 DIV.

Calcium imaging recordings

Nunc™ Lab-Tek™ II chamber slides™ cultured neurons were incubated with 0.5 µM Fluo4-AM (Thermo Fisher, Cat No. F14217) and placed in an imaging chamber at 37°C with 5% CO2 and 95% humidity at 90 DIV. Image sequences were recorded using a Deltavision Elite live cell imaging system (GE Healthcare) equipped with PLAPON 60x oil, NA 1.42, WD 0.15 mm (Olympus) and a 15-bit EDGE/sCMOS camera (PCO) with GFP live filter wheel settings. Image sequences were recorded for 2 min intervals at 0.5 s per frame at 3.2% illumination intensity. Time series analysis was done using ImageJ (1.49s), plotting y-axis profiles for regions of interest (ROIs). Neuronal calcium events were defined as a sharp transient increase in fluorescence intensity (Fluo-4 AM, dF/F >5%, fast rise, slower decay). Images are presented using Green Fire Blue lookup tables.

Immunocytochemistry

Borosilicate glass coverslips containing neuronal cells were fixed in paraformaldehyde 4% for 15 min at room temperature and stored at 4°C. Permeabilization and blocking were done in PBS containing 0.1% Triton, 1% BSA and 5% normal goat serum for ~60 min at RT. Primary antibody incubation was done overnight at 6°C, followed by three PBS

washes (5 min each), after with a fluorescent conjugated secondary antibody and Hoechst 33258 (Sigma, 14530) were added. In the case of using MitoTracker® Orange, live cells were incubated prior to fixation, since the dye fluorescence is retained after fixation. Mowiol® 4-88 (Sigma) was used as mounting medium to attach coverglasses to a coverslip. Samples were stored at 4°C until further analysis.

Confocal images were acquired using a Leica SP8 confocal microscope, equipped with an HC PLAPO CS2 63x oil lens, with NA 1.4. Other epifluorescence images were acquired using a Leica AF-6000 fluorescent microscope, using a PL FLUOTAR 20x/NA 0.4, Dry lens.

Mitochondrial trafficking using MitoTracker® Orange

At 90 DIV, cells were incubated with 50nM MitoTracker® Orange CMTMRos (Invitrogen) for 30 min, after which medium was changed to fresh NBA supplemented medium. Live imaging was performed using a Deltavision Elite live cell imaging system (GE Healthcare) equipped with PLAPON 60x oil, NA 1.42, WD 0.15 mm (Olympus) and a 15-bit EDGE/sCMOS camera (PCO) with mCherry live filter wheel settings, using 1 % illumination intensity. During live imaging, cells were maintained in a humidified imaging chamber at 37°C with 5%CO_2. Data sets were recorded at 2.5 s intervals, with a total of 301 frames per recorded image sequence at 2024x2024 pixels.

Analysis using ImageJ plugin Difference tracker

Supplemental figureS3 A-C illustrates a simplified example of the method we have used for analysing mitochondrial trafficking images. The ImageJ plugin DifferenceTracker can compare time series images to their previous frames to determine if pixels have shifted. Using a frame offset value determines if pixels have moved over a number of frames.

Comparing figure S3C to figure S3B, the plugin is unable to detect changes in the red boxed pixel, since it still records a positive pixel value in this frame. However, when looking at figure S3A a difference is

observed, and the pixel can be classified as moving. In our approach, we have used a frame offset of four. Apart from frame offset, we used a difference in pixel intensity of at least 20 to be observed in an 8-bit image (256 grey values) to classify the pixel as moving. This is correlated to total number of pixels present, as this corrects between cell densities between groups. This leads to the reported % of pixels moving (i.e. % moving mitochondria), and % of moving intensities (i.e. %moving mitochondria corrected for fluorescent signal). Overlay images were generated using ImageJ software, with pseudocolor red for DifferenceTracker generated images.

Statistical analysis

All statistical tests were performed using Sigmaplot 13.0. Statistical significance was determined using one-way ANOVA followed by Tukey or Bonferroni post hoc test. A p-value < 0.05 was considered significant. Data are presented as the minimum to maximum whisker box plots or dot plots.

Results

PD patient iPSCs DA differentiation

iPSCs were generated from three fibroblast samples (one age-matched control and two PD patients) and characterized using standardized procedures. Supplemental figure S1 shows the characterization of iPSCs during different stages of generation.

We successfully differentiated all iPS lines into neurons with tyrosine hydroxylase (TH) expression in 10-20% of cells at 60 days in vitro (DIV) (figure1A). TH-positive differentiated cells show robust expression of α-synuclein compared to non-neuronal cells, which can be recognized by a larger nucleus (figure 1B), but no differences were observed between lines. To remove non-neuronal cells from culture, we applied a metabolic selection procedure developed by our lab (figure 1C). We found similar efficiencies in dopaminergic differentiation in all the different cell lines after

metabolic selection (figure 1D-F). Calcium imaging revealed the generation of spontaneous action potentials in PD1 derived neuronal cells at 90 DIV indicating that these neurons were viable and active at the time of mitochondrial trafficking analysis (see supplemental figure S2 and movie S2).

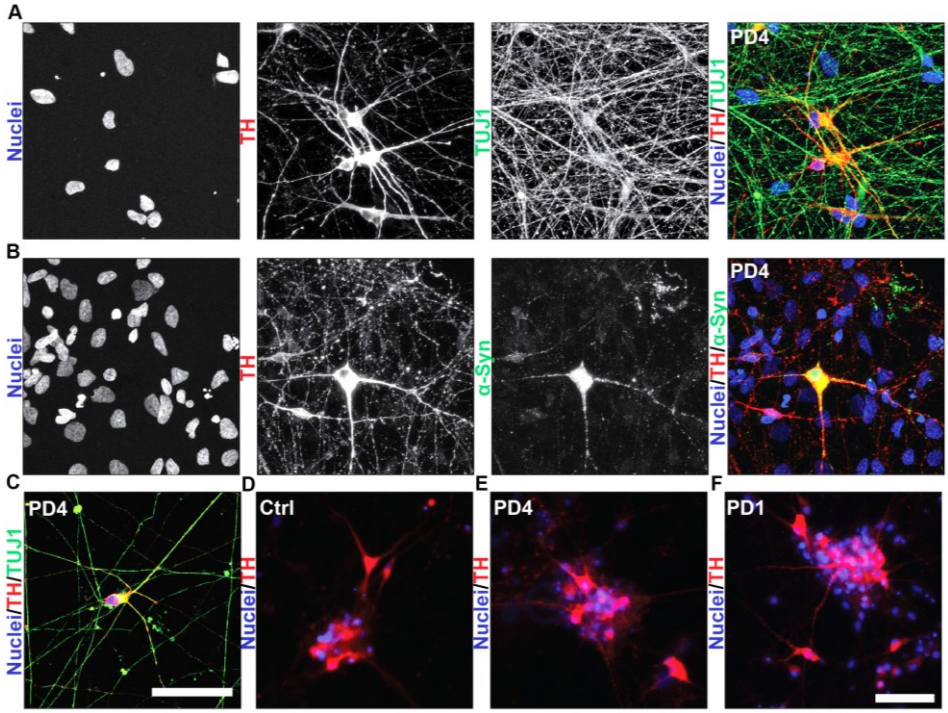

Figure 1. Patient hiPSCs can be differentiated into DA neurons (A) *Differentiation of hiPSCs to neuronal cells at 60 DIV. Immunofluorescence imaging for TUJ1 (green), TH (red) and Hoechst (blue).* ***(B)*** *Neuronal cells display expression of α-synuclein (green), TH (red) and Hoechst (blue).* ***(C)*** *DA cultures can be purified to enrich for neuronal cells, staining for TUJ1 (green), TH (red) and Hoechst (blue) at 60 DIV.* ***(D)*** *Phase contrast image overlay with MitoTracker® Orange labeled neurons used in mitochondrial trafficking experiments at 90 DIV.* ***(E-G)*** *Comparison of purified cultures of Ctrl* ***(E)****, PD4* ***(F)*** *and PD1* ***(G)*** *at 60DIV. Cells are labeled for TH (red) and Hoechst (blue). All bars represent 50 µm.*

MitoTracker® Orange can be used as a specific marker for mitochondria in iPSC derived DA neurons

To validate the specificity of MitoTracker® Orange as a selective live dye for mitochondria in iPSC-derived dopaminergic neurons, a triple staining was performed using TOM20, an outer membrane protein of mitochondria, TH and Hoechst33342. Fluorescence co-localization analysis was done using the ImageJ plugin Coloc2. The resulting Pearson's R^2 value of 0.89 points to a strong co-localization of TOM20 with MitoTracker® Orange in whole image analysis, indicating that most mitochondria are stained with the live dye in dopaminergic neurons (figure 2A). Zooming in on axonal structures (figure 2B) reveals a higher correlation with a Pearson's R^2 value of 0.91, further validating proper use of this live dye. On average, bleaching during 5 minutes of live imaging when using this dye was to less than 10% and was not significantly different between groups (see supplemental figure S3H).

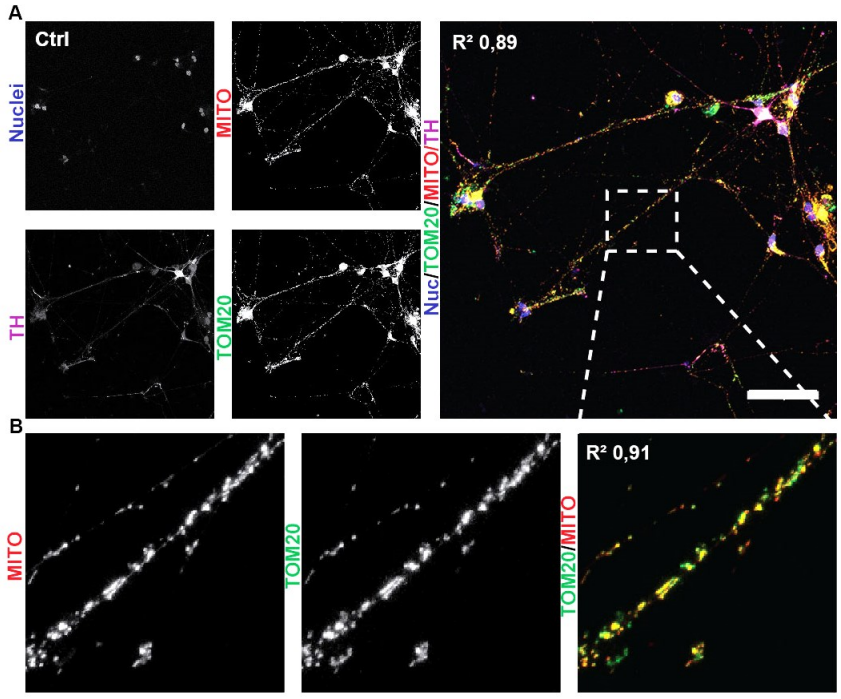

Figure 2. MitoTracker® Orange co-localizes with TOM20 (A) *Staining of MitoTracker® Orange labeled cells at 60DIV labeled with TH (magenta), MitoTracker® Orange (red), TOM20 (green) and Hoechst (blue) (bars 50 µm). Pearson's correlation R^2 for TOM20 and MitoTracker® Orange in the whole image has a value of 0.89.* ***(B)*** *An axonal excerpt of figure* ***A****, for MitoTracker® Orange (red) and TOMM20 (green) has a Pearson's correlation R^2 value of 0.91.*

Analysis of mitochondrial trafficking in hiPSC-derived neurons

To evaluate the process of mitochondrial trafficking, fission and fusion we used an automated approach to identify trafficking of these organelles by employing the ImageJ plugin DifferenceTracker (see Materials & Methods) [14]. A simplified explanation, based on the authors' instructions is illustrated in supplemental figure S3. All trafficking events were recorded at 90 DIV, without use of neurotoxins, and under identical experimental conditions.

An analysis of an image of the control cell line at a window of 222.5 µm by 222.5 µm is depicted in figure 3B. In this image, moving pixels are pseudocolored in red, while stationary pixels are pseudocolored green. An excerpt of this image in figure 3A shows a more detailed image measuring 70 µm by 70 µm. A time series of 40 seconds of an even more detailed excerpt with dimensions 32.5 µm by 32.5 µm is presented in figure 3C. In this time series, we show a moving mitochondrion in red followed by the arrow over different frames, moving approximately 25 µm before moving out of frame. Calculation of the whole image with difference tracker on this excerpt revealed that 11.6 % of the pixels are moving over a total of 297 imaging frames. A movie is available as Movie S1.

The kymograph, corresponding to the line drawn in the last timeframe in figure 3C, provides an accurate representation of mitochondrial trafficking (figure 3D). However, we have chosen to show DifferenceTracker overlay images since these depict whole image trafficking events. Additional kymographs are presented as supplementary images (see figure S4).

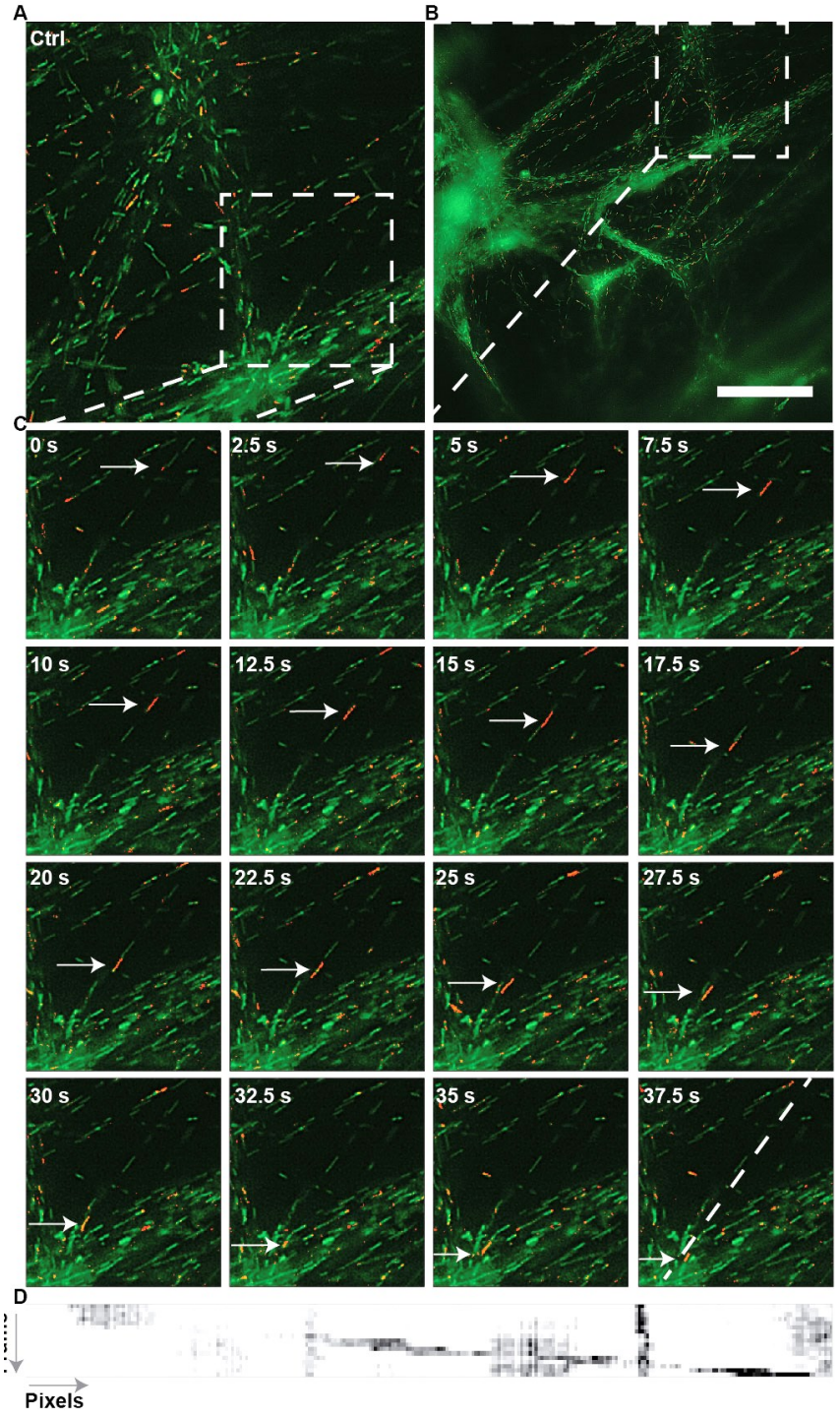
A
Ctrl
B
C
0 s
2.5 s
5 s
7.5 s
10 s
12.5 s
15 s
17.5 s
20 s
22.5 s
25 s
27.5 s
30 s
32.5 s
35 s
37.5 s
D
Pixels

Figure 3. Difference tracker can be used to identify trafficking mitochondria. *(**A**) MitoTracker® Orange labeled culture analyzed using difference tracker. Red pseudo colors moving mitochondria, determined using the ImageJ plugin Difference Tracker, while green shows stationary mitochondria (bars 50 µm). (**B**) Shows an excerpt from (**A**) with enhanced detail, while (**C**) illustrates an even more enhanced excerpt with 16 consecutive frames to show movement of mitochondria. (**D**) Kymograph representation of the line drawn in (**C**), depicts mitochondrial trafficking over 16 frames.*

Mitochondrial trafficking is impaired in PD neurons

Trafficking analysis was assessed using large frame images (as in figure 3) and images were excluded if the image moved out of focus or if cells moved, leading to false positive trafficking events. We determined the percentage of moving pixels in whole image analysis (figure 4A), and the percentage of moving pixel intensity, correlating to the percentage of moving mitochondria (figure 4B-D, see also corresponding kymographs in supplemental figure S4). Both graphs show a significant difference in trafficking of mitochondria in neurons between Ctrl and PD1 patient lines, but not between PD lines. The corresponding p-value for Ctrl and PD4 is 0,024, while p-value for PD1 and Ctrl is 0,002. When correcting for pixel intensity, the p-value between Ctrl and PD4 is 0,017 and the p-value between PD1 and Ctrl is 0,005. Movies are available as Movie S2-4.

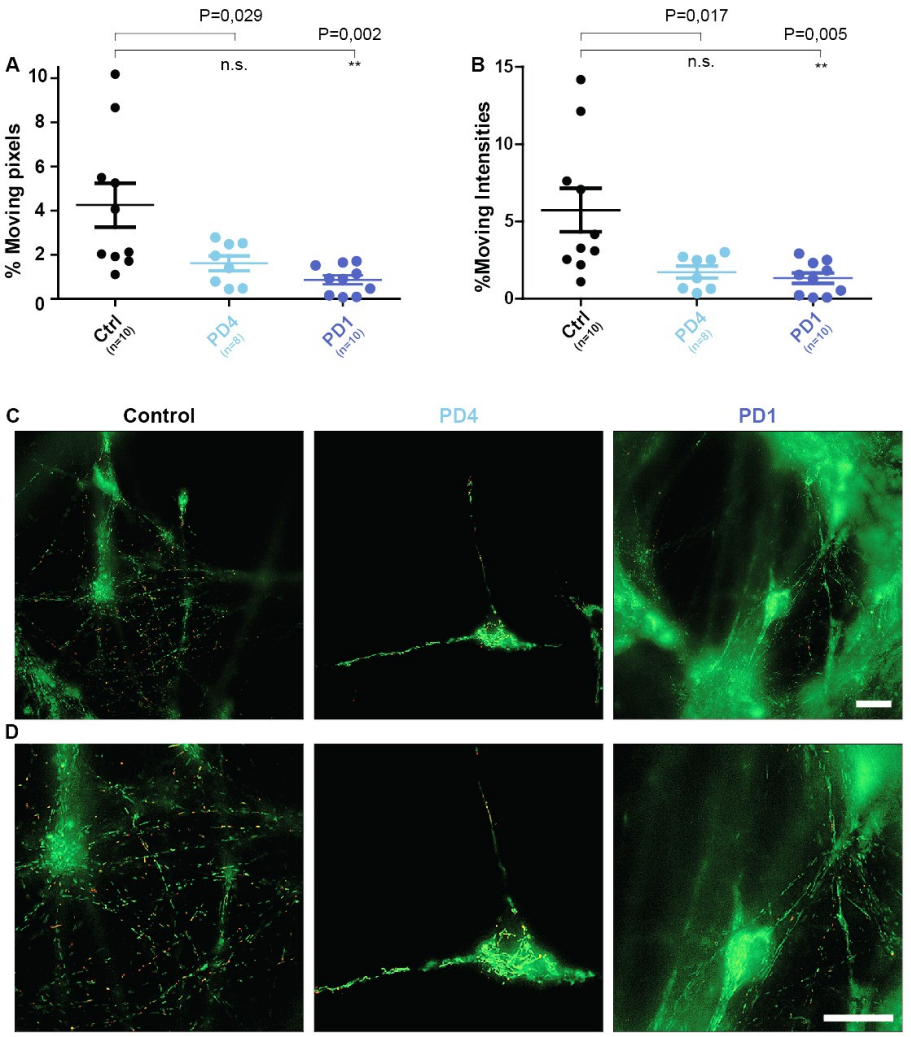

Figure 4. PD lines show mitochondrial trafficking impairment. ***(A)*** *Movement of mitochondria referenced to pixels shows a significant difference between control and PD lines (Ctrl vs. PD4 p=0,049 and Ctrl vs. PD p=0,006), but not between PD lines.* ***(B)*** *Moving intensity percentages are significantly different between control and PD lines (Ctrl vs. PD4 p=0,023 and Ctrl vs. PD p=0,007), but not between PD lines.* ***(C)*** *Example of mitochondrial trafficking analysis of control.* ***(D)*** *Excerpt of* ***(C)*** *shows less trafficking in PD4 and PD1 compared to control. Red indicates moving mitochondria, while green indicates stationary mitochondria. (Scalebar 25µm). Corresponding kymographs are illustrated in supplemental figure S4.*

Whole image analysis was validated by small frame analysis

While whole image analysis has the benefit of unbiased analysis, a downside of using automated trafficking software is the inability to distinguish between mitochondrial movement and (particularly sideways) movement of axons (see Supplemental figure S3D-E). It should be noted that these events take place in both patient and control cells, but we have chosen to further analyse data in smaller excerpts that showed no sideways movement during frame acquisition. To improve the accuracy of analysis, we have chosen to analyse excerpts away from the cell body, thereby focussing on axonal mitochondrial trafficking dynamics. Analysis of 20 smaller frame images, where no sideways movement occurred, again resulted in a significant difference in trafficking between PD and control lines (see supplemental figure S5). Since axonal excerpts with mitochondria are analysed, trafficking speed was higher than those observed in whole image analysis. These results confirm that mitochondrial trafficking in DA neurons of PD iPSC lines is impaired in comparison to mitochondrial trafficking in DA neurons of control iPSC lines. The corresponding p-value for Ctrl and PD4 is 0,001 and the p-value for PD1 and Ctrl is 0,001 in both percentage of pixels and percentage of pixel intensities moving.

PD lines show mitochondrial fragmentation

In neurons, healthy mitochondria are typically elongated and undergo fusion and fission to maintain proper mitochondrial viability and functionality [15]. In our experiments, patient-derived PD DA neurons showed increased fragmentation of mitochondria (figure 5B-C), while control DA neurons (figure 5A) show healthy, elongated mitochondria. The increased presence of fragmented mitochondria hints to lowered mitochondrial integrity.

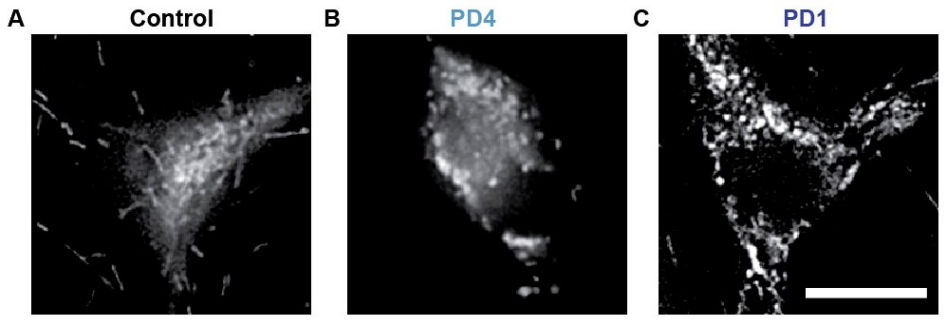

Figure 5. Mitochondrial fragmentation is observed in PD4 and PD1 line, but not in control. (A) *In all imaging conditions, control line mitochondria showed an elongated phenotype, while in the PD4* ***(B)*** *and PD1* ***(C)*** *line mitochondrial fragmentation and round mitochondria were observed (bars 10μm).*

Discussion and Conclusion

In our experiments, we have demonstrated that mitochondrial trafficking is impaired in familial PD neurons generated from iPSCs compared to healthy age-matched control cells. Our data extends to previous data published by our group [16] and supports the hypothesis that intracellular trafficking dynamics impairment precedes the onset of PD [12]. Being able to culture pure neuronal cultures for extended periods of time has given us the opportunity to study mitochondrial trafficking without the use of environmental toxins, when compared to other PD studies [9, 17-19]. Use of environmental toxins has led to a link between α-synuclein and mitochondrial pathology in previous studies, but these approaches mainly highlight the vulnerability of patient DA neurons for these toxins. In contrast, our data gives insight to early pathology and mitochondrial dysfunction as opposed to a rapid onset of the disease phenotype. While mutations in parkin (PARK2) and PTEN-induced kinase 1 (PINK1) have provided a strong link between mitochondrial dysfunction and PD in iPSC studies [20], a link to early mitochondrial dysfunction in SNCA-mutated iPSCs has remained elusive.

Acknowledgements

This study was supported by research grants from Fundacao de Amparo a Pesquisa do Estado de Sao Paulo (FAPESP) (2011/06434-7; 2013/08028-1; 2015/18961- 2), Conselho Nacional de desenvolvimento Cientifico e Tecnologico (CNPq) (471999/2013-0; 401670/2013-9). T.Q.M. received fellowship from CAPES.

References

1. Priyadarshi, A., et al., *A meta-analysis of Parkinson's disease and exposure to pesticides.* Neurotoxicology, 2000. **21**(4): p. 435-40.
2. Jenner, P., *Parkinson's disease, pesticides and mitochondrial dysfunction.* Trends Neurosci, 2001. **24**(5): p. 245-7.
3. Polymeropoulos, M.H., et al., *Mutation in the alpha-synuclein gene identified in families with Parkinson's disease.* Science, 1997. **276**(5321): p. 2045-7.
4. Desplats, P., et al., *Inclusion formation and neuronal cell death through neuron-to-neuron transmission of alpha-synuclein.* Proc Natl Acad Sci U S A, 2009. **106**(31): p. 13010-5.
5. Braak, H., et al., *Stages in the development of Parkinson's disease-related pathology.* Cell Tissue Res, 2004. **318**(1): p. 121-34.
6. Martin, L.J., et al., *Mitochondrial permeability transition pore regulates Parkinson's disease development in mutant alpha-synuclein transgenic mice.* Neurobiol Aging, 2014. **35**(5): p. 1132-52.
7. Smith, W.W., et al., *Endoplasmic reticulum stress and mitochondrial cell death pathways mediate A53T mutant alpha-synuclein-induced toxicity.* Hum Mol Genet, 2005. **14**(24): p. 3801-11.
8. Takahashi, K. and S. Yamanaka, *Induction of pluripotent stem cells from mouse embryonic and adult fibroblast cultures by defined factors.* Cell, 2006. **126**(4): p. 663-76.
9. Ryan, S.D., et al., *Isogenic human iPSC Parkinson's model shows nitrosative stress-induced dysfunction in MEF2-PGC1alpha transcription.* Cell, 2013. **155**(6): p. 1351-64.

10. Sanchez-Danes, A., et al., *Disease-specific phenotypes in dopamine neurons from human iPS-based models of genetic and sporadic Parkinson's disease.* EMBO Mol Med, 2012. **4**(5): p. 380-95.
11. Cheng, H.C., C.M. Ulane, and R.E. Burke, *Clinical progression in Parkinson disease and the neurobiology of axons.* Ann Neurol, 2010. **67**(6): p. 715-25.
12. Hunn, B.H., et al., *Impaired intracellular trafficking defines early Parkinson's disease.* Trends Neurosci, 2015. **38**(3): p. 178-88.
13. Kriks, S., et al., *Dopamine neurons derived from human ES cells efficiently engraft in animal models of Parkinson's disease.* Nature, 2011. **480**(7378): p. 547-51.
14. Andrews, S., J. Gilley, and M.P. Coleman, *Difference Tracker: ImageJ plugins for fully automated analysis of multiple axonal transport parameters.* J Neurosci Methods, 2010. **193**(2): p. 281-7.
15. Knott, A.B., et al., *Mitochondrial fragmentation in neurodegeneration.* Nat Rev Neurosci, 2008. **9**(7): p. 505-18.
16. Melo, T.Q., et al., *Impairment of mitochondria dynamics by human A53T alpha-synuclein and rescue by NAP (davunetide) in a cell model for Parkinson's disease.* Exp Brain Res, 2016.
17. Mazzulli, J.R., et al., *alpha-Synuclein-induced lysosomal dysfunction occurs through disruptions in protein trafficking in human midbrain synucleinopathy models.* Proc Natl Acad Sci U S A, 2016. 113(7): p. 1931-6.
18. Reinhardt, P., et al., *Genetic correction of a LRRK2 mutation in human iPSCs links parkinsonian neurodegeneration to ERK-dependent changes in gene expression.* Cell Stem Cell, 2013. **12**(3): p. 354-67.
19. Zagoura, D., et al., *Evaluation of the rotenone-induced activation of the Nrf2 pathway in a neuronal model derived from human induced pluripotent stem cells.* Neurochem Int, 2016.
20. Chung, S.Y., et al., *Parkin and PINK1 Patient iPSC-Derived Midbrain Dopamine Neurons Exhibit Mitochondrial Dysfunction and alpha-Synuclein Accumulation.* Stem Cell Reports, 2016. **7**(4): p. 664-677.

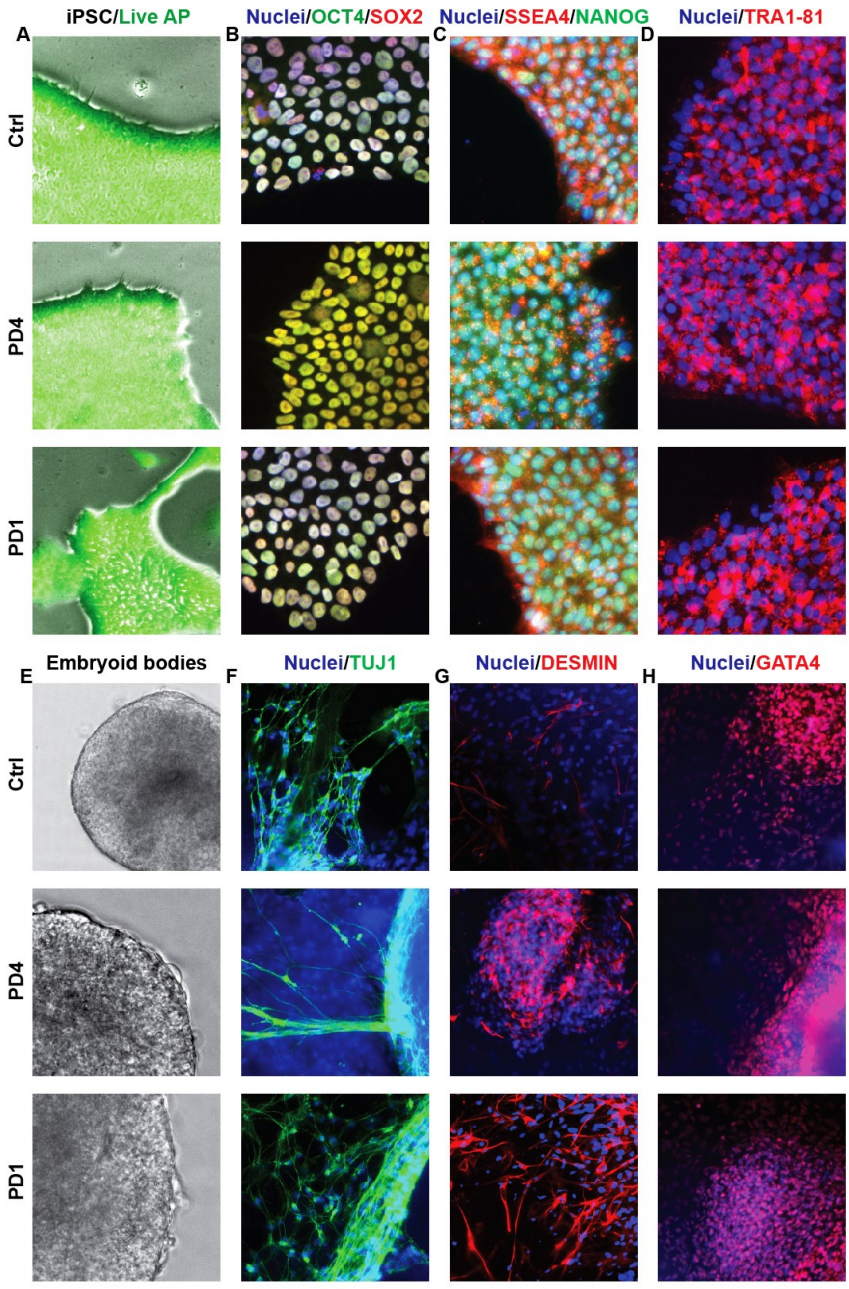

Supplemental figure S1. Characterization of iPSC lines. (A) *iPSC cultures stained with Live Alkaline Phosphatase staining (Thermo Scientific).* ***(B-D*** *iPSC immunocytochemistry for pluripotency markers.* ***(B)*** *Staining for OCT4 (green),*

SOX2 (red) and Hoechst (blue). ***(C)*** *Staining for NANOG (green), SSEA4 (red) and Hoechst (blue)* ***(D)*** *Staining for TRA1-81 (red) and Hoechst (blue)* ***(E)*** *Embryoid body formation in all lines.* ***(F-H)*** *Embryoid body immunocytochemistry for DESMIN (red) and Hoechst (blue)* ***(F)****, TUJ1 (green) and Hoechst (blue)* ***(G)*** *and GATA4 (red) and Hoechst (blue)* ***(H)****.*

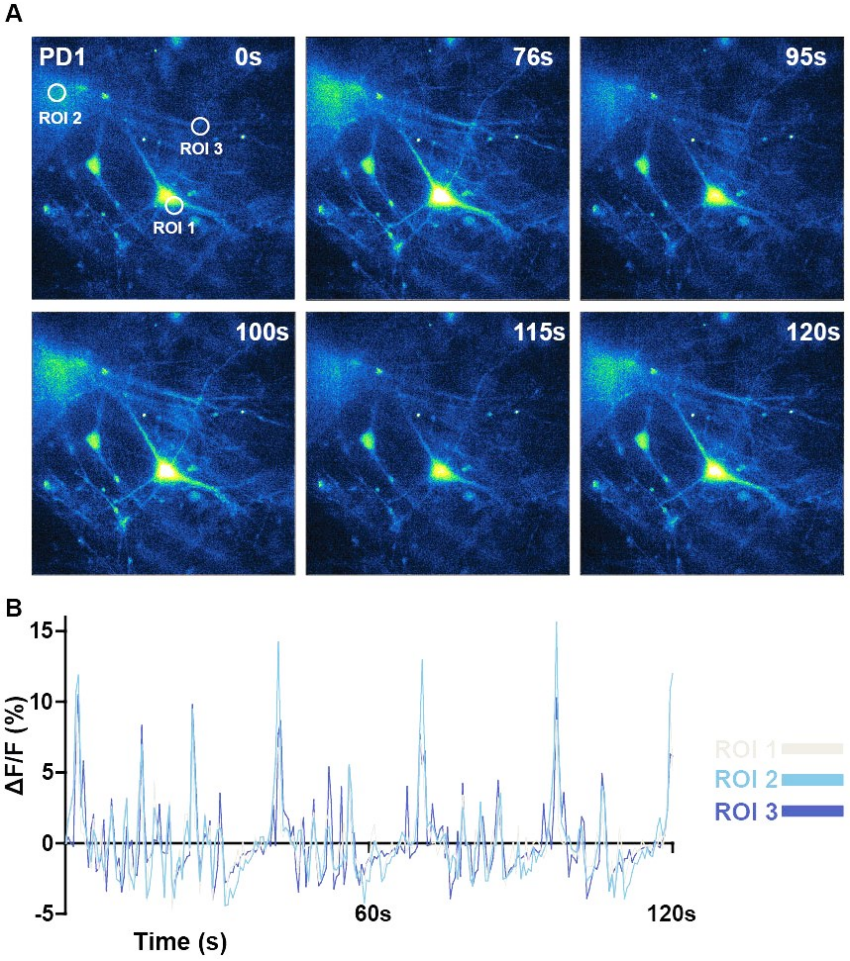

Supplemental figure S2. Calcium imaging of PD1 line at 90 DIV shows spontaneous neuronal activity patterns. ***(A)*** *Shows PD1 derived neuronal cells labeled with Fluo-4 AM over a period of 120 seconds. Spontaneous depolarization events are characterized by increasing presence of the green color.* ***(B)*** *Depicts the change in pixel values corresponding to ROI1, ROI2 and ROI3, showing similar activation patterns of these different locations. Data is represented as* $\Delta F/F_0$.

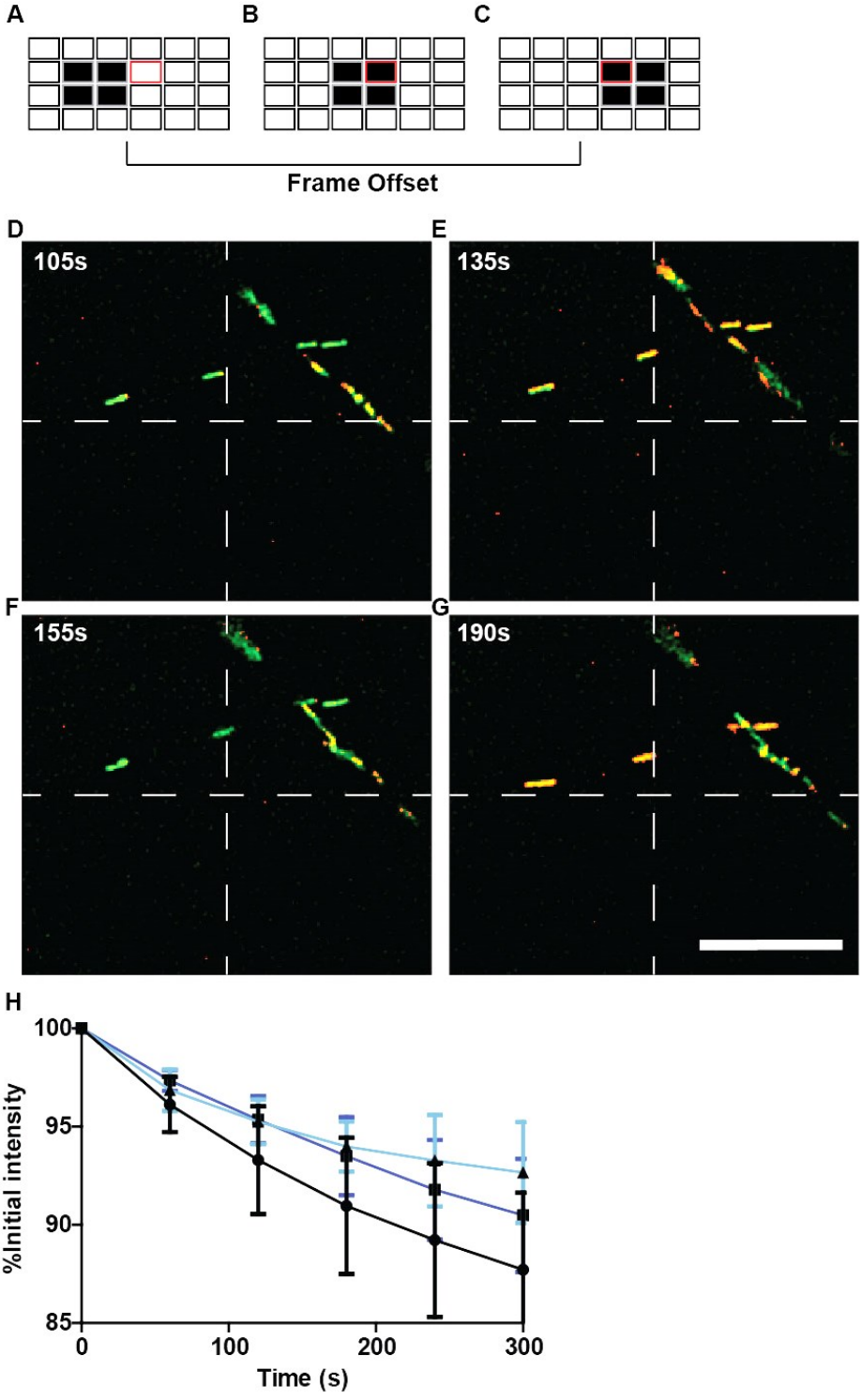
A
B
C
Frame Offset
D
105s
E
135s
F
155s
G
190s
H
100
95
90
85
%Initial intensity
0
100
200
300
Time (s)

Supplemental figure S3. Simplified example of difference tracker software and experimental validations. *From* ***(C)*** *to* ***(B)****, the plugin is unable to observe changes in the red boxed pixel, since it still records a positive pixel value in this frame. However, when looking at* ***(A)*** *a difference is observed, and the pixel can be classified as moving. It should be noted that in the actual 8-bit image, as opposed to this binary example, the pixel can have 256 intensity values, allowing for offset values to classify pixels as moving.* ***(D)*** *An axonal shift results in a positive trafficking event* ***(E),*** *while in reality mitochondria are stationary. The axonal positions in* ***(F)*** *shift down* ***(G)*** *again resulting in false positive events. Since the software is not able to recognize these events, screening of smaller excerpt has to be performed to prevent a false positive bias of results.* ***(E)*** *Fluorescence intensity loss shows bleaching effects observed during imaging. While minor differences between groups were observed, the difference in bleaching was not significant, and in amounted on average 9,8%.*

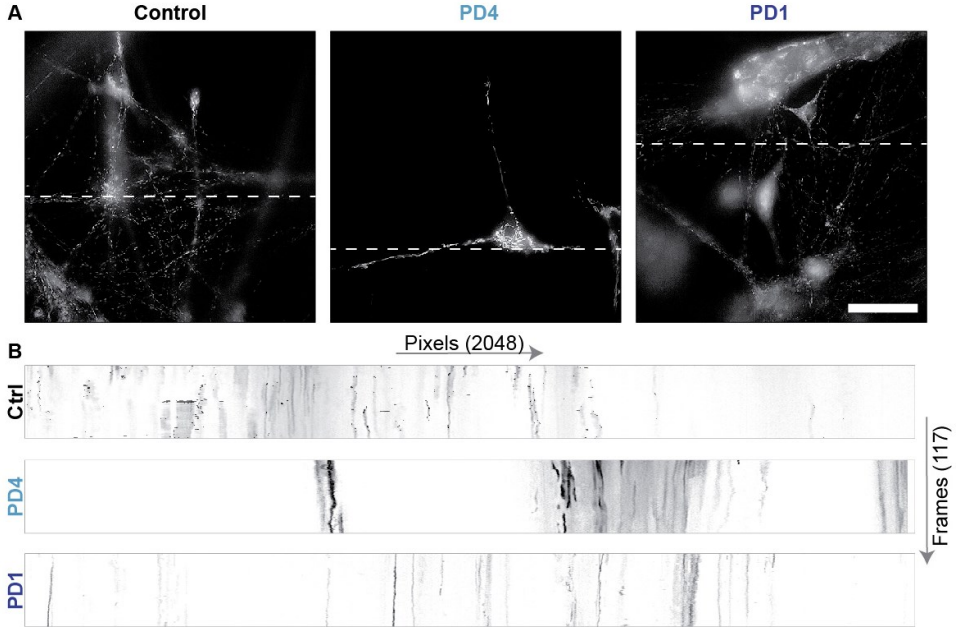

Supplemental figure S4. Kymographs of trafficking experiments. ***(A)*** *Grey scale images containing MitoTracker® Orange labelled neuronal cells from control and PD patient lines.* ***(B)*** *Kymographs corresponding to figure 4, consisting of 117 frames, containing an average of a 5 pixel line indicated in the images depicted in* ***(A)****.*

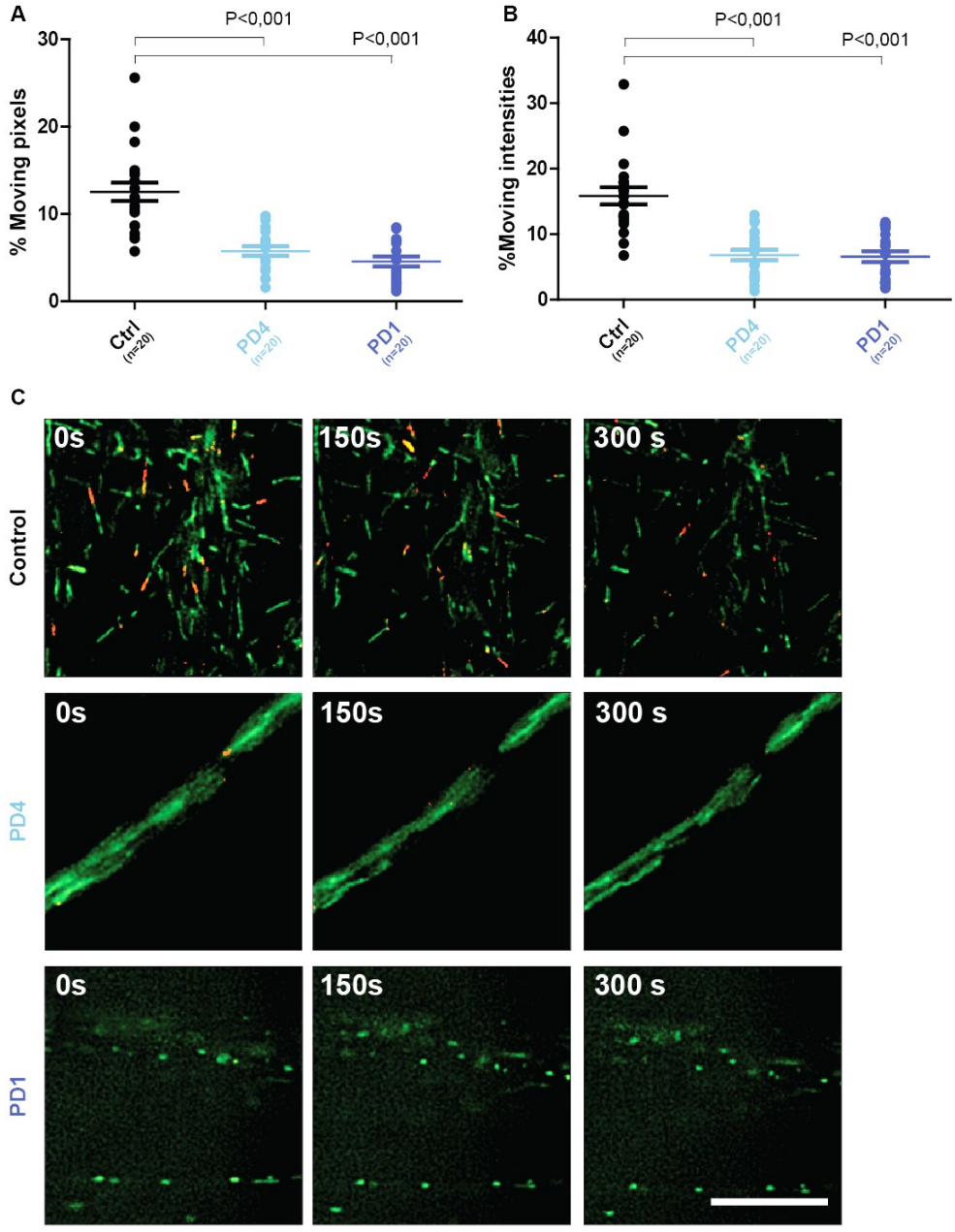

Supplemental figure S5. Trafficking impairment is observed when analyzing more detailed images. (A) *Movement of mitochondria referenced to pixel intensities shows a significant difference between control and PD lines, but not*

between PD lines. ***(B)*** *Absolute moving percentages are significantly different between control and PD lines, but not between PD lines.* ***(C)*** *Example of mitochondrial trafficking analysis of control.* ***(D)*** *Excerpt of* ***(C)*** *shows less trafficking in PD4 and PD1 compared to control. Red indicates moving mitochondria, while green indicates stationary mitochondria. (Scalebar 10µm).*

Chapter 5

Modelling age-associated diseases using transgenic progerin expression

Zomeren, K.C. van[a], Hoes, M.F.[b], Tromp, J.[b], Boddeke, H.W.G.M[a], Meer, P. van der[b], Copray, J.C.V.M.[a]

a) Department of Neuroscience, section Medical Physiology, University Medical Center Groningen, Antonius Deusinglaan 1, 9713 AV, Groningen, The Netherlands
b) Department of Experimental Cardiology, University Medical Center Groningen, Antonius Deusinglaan 1, 9713 AV, Groningen, The Netherlands

Manuscript in preparation

Abstract

Human induced pluripotent stem cells (hiPSC) have transformed research since their discovery. The hiPSC technology enables detailed cellular studies on pathogenic processes in patient-derived somatic cell types that are specifically affected by the disease of the patient. However, due to the fact that these somatic cells are effectively rejuvenated during the iPSC reprogramming process, they have been considered less suitable for pathogenic studies on late-onset diseases, such as Parkinson's disease. We introduce a human in-vitro model to accelerate ageing of the iPSC-derived somatic cells using transgenic expression of progerin. Before application to our PD patient-derived DA neurons, we have chosen to test and implement our progerin-associated ageing model on embryonic stem cell differentiated cardiomyocytes. These cells can be easily differentiated, have a large soma easily accessible for microscopic analysis and display high mitochondrial activity allowing accurate evaluation of aging hallmarks. Differentiated cells that express progerin indeed displayed several hallmarks of ageing, including nuclear folding, chromosomal instability and mitochondrial dysfunction. Crucially, compared to earlier work by other groups, we can sustain progerin expression for up to at least 30 days, without apparent toxicity associated with the method for transgenic expression. Progerin-induced ageing on Parkinson's disease patient hiPSC-derived dopaminergic neurons resulted in neuronal cells with increased amounts of α-synuclein compared to control populations. This chapter presents the stem cell community with new tools to study ageing differentiated cells.

Introduction

Age-associated diseases pose an increasing burden on society and are often related to cellular senescence. Hallmarks of ageing are currently considered to be comprised of genomic instability, telomere attrition, epigenetic alterations, loss of proteostasis, deregulated nutrient

sensing, mitochondrial dysfunction, cellular senescence, stem cell exhaustion, and altered intercellular communication [1]. To properly model these processes in an ageing model for cell culture applications, scientists have come up with a number of ways to recapitulate parts of the ageing process. But, while most models mimic one hallmark of ageing, it remains difficult to tackle the multiple aspects of the ageing process. Cell models for late onset disorders, such as Parkinson's disease (PD), often use mitochondrial toxins [2-4], proteasome inhibitors [5], mimicking only part of the ageing process. Apart from this, cell models often consist of immortalized proliferating cells [6, 7], which are vastly different from somatic cells and make it difficult to model a senescent cell.

The use of human induced pluripotent stem cells (hiPSCs) and human embryonic stem cells (hESCs) has overcome part of this challenge since they can be differentiated into lineage-specific cells with a low mitotic index. However, reprogramming of somatic cells into iPSCs leads to their rejuvenation [8]. Telomere elongation, increased mitochondrial fitness and chromatin remodelling effectively restore iPSCs to an embryonic state that is beneficial for stemness. Thus, the reprogramming event also reverses several hallmarks of ageing making the resulting differentiated cells less suitable for modelling age-related disorders. Direct reprogramming of somatic cells is one way to overcome these challenges [9], but resulting cells are often unlike their somatic counterparts [10], and present epigenetic marks of the original cells after transdifferentiation [11].

An alternative method to overcome these challenges is using a mutated protein of Hutchinson-Gilford progeria syndrome (HGPS), a rare autosomal dominant disorder involving a splice variant of the *LMNA* gene [12]. The *LMNA* G608G (GGC>GGT) mutation in exon 11 activates a cryptic splice site leading to an aberrant form of the Lamin A/C protein, named progerin. Affected cells display a multiple hallmarks of ageing including nuclear deformation, DNA damage and mitochondrial

dysfunction [13]. Affected individuals usually die in the second decade of life from disorders usually associated with an aged population. Mental development is unaffected, and patients show no predisposition of neurodegeneration. This is due to a lack of Lamin A expression in the brain, where Lamin B and Lamin C are predominantly expressed [14].

Using progerin in a cell culture model for ageing has previously been introduced by Miller et al. [15], where it was elegantly shown that cells could be aged using progerin. However, procedural limitations prevented cells to be cultured for more than five days after progerin expression. Using modified RNA, cells were put under high transfection stress, resulting in major cell death even in the control group. To circumvent this problem, we decided to devise a lentiviral approach to expose cells to prolonged progerin expression.

This model has been extensively tested on hESC-derived cardiomyocytes (hESC-CMs), since *LMNA* laminopathies are usually associated with cardiac disease [16]. Furthermore, cardiac cells have high mitochondrial activity and are relatively easy to differentiate [17, 18]. By using the cardiac expression pattern during differentiation, transgenic progerin expression can be achieved using a conditional promoter. The ability to use cardiac cells at 30 days in vitro (DIV) compared to neurons at 60 DIV, allows for optimization of the method in a disease relevant cell type. After introduction and evaluation of the model in cardiomyocytes, we have used the same model on PD patient-derived neurons obtained via iPSC differentiation, to use it as a model for ageing.

In this chapter, we show that lentivirus-induced progerin expression in ESC-derived CMs leads to increased mitochondrial stress, nuclear deformation and an increase in double stranded break (DSB) formation of DNA. Additionally, we improved this ageing model for CMs by introducing a conditional promoter system for cardiac cell specific expression of progerin. Progerin expression in PD iPSC-derived neuronal cells leads to a typical accumulation of α-synuclein, a hallmark

of altered proteostasis not seen in control transduced PD iPSC-derived neuronal cells.

Materials and Methods

Culture of hESCs and hiPSCs

Human iPSCs were generated using a protocol described in chapter 3 of this thesis. Human HUES9 embryonic stem cells were provided by Harvard University HSCI iPS Core Facility.

Geltrex®-coated plates and Essential 8™ medium (Thermo Fisher Scientific) were used to maintain cells according to the manufacturer's instruction. Passaging of iPSCs was done using ReLeSR™ (Stemcell Technologies) according to the manufacturer's instruction, while passaging of ESCs was done using TrypLE™ Express (Thermo Fisher Scientific). All cells were maintained in a humidified incubator at 37°C with 5%CO_2. ESCs were used below passage 50, while iPSCs were used between passage 25 and 35.

Dopaminergic differentiation

Dopaminergic differentiation was achieved using a slightly adapted protocol from Kriks et al. [19], described in chapter 3 of this thesis. At day 20 of differentiation, cells were dissociated with Accutase (Sigma-Aldrich) and plated on Geltrex®-coated tissue culture treated plates. To purify cultures, cultures were exposed to glucose deprivation and lactate (5mM) supplementation (GDLS) at 26 days in vitro (DIV) after which neurons were maintained to 60 DIV. At 60DIV, transduction was performed after which cells were cultured for 30 DIV.

Cardiac differentiation

CMC differentiation of ESCs was achieved by dissociating HUES9 ESCs with 1x TrypLE Express for 4 minutes and plating them as single cells in Essential 8 medium containing 5 μM Y26732 (Selleck Chemicals). Once cultures reached 80% confluency, cells were washed with PBS and

differentiation was initiated (day 0) by culturing cells in RPMI1640 medium (Thermo Fisher Scientific) supplemented with 1x B27 minus insulin (Thermo Fisher Scientific) and 6 μM CHIR99021 (Cayman Chemical). At day 2, cells were washed with PBS and medium was refreshed with RPMI1640 supplemented with 1x B27 minus insulin and 2 μM Wnt-C59 (Tocris Bioscience). From day 4, medium was changed to CDM3 [17] medium and refreshed every other day as CM maintenance medium. This resulted in cultures with >90% spontaneously contracting CM at day 8-10. To further enrich these cultures, starting from day 12, differentiated CM were cultured in glucose-free RPMI1640-based (Thermo Fisher Scientific) CDM3 medium supplemented with 5 mM sodium DL-lactate (Sigma-Aldrich) for 6-10 days [20]. At 20DIV, medium was supplemented with triiodothyronine (Sigma-Aldrich) to enhance cardiomyocyte maturation and increase *MYH6* expression [21].

Vector construction

PCR amplification (Phusion High-Fidelity DNA Polymerase, Thermo Fisher Scientific) for AcGFP and AcGFP-progerin (a generous gift by Justine Miller) with overhangs for SpeI and KpnI was performed, and purified fragments were ligated in CloneJET vector (Thermo Fisher Scientific). Resulting CloneJET vectors and the pSin-EF2-Nanog-Pur vector (addgene plasmid 16578) were restricted using BcuI (SpeI, Thermo Fisher Scientific) and KpnI (Thermo Fisher Scientific), subsequently ligated using T4 ligase (Thermo Fisher Scientific) after which the product was transformed in DH5α competent cells. Colony PCR screening was performed to select positive colonies, which were checked by restriction analysis. Correct plasmids were sent for sequencing and transfected in HEK293T to validate expression.

A conditional vector for AcGFP and AcGFP-progerin expression was created at Oxford Genetics. To achieve expression, inserts were placed under control of the α-MHC promoter, which is flanked by an EF1a-PuroR cassette to allow puromycin selection of transduced cells.

The cassette is flanked by a Woodchuck Hepatitis Virus (WHP) Posttranscriptional Regulatory Element (WPRE) for stable expression of the transgenes.

Viral transduction

Viral transduction was using a slightly modified protocol by Trono et al. (Production and titration of lentiviral vectors) achieved by transfecting a T75 of HEK-293T cells when cells were 70-80% confluent. A mixture containing 900 µl OPTIMEM (Thermo Fisher Scientific) 9 µg viral vector, 3 µg pMD2-VSV-G and 7.5 µg pCMV-D8.91, was supplemented with 45 µl FUGENE HD (Lonza) and incubated for 15 min at room temperature (RT) to generate transfection complexes. The next day medium was changed with 20 ml RPMI 1640 (Thermo Fisher Scientific) and viral particles were harvested between 36 and 48 h. Viral supernatant was collected and sterilized using a 0.45 µm filter (Nalgene), subsequently mixed with CDM3 in a 1:1 ratio for AcGFP-progerin, and a 1:4 ratio for AcGFP. The resulting mixture was supplemented with polybrene (8 µg/ml). HUES9 derived CMs were dissociated using 1x TrypLE Express, spun down at 200g, resuspended in low volume and added to the viral mixture. The next day cells were washed with dPBS, and medium was changed to CDM3.

Transducing HUES9 ES cells with the conditional promoter system was achieved using a similar protocol as described above, with minor modifications. HEK293T cells were transfected with the pSF-OxG-Lenti-aMHC-AcGFP-(Progerin)-Puro-WPRE vector, constructed by Oxford Genetics custom cloning and viral supernatant was collected in E8 medium w/o supplement. After transduction, HUES9 cells were cultured with 50µg puromycin to obtain clones with similar integration profiles. Resulting cultures were single cell sorted using a flow cytometer and expanded to be analysed using genomic DNA qPCR.

Immunocytochemistry

Borosilicate glass coverslips containing cells were fixed in paraformaldehyde 4% for 15 min at room temperature and stored at 4°C. Permeabilization and blocking were done in PBS containing 0.1% Triton, 1% BSA and 5% normal goat serum for ~60 min at RT. Primary antibody incubation was done overnight at 6°C, followed by three PBS washes (5 min each), after which a fluorescent conjugated secondary antibody and Hoechst 33258 (Sigma-Aldrich, 14530) were added. Mowiol® 4-88 (Sigma-Aldrich) was used as mounting medium to attach the coverslips to glass slides. Samples were stored at 4°C until further analysis. Primary antibodies used were monoclonal anti-α-actinin IgG1 (1:100; A7811, Sigma-Aldrich), polyclonal anti-cardiac troponin T IgG (1:100; ab45932, Abcam) polyclonal anti-TOM20 IgG (1:250; sc-11415, Santa Cruz Biotech), monoclonal Anti-phospho-Histone H2A.X (Ser139) (1:100, clone JBW301, Millipore).

Imaging

Phase contrast imaging was performed on a Leica AF-6000 microscope, using a 20x objective (PL FLUOTAR 20x/NA 0.4, Dry).

Confocal images were acquired using a Leica SP8 confocal microscope, equipped with an HC PLAPO CS2 63x oil lens, with NA 1.4. Epifluorescence images were acquired using a Leica AF-6000 fluorescent microscope, using a PL FLUOTAR 20x/NA 0.4, Dry lens.

CellROX™ assay

To perform CellROX™ (Thermo Fisher Scientific) assays, cells were plated and transduced in a Geltrex®-coated 96 well plate. After two weeks of transgenic expression, medium was changed to CDM3 without phenol red 2 hours prior to measurement. For measurement, 25µl of CDM3 without phenol red supplemented with 5µM CellROX™ orange and 10mM HEPES was added to the wells. Fluorescent signal (Ex/Em: 540/570) was measured every minute for 2h by a SYNERGY H1 plate

reader (BIOTEK), and the area under curve (AUC) was calculated from the resulting data. Experiments were performed in n=5 independent differentiations.

Genomic DNA qPCR

Single cell sorted HUES9 clones were expanded for two passages, and genomic DNA was extracted using a QIAamp DNA Mini Kit (QIAGEN). In order to find the right conditions for qPCR on gDNA, primer test experiments were performed for the GAPDH (Fw: GGCTCCCACCTTTCTCATCC, Rev: CTCCCCACATCACCCCTCTA) and AcGFP (Fw: CGAGCTGAATGGCGATGTGA, Rev: CCGGTGGTGCAGATGAACT) primer using different primer concentrations, and different input of genomic DNA. Using this data, we determined the optimal concentration to compare the amount of AcGFP integration between clones. To determine the amount of integration samples were mixed with primers (5nM) and IQ SYBR Green (170-8885, BioRad). Samples were run on a Biorad C1000 Touch thermal cycler and analyzed with Biorad CFX manager™ software.

Statistical analysis

All statistical tests were performed using Prism 7.0. Statistical significance was determined using one-way ANOVA followed by Tukey post hoc test. A p value < 0.05 was considered significant. With biological replicates lower than n=3 no significance was indicated.

Results

To introduce viral expression of AcGFP and AcGFP-progerin, several vectors were used. To introduce progerin expression in initial experiments, a vector with a strong promoter and easy vector design was chosen to directly transduce differentiated cardiomyocytes. After initial findings a second expression system was introduced, using conditional promoter driven expression of AcGFP and AcGFP-progerin. This design

enables the study of clonal lines, allowing more stable expression between control and progerin expressing lines and takes away the need for directly transducing differentiated cultures.

HUES9 CMs can be successfully transduced by an AcGFP-progerin viral vector

Construction of the viral vector was based on the pSinEF2 vector with AcGFP or AcGFP-progerin placed under expression of the EF1a promoter (Figure 1A). Testing of the vector in HEK293T cells showed a robust expression of the viral vector (Figure 1B). Additionally, CMs were transduced successfully (Figure 1C). Transgenic AcGFP-progerin expression showed progerin localisation around the nuclear lamina (Figure 1C).

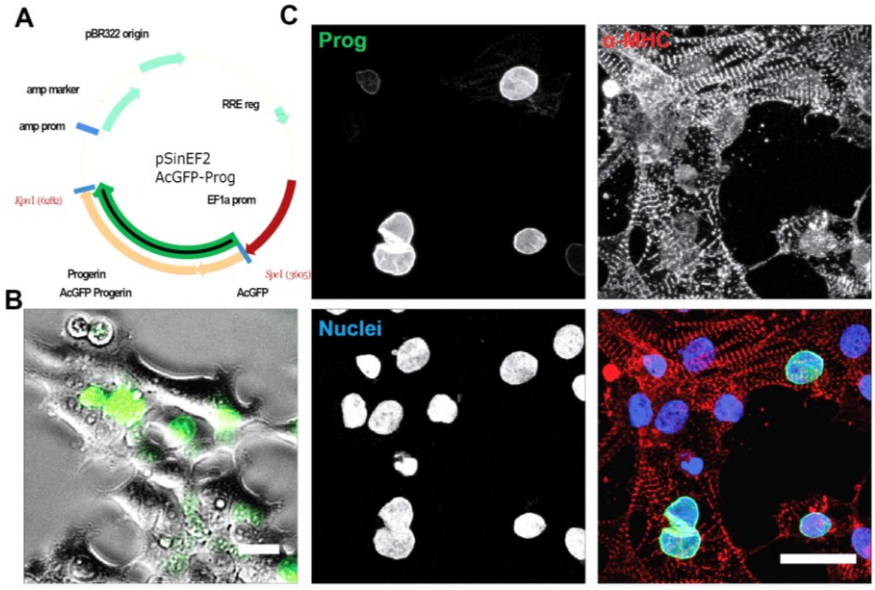

Figure 1. AcGFP-progerin can be successfully expressed in CMs. (A) *Vector map of the pSinEF2-AcGFP-progerin viral vector. AcGFP-progerin is placed under control of the EF1-α promoter.* ***(B)*** *HEK293T cells expressing the AcGFP-progerin vector.* ***(C)*** *CMC cultures successfully transduced by AcGFP-Progerin. Striated α-actinin structures (red), AcGFP-progerin and Hoechst (blue) are shown at 40DIV. All bars represent 25 μm.*

Progerin expression leads to oxidative stress

AcGFP-progerin-expressing CMs produced significantly more ROS compared to AcGFP expressing and control CMs. Figure 2A displays fluorescent images of measured CMs. The amount of transduced cells was similar between AcGFP and AcGFP-progerin. Expression of AcGFP-progerin showed a significant increase (19.4%) in ROS production compared to control ($p<0.0001$) and to AcGFP-expressing CMs ($p<0.0001$) (Figure 2B).

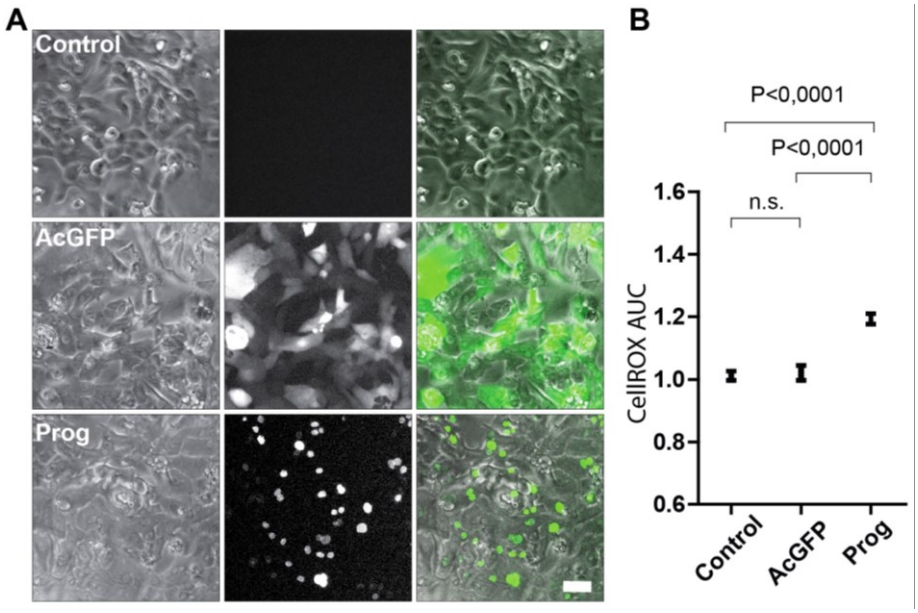

Figure 2. AcGFP-progerin expression leads to an increase in ROS production. (A) *Transduction with AcGFP and AcGFP-progerin vectors. AcGFP-progerin co-localizes with the nuclear membrane, while AcGFP is expressed diffusely in the cytoplasm. Scalebar represents 25 µm.* ***(B)*** *ROS production is higher in AcGFP-progerin expressing cells (19.4% increase), while it remains similar between control and AcGFP (2.1%, n.s.). All data were produced with n=5 biological replicates.*

Progerin expression leads to an increase in double stranded breaks

Double stranded break (DSB) incidence was quantified by counting γH2AX-positive foci-containing cells, where only cells with 2 or

more γH2AX foci are considered positive and included, as sporadic incidence of DSBs is a normal consequence of mammalian cell culture. AcGFP-progerin expressing cells were frequently observed to have more than 20 of such foci. Figure 3A shows an example of a quantified image, with a high incidence of DSBs in AcGFP-progerin-expressing CMs compared to control and AcGFP-expressing CMs. Transduction efficiencies for AcGFP and AcGFP-progerin were 55.0% and 53.3% respectively (Figure 3B). Incidence of γH2AX foci in control cells was 10.5%, while incidence in the cells in the AcGFP images was 12.1% and 12.35%, respectively for AcGFP-negative and AcGFP-positive foci. Interestingly, AcGFP-progerin images showed an increase in cells with foci for both AcGFP-progerin-positive (53.3%) and -negative cells (20.3%).

Transgene expression in a conditional CMC promoter

To validate our findings using direct transduction of CMs, we have chosen to develop a model that allows conditional expression of AcGFP-progerin; the set-up of the viral vector is shown in figure 4a. Figure 4B displays the expression of the vector in mixed cultures, after culture for 34DIV. At this time point, CMs are active and contract as evidenced by analysis with difference tracker (Figure 4C). The highlighted section at 7.75s is an overlay with the moving pixels in the image, indicating the contraction of cells in red. To select individual clones for further analysis, we decided to screen integration sites using a qPCR assay on genomic DNA. For this purpose, previously puromycin-selected transduced HUES9 cells were single cell sorted and cultured after which gDNA was extracted. Optimal primer conditions and gDNA input were determined and AcGFP integration was normalized to genomic GAPDH content. From our data we selected two AcGFP and two AcGFP-progerin clones which had closely matching integration of the viral vector (Figure 4D).

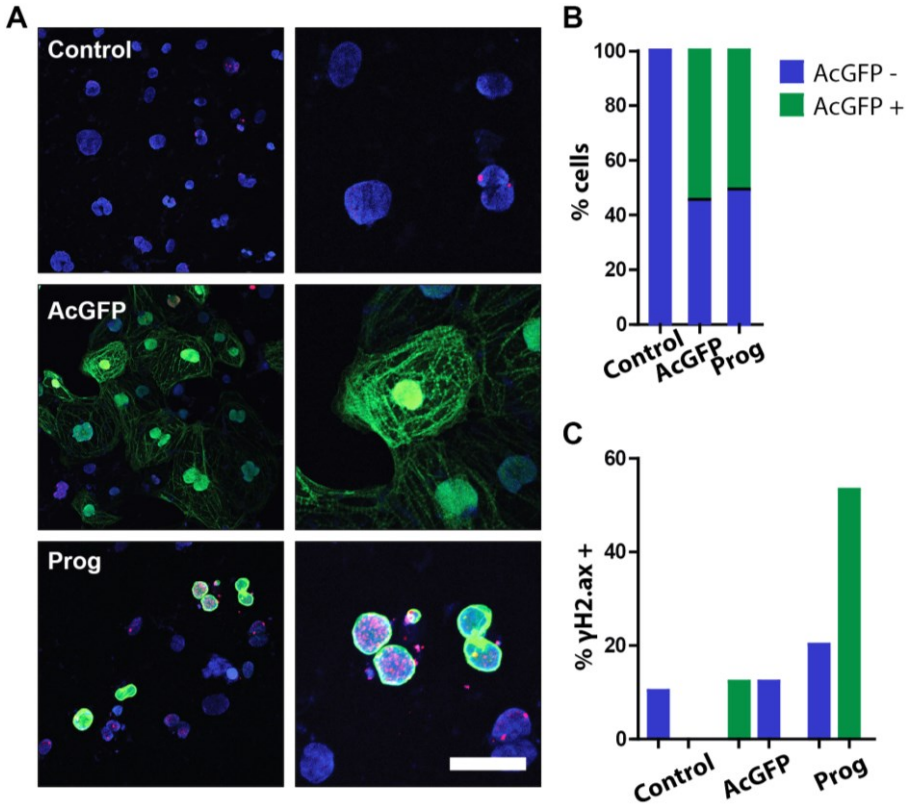

Figure 3. AcGFP-progerin expression leads to increased DSB incidence. (A) *Corresponding images of control and AcGFP (green) and AcGFP-progerin (green) transduced cells. A γH2AX staining is presented in the red channel, and Hoechst is depicted in blue. Scalebar represents 25 µm.* ***(B)*** *Transduction efficiency in CMs is presented as AcGFP positive (green) and negative cells (blue).* ***(C)*** *Occurrence of DSBs as assessed by the percentage of cells containing 2 or more γH2AX positive foci is more frequent in AcGFP-progerin-transduced cells compared to control and AcGFP-transduced cells. Non-transduced cells present in the progerin condition also display an increase in γH2AX foci. Data was produced with n=2 biological replicates.*

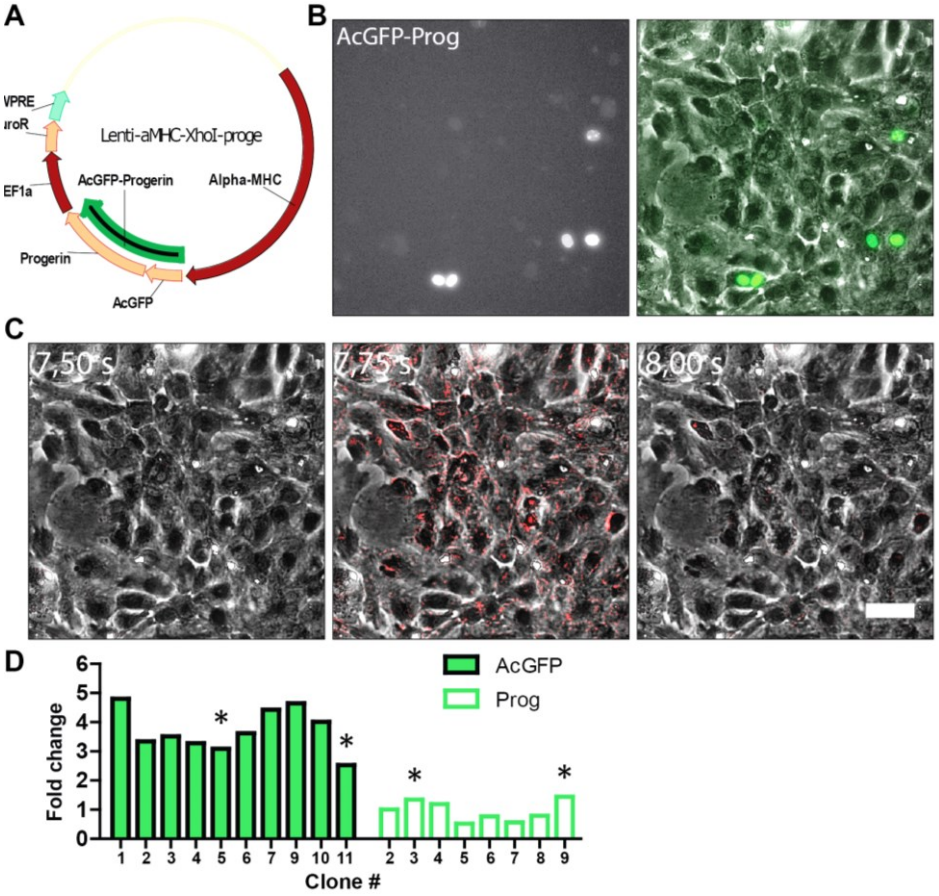

Figure 4. AcGFP-progerin can be expressed under the αMHC promoter in CMs. ***(A)*** *Viral vector map of pSF-OxG-Lenti-aMHC-AcGFP-(Progerin)-Puro-WPRE. AcGFP-progerin is placed under control of the α-MHC promoter, and flanked by an EF1α-PuroR cassette.* ***(B)*** *CMC cultures successfully express AcGFP-progerin (green) under the α-MHC promoter at 30DIV. The observed heterogeneity is the result of culturing a non-clonal cell population.* ***(C)*** *CMC cultures are functional at 30DIV, as evidenced by contraction highlighted by difference tracker. Bar represents 25 µm.* ***(D)*** *AcGFP integration normalized to GAPDH for AcGFP and AcGFP-progerin transduced HUES9 ESCs. Selected clones are denoted by an asterisk*.*

AcGFP-progerin can be expressed under the conditional α-MHC promoter in CMs

Figure 5A demonstrates the expression of AcGFP-progerin (white) in a cardiomyocytes culture. Alpha-actinin (green) staining shows the sarcomeric structure of CMs, with co-localizing expression of troponin-T (red). Expression of LAMINA/C is illustrated in Figure 5B, and shows co-localisation with AcGFP-progerin, indicating correct nuclear localisation. A staining with the gap junction protein Connexin-43 (Cx43) highlights the connections between adjacent cells. A mitochondrial TOMM20 (red) staining in Figure 5C displays no apparent defects in mitochondrial integrity in AcGFP-progerin (green) expressing cells. Although γH2AX (white) positive foci were occasionally observed in AcGFP-progerin expressing cells, their frequency was low.

Neuronal AcGFP-progerin expression results in increased levels of α-synuclein

To use our progerin expression model system in neuronal cells, we used the earlier described pSinEF2-AcGFP-progerin vector for direct transduction of differentiated cultures. Transgenic expression was achieved at 60DIV and maintained for 30DIV in purified neuronal cultures. This resulted in a marked increase of the amount of α-synuclein fluorescence when compared to AcGFP control. Expression of AcGFP-progerin in differentiated PD patient iPSCs led to increased levels of α-synuclein in these cells as assessed by confocal microscopy (Figure 6). Figure 6A shows expression of the AcGFP control vector, combined with TH (red), α-synuclein (yellow) and Hoechst (blue). Figure 6B shows expression of the AcGFP-progerin vector, combined with TH (red), α-synuclein (yellow) and Hoechst (blue).

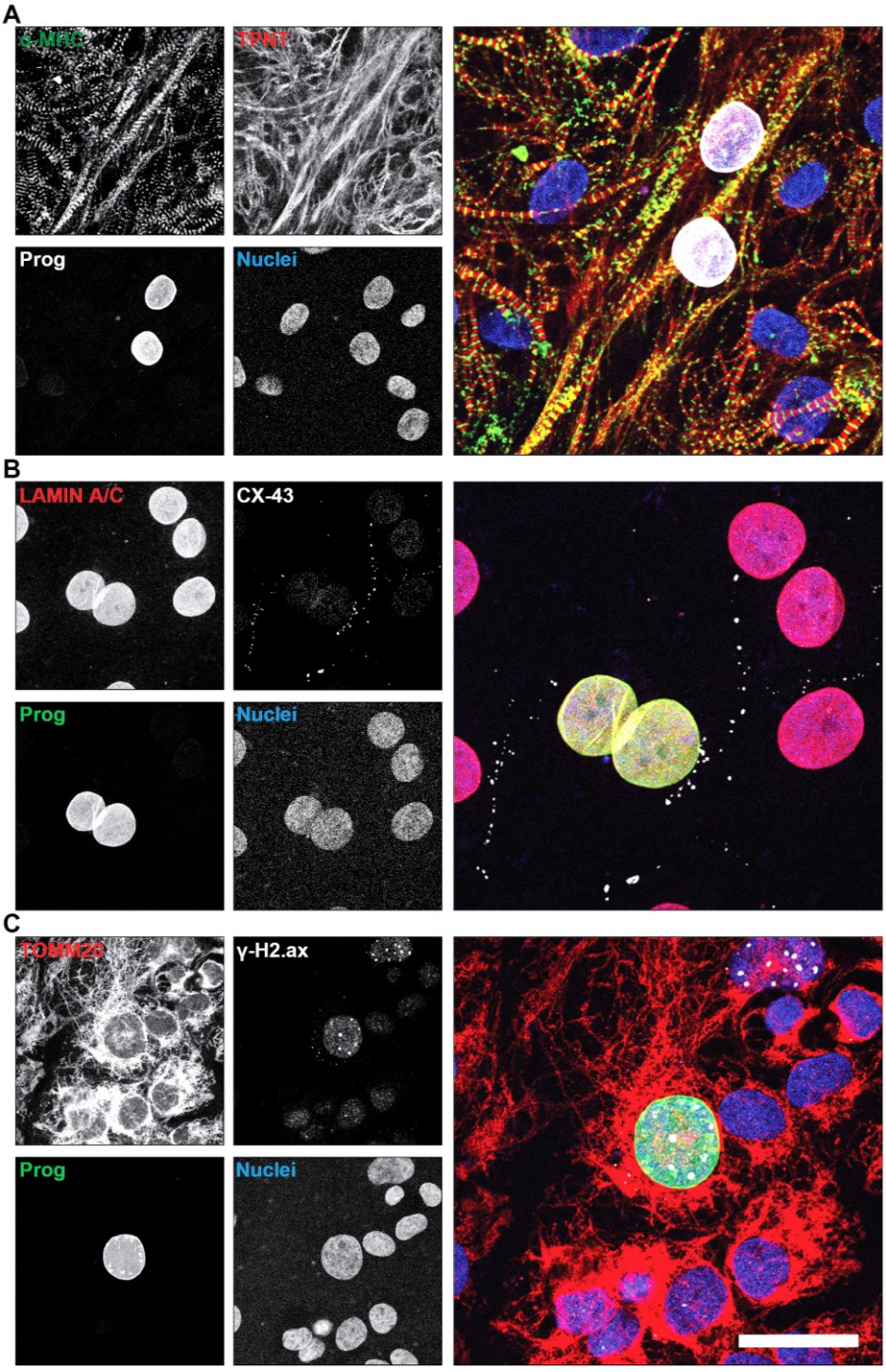
A
c-MHC
TPNT
Prog
Nuclei
B
LAMIN A/C
CX-43
Prog
Nuclei
C
TOMM20
γ-H2.ax
Prog
Nuclei

Figure 5. CMs confocal microscopy highlights functional characteristic. (A) *CMs express striated α-actinin (red) structures and a structural distribution of troponin-T (green). AcGFP-progerin and Hoechst are presented in white and blue respectively.* ***(B)*** *CMs express laminA/C, which shows overlap with the AcGFP-progerin signal (green). Connexin43 staining highlights the gap junctions between CMs, and Hoechst is depicted in blue.* ***(C)*** *CMs show no abnormalities in mitochondrial networks as evidenced by TOMM20 (red). γH2AX foci (white) were present, but not frequently observed. AcGFP-progerin and Hoechst are presented in white and blue respectively. Bar represents 25 μm.*

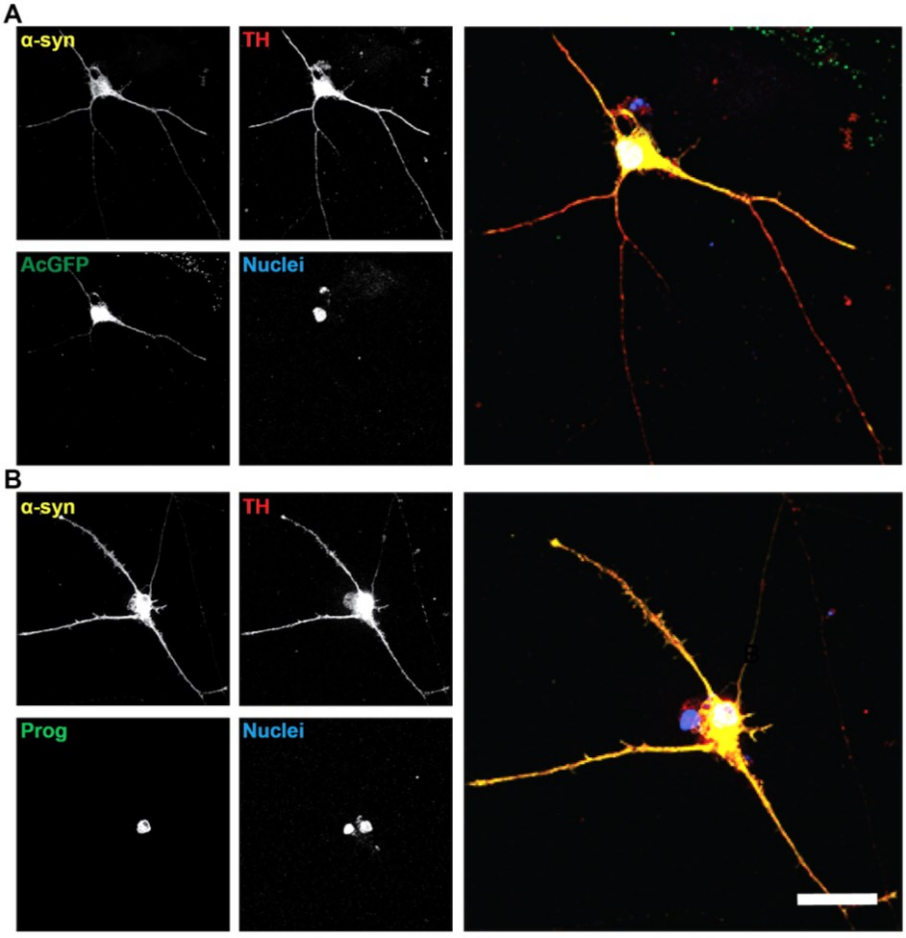

Figure 6. DA neurons expressing AcGFP-progerin have increased levels of α-synuclein.

(A) *PD4 iPSC-derived DA neuron expressing AcGFP (green), stained for TH (red), α-synuclein (yellow) and Hoechst (blue).* ***(B)*** *PD4 iPSC-derived DA neuron expressing AcGFP-progerin (green), stained for TH (red), α-synuclein (yellow) and Hoechst (blue). Comparison of α-synuclein-associated fluorescence shows a marked increase between AcGFP and AcGFP-progerin transduced iPSC-derived DA neurons. Bar represents 25 µm.*

Discussion and conclusion

In this chapter, we successfully recapitulated ageing hallmarks by inducing overexpression of progerin in both neuronal and cardiac cells. The lentiviral approach allowed us to induce transgenic expression of progerin for prolonged periods of time (>30DIV). Our model recapitulates hallmarks of ageing which could not be produced by the approach of Miller et al. [15]. However, a downside of our viral approach is the uncontrolled integration of the viral vector, which can interfere with gene integrity and expression. This is solved by using a large population of post-mitotic cells, that will create a heterogeneous profile of viral integrates, effectively diluting any negative effects of viral integration. In our conditional promoter approach, however, viral integration might produce a problem since we are using clonal cells. To prevent harmful viral integration in these models, a non-restrictive linear amplification-mediated PCR should be performed to identify integration sites [22].

The occurrence of increased oxidative stress and the increase in γH2AX-positive foci indicates that our model captures both genomic instability and mitochondrial dysfunction. Interestingly, mitochondrial ROS production is significant but not as pronounced compared to other model systems. Over two-fold increases in ROS generation are common when exposing cells to mitochondrial toxins like rotenone or paraquat, but our approach reports an increase of only 19.4%. In this light, our model recaptures more physiological levels of ROS increase that might lead to cellular damage over time. Mitochondrial abnormalities were not apparent

in confocal microscopy and it remains to be investigated whether the mitochondrial membrane potential is affected. The ability to induce long-term mitochondrial toxicity by nuclear stress provides an indirect mechanism for manipulating mitochondrial function and so provides a relevant tool for studying mitochondrial function in ageing. Mitochondrial function will be further analysed in mitochondrial respiration and glycolysis assays using the Agilent Seahorse XF Technology, as oxidative phosphorylation has been proposed to be progressively impaired during ageing [23].

The increase in γH2AX was an expected effect in progerin pathology. The large number of foci present in some of the cells point to extensive nuclear instability. Surprisingly, non-transduced cells in the progerin-transduced cultures also presented a higher number of foci indicating that an indirect effect may contribute to nuclear pathology. The overall increase in ROS production in these cultures might increase the indirect formation of DSBs in non-transduced cells [24] or might be the result of senescent paracrine signalling by progerin transduced cells [25].

In human iPSC derived DA neurons, progerin-induced ageing in resulted in higher levels of α-synuclein compared to controls. The underlying cause for this increase remains to be investigated, but might stem from altered proteostasis in these neurons. Another option is the induction of aggregation by increased oxidative stress, which has a direct effect on α-synuclein oligomerization [26, 27]. It should be noted that while progerin can be used as an ageing model in these cells, neurons do not express Lamin-A or progerin in vivo *[28]*. Progerin induced ageing might therefore not be as physiologically relevant to the brain as it is to other organs, i.e. cardiomyocytes. It does, however, represent a model that recaptures multiple hallmarks of ageing.

In summary, we present an alternative method to age cells, and show that functional CMs generated from HUES9 ESCs exposed to this method exhibit several characteristics of aging. Future experiments will

rely on a conditional promoter approach, and will validate earlier findings done in directly transduced CMs.

References

1. Lopez-Otin C, Blasco MA, Partridge L et al. The hallmarks of aging. **Cell**. 2013;153:1194-1217.
2. Gen W, Tani M, Takeshita J et al. Mechanisms of Ca2+ overload induced by extracellular H2O2 in quiescent isolated rat cardiomyocytes. **Basic research in cardiology**. 2001;96:623-629.
3. Ryan SD, Dolatabadi N, Chan SF et al. Isogenic human iPSC Parkinson's model shows nitrosative stress-induced dysfunction in MEF2-PGC1alpha transcription. **Cell**. 2013;155:1351-1364.
4. Zhang HY, McPherson BC, Liu H et al. H(2)O(2) opens mitochondrial K(ATP) channels and inhibits GABA receptors via protein kinase C-epsilon in cardiomyocytes. **American journal of physiology Heart and circulatory physiology**. 2002;282:H1395-1403.
5. Rideout HJ, Larsen KE, Sulzer D et al. Proteasomal inhibition leads to formation of ubiquitin/alpha-synuclein-immunoreactive inclusions in PC12 cells. **Journal of neurochemistry**. 2001;78:899-908.
6. White SM, Constantin PE, Claycomb WC. Cardiac physiology at the cellular level: use of cultured HL-1 cardiomyocytes for studies of cardiac muscle cell structure and function. **American journal of physiology Heart and circulatory physiology**. 2004;286:H823-829.
7. Xie HR, Hu LS, Li GY. SH-SY5Y human neuroblastoma cell line: in vitro cell model of dopaminergic neurons in Parkinson's disease. **Chinese medical journal**. 2010;123:1086-1092.
8. Lapasset L, Milhavet O, Prieur A et al. Rejuvenating senescent and centenarian human cells by reprogramming through the pluripotent state. **Genes & development**. 2011;25:2248-2253.
9. Mertens J, Paquola AC, Ku M et al. Directly Reprogrammed Human Neurons Retain Aging-Associated Transcriptomic Signatures and Reveal Age-Related Nucleocytoplasmic Defects. **Cell stem cell**. 2015;17:705-718.
10. Hanna JH, Saha K, Jaenisch R. Pluripotency and cellular reprogramming: facts, hypotheses, unresolved issues. **Cell**. 2010;143:508-525.

11. Zhou Q, Melton DA. Extreme makeover: converting one cell into another. **Cell stem cell**. 2008;3:382-388.
12. Moulson CL, Fong LG, Gardner JM et al. Increased progerin expression associated with unusual LMNA mutations causes severe progeroid syndromes. **Human mutation**. 2007;28:882-889.
13. Cao K, Blair CD, Faddah DA et al. Progerin and telomere dysfunction collaborate to trigger cellular senescence in normal human fibroblasts. **The Journal of clinical investigation**. 2011;121:2833-2844.
14. Jung HJ, Coffinier C, Choe Y et al. Regulation of prelamin A but not lamin C by miR-9, a brain-specific microRNA. **Proceedings of the National Academy of Sciences of the United States of America**. 2012;109:E423-431.
15. Miller JD, Ganat YM, Kishinevsky S et al. Human iPSC-based modeling of late-onset disease via progerin-induced aging. **Cell stem cell**. 2013;13:691-705.
16. van der Kooi AJ, Bonne G, Eymard B et al. Lamin A/C mutations with lipodystrophy, cardiac abnormalities, and muscular dystrophy. **Neurology**. 2002;59:620-623.
17. Burridge PW, Holmstrom A, Wu JC. Chemically Defined Culture and Cardiomyocyte Differentiation of Human Pluripotent Stem Cells. **Current protocols in human genetics**. 2015;87:21 23 21-15.
18. Lian X, Hsiao C, Wilson G et al. Robust cardiomyocyte differentiation from human pluripotent stem cells via temporal modulation of canonical Wnt signaling. **Proceedings of the National Academy of Sciences of the United States of America**. 2012;109:E1848-1857.
19. Kriks S, Shim JW, Piao J et al. Dopamine neurons derived from human ES cells efficiently engraft in animal models of Parkinson's disease. **Nature**. 2011;480:547-551.
20. Tohyama S, Hattori F, Sano M et al. Distinct metabolic flow enables large-scale purification of mouse and human pluripotent stem cell-derived cardiomyocytes. **Cell stem cell**. 2013;12:127-137.
21. Lee YK, Ng KM, Chan YC et al. Triiodothyronine promotes cardiac differentiation and maturation of embryonic stem cells via the classical genomic pathway. **Molecular endocrinology**. 2010;24:1728-1736.
22. Gabriel R, Kutschera I, Bartholomae CC et al. Linear amplification mediated PCR--localization of genetic elements and characterization of unknown flanking DNA. **Journal of visualized experiments : JoVE**. 2014:e51543.
23. Lesnefsky EJ, Hoppel CL. Oxidative phosphorylation and aging. **Ageing research reviews**. 2006;5:402-433.

24. Vilenchik MM, Knudson AG. Endogenous DNA double-strand breaks: production, fidelity of repair, and induction of cancer. **Proceedings of the National Academy of Sciences of the United States of America**. 2003;100:12871-12876.
25. van Deursen JM. The role of senescent cells in ageing. **Nature**. 2014;509:439-446.
26. Paxinou E, Chen Q, Weisse M et al. Induction of alpha-synuclein aggregation by intracellular nitrative insult. **The Journal of neuroscience : the official journal of the Society for Neuroscience**. 2001;21:8053-8061.
27. Esteves AR, Arduino DM, Swerdlow RH et al. Oxidative stress involvement in alpha-synuclein oligomerization in Parkinson's disease cybrids. **Antioxidants & redox signaling**. 2009;11:439-448.
28. Nissan X, Blondel S, Navarro C et al. Unique preservation of neural cells in Hutchinson- Gilford progeria syndrome is due to the expression of the neural-specific miR-9 microRNA. **Cell reports**. 2012;2:1-9.

Chapter 6

Summary and discussion

In two hundred years after the first description, the understanding of Parkinson's disease (PD) has evolved from a classical motor disease to a disease with complex heterogeneous symptoms [1]. Pathological hallmarks such as Lewy bodies (LB) and neuronal cell death have been found outside the substantia nigra pars compacta (SNc), and it is now accepted that PD pathology involves large regions of the nervous system [2]. This complexity is also reflected in our current understanding of the cause of disease: a complex interplay between genetic and environmental factors [1]. Despite a large increase in understanding of the molecular and cellular basis of the disease there are no treatments that slow the neurodegenerative process, and management of disease symptoms by administration of L-Dopa has been used for over 50 years [3]. In part, this is attributable to difficulties with proper clinical diagnosis of a disease that develops slowly over many years, and consequently results in the study of only the latter stages of disease [4]. Recent advancements in genetics and biotechnology, such as the discovery of genetic contributors to PD [5, 6] and the introduction of induced pluripotent stem cells (iPSCs) [7] and embryonic stem cells (ESCs) [8], have presented new opportunities in understanding PD [9]. In this dissertation, patient-derived iPSCs carrying the PD donors' genetic background were used to study the early onset of familial PD.

Chapter 1 provides a concise introduction into the history and current literature of PD research. This is followed by a study in a neuroblastoma cell PD model in Chapter 2, which focusses on mitochondrial trafficking in these cells. To validate results of this study in iPSCs, a method for purification of iPSC derived dopaminergic (DA) neurons is introduced in Chapter 3. In Chapter 4 mitochondrial trafficking

in these neurons is assessed, to validate the findings of Chapter 2. Finally, Chapter 5 introduces a method based on the Hutchinson–Gilford progeria syndrome, to accelerate the in-vitro ageing of hiPSC- and hESC-derived cells. Box 1 contains an overview of the findings of this dissertation, which will be discussed in the following sections.

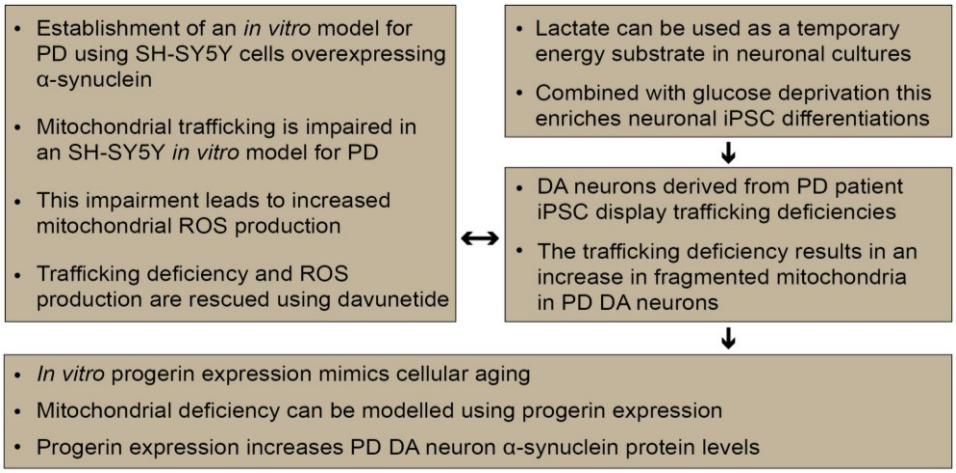

Box 1. Main conclusions and findings of this dissertation.

Mitochondrial trafficking in Parkinson's disease

As highlighted in the general introduction, the selective vulnerability of SNc DA neurons is likely attributable to a combination of constant pace-making activity and a complex axonal arbor [10]. Many proteins critical to synaptic function are produced in the soma and require functional anterograde transport along the axon [11]. Conversely, retrograde transport is necessary for the removal of dysfunctional organelles and the transport of neurotrophic factors [12]. We hypothesized that SNc DA neurons are more vulnerable to mitochondrial trafficking deficiencies as mitochondrial activity in these neurons is high and trafficking processes are more complex compared to other neuronal cells. Mitochondrial trafficking deficiencies have been associated with many different neurodegenerative disorders [11], but the underlying mechanisms and effects of these deficiencies differ and have not been completely explored. A heterozygous mutation in the *DNM1L* gene, for

instance, results in severe infantile neurodegenerative disease characterized by microcephaly and abnormal brain development [13]. *DNM1L* encodes the protein Drp1, which is involved in normal mitochondrial fission [14]. Mutations in the middle domain of Drp1 lead to elongated mitochondria, resulting in an incorrect distribution of mitochondria in neurons [15]. Interestingly, *DNM1L* mutations primarily affect neuronal cells, indicating that correct mitochondrial fission is essential for their function, development and maintenance through proper axonal trafficking [16]. Conversely, compound heterozygous and homozygous mutations in the protein mitofusin 2 (Mfn2) lead to the axonal peripheral sensorimotor neuropathy Charcot-Marie-Tooth neuropathy type 2A [17]. Improper mitochondrial fusion by Mfn2 leads to small fragmented mitochondria, which display significant impairment in neuronal mitochondrial trafficking [18]. Strikingly, conditional knockout mice for Mfn2 in DA neurons display nigrostriatal degeneration in a dying-back phenotype [19]. In these mice, increased mitochondrial fragmentation led to a decrease of transport within the axon. Similar to this, the early onset familial PD mutations in PINK1 and Parkin also result in abnormal mitochondrial morphology and trafficking deficiencies [20, 21]. These mutations illustrate the importance of a fine balance between fusion and fission of mitochondria required for proper mitochondrial dynamics.

To investigate if mitochondrial trafficking is also involved in cellular pathology of familial PD with mutations in the *SNCA* gene, we established both a neuroblastoma cell model and an iPSC in-vitro PD model. In Chapter 2, SH-SY5Y cells were used to generate an in-vitro model using transgenic overexpression of α-synuclein mutants. This model uses neuroblastoma cells with a high mitotic index that can be lowered by exposing the cells to retinoic acid [22], resulting in neurite outgrowth and axon formation. Chapter 2 demonstrates that retrograde mitochondrial trafficking is significantly impaired in the A53T mutant expressing cells in comparison to control at 6 days in vitro (DIV); both retro- and anterograde

trafficking are impaired at 8 DIV. Trafficking in the A30P mutant and WT α-synuclein was not significantly impaired compared to control, but the cells did display increased ROS production associated with mitochondrial dysfunction. Impairment of normal mitochondrial dynamics has been previously reported in PD animal models and cell models [23-25], but a directional bias and the time-dependent changes in mitochondrial dynamics had not yet been elucidated. Furthermore, α-synuclein induced trafficking impairment and ROS production can be rescued using the small interfering peptide davunetide (NAP) [26].

Although expression of mature DA markers has been reported in SH-SY5Y, expression levels are low and represent less than half of the proteins associated with mature DA neurons [27]. Therefore, to further assess trafficking impairment, proper ventral midbrain dopaminergic neurons derived from iPSCs were used. These differentiated DA neurons contain more in-vivo like axonal structures, which are way more complex than the simple axonal structures in the neuroblastoma cell model, and have a physiologically normal neuronal expression pattern. Additionally, these neurons have a very low mitotic index, can be cultured for prolonged duration and display spontaneous electrical activity. Chapter 4 describes a decrease in mitochondrial trafficking in DA neurons from PD patients compared to an age-matched control, similar to the defects described in Chapter 2. However, while wild-type α-synuclein displays no trafficking deficiencies in the SH-SY5Y overexpression model, iPSC DA neurons harbouring an *SNCA* triplication do reveal trafficking deficiencies. This is likely the result of prolonged culture duration, higher levels of oxidative metabolism, and intrinsic electrical activity in these neurons.

However, the mechanisms by which α-synuclein causes these trafficking differences remain elusive and numerous candidates for trafficking deficiencies have been described. Figure 1 illustrates several mechanisms related to mitochondrial trafficking impairments.

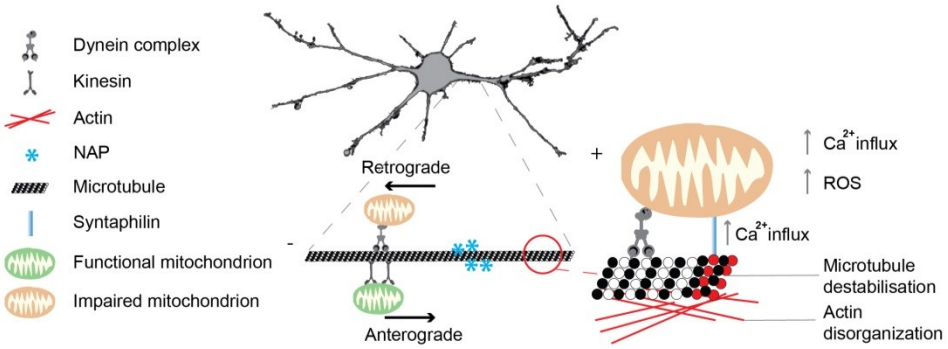

Figure 1. Proposed mechanisms leading to mitochondrial trafficking impairments. *Increased ROS production is a result of distal accumulation of impaired mitochondria. Increased Ca^{2+} influx leads increased cellular stress and to microtubule anchoring of mitochondria by syntaphilin. α-Synuclein-mediated disorganisation of microtubules and actin is thought to contribute to trafficking deficiencies. Using NAP stabilizes microtubules and rescues the observed trafficking deficiencies in our SH-SY5Y PD cell model.*

Different species of α-synuclein oligomers increase calcium influx in SH-SY5Y cells through a pore-forming mechanism, which can indirectly lead to cell damage [28]. Direct disruption of isolated mitochondrial membranes by α-synuclein has also been reported, but no evidence for this model has been presented in cell models [29]. Combined with the intrinsic pace-making activity of DA neurons through L-type calcium channels, α-synuclein pore-formation can result in high calcium levels in α-synuclein-overexpressing cells and make these neurons more vulnerable to cellular stress [30]. Additionally, increased calcium influx can directly disrupt neuronal trafficking of mitochondria, arresting mitochondria in distal regions of the axon by anchoring syntaphilin [31, 32]. Other mechanisms for disruption of trafficking might result from the interaction of α-synuclein with microtubule associated protein tau (MAPT) and actin [33, 34]. Overexpression of α-synuclein resulted in slowed actin polymerization, thereby decreasing reassembly of actin filaments [33]. MAPT on the other hand aggregates under the influence of α-synuclein fibrils, thereby inhibiting its function to stabilize microtubules [35]. Single

nucleotide polymorphisms in the *MAPT* locus have been frequently associated with PD, underscoring its implication in disease [6, 36]. Incorrect trafficking of mitochondria can lead to distal accumulation of impaired mitochondria, ultimately leading to an increase in ROS production in axonal regions. To enhance microtubule stability, a small protein named davunetide (NAP) can be used, which is based on the activity dependent neuroprotective protein (ADNP). Introduced as a possible therapy for progressive supranuclear palsy [37], NAP is currently considered as a therapeutic in Alzheimer's disease [38] and has been shown to alleviate PD pathology in an α-synuclein mouse model [26]. The eight amino-acid peptide (NAPVSIPQ) has been shown to provide microtubule stability and reduce tau phosphorylation [37, 39]. Protecting the cytoskeleton and increasing the microtubule-tau interaction [40], NAP is likely able to counter the negative effects of α-synuclein on mitochondrial trafficking.

It remains to be elucidated whether one or several of the above mentioned mechanisms are responsible for the observed trafficking deficiencies in Chapter 2 and 4. It is clear, however, that mitochondrial trafficking deficiencies precede neuronal cell death in these cell models for PD.

Energy metabolism in human neurons derived from iPSC

Energy metabolism of human pluripotent stem cells is extensively studied and is well recognized as being an important roadblock on the way to pluripotency [41]. While many somatic cells use oxidative phosphorylation (OXPHOS) as an important source of energy [42], a switch to a glycolytic metabolism is characteristic of stem cells [43]. This process is preceded by a burst in OXPHOS activity, which provides a metabolic gate to pluripotency [44]. Self-renewal in cultured ESCs and iPSCs is characterized by glycolysis, lactate production and the presence of round mitochondria near the nucleus [45]. Glycolysis-mediated histone acetylation in pluripotent stem cells has been revealed to play a role in

maintaining pluripotency [46], and is currently recognized as an active regulatory mechanism of the pluripotent state [47]. Conversely, differentiating pluripotent stem cells to fibroblasts causes elongation of mitochondria accompanied by a shift to OXPHOS [45].

In Chapter 3, these characteristics of stem cells and their somatic progeny were utilized to purify neuronal cells based on their metabolic capacity to use lactate as a substrate. The ability of cells to metabolize lactate varies between different cells types and is dependent on the presence of specific transporters and enzymes to metabolize lactate. By using glucose deprivation and lactate supplementation (GDLS), neuronal cells can be purified from their undifferentiated counterparts as illustrated in Chapter 3. Purified cultures displayed over 90% purity, while normal cultures contained fewer than 40% of neuronal cells at 60 DIV. While various articles have reported higher initial yields, estimates are usually done below 40 DIV [48, 49]. Contaminating populations often arise at later time points, and reproducing results reported by other labs can be challenging due to differences in culture methods or because of intrinsic differences between iPSC lines [50]. Intrinsic differentiation potential varies between pluripotent cells, which can be illustrated by spontaneous differentiations [51]. H9 ESCs have a propensity towards an ectodermal lineage, which makes these cells suitable for neuronal differentiations. HUES9 ESCs on the other hand spontaneously differentiate to the mesoderm and endoderm linage, making these cells suitable for cardiomyocyte differentiations [51]. To homogenize differentiated populations cells are often cell-sorted based on surface markers [52], but these techniques are laborious and cell-straining. The introduction of GDLS creates a simple purification method to serve as an alternative tool to homogenize different neuronal cultures. Figure 2 highlights the principles on which GDLS neuronal purification is based.

Neuronal metabolism of lactate was emphasized in the astrocyte-neuron lactate shuttle (ANLS) hypothesis, proposed in 1998 by Pellerin [53]. While the theory initially sparked critical reviews [54], refinements

have been made over the years [55], and recent in-vivo evidence of a lactate gradient has created renewed interest for the theory [56, 57]. Current understanding of the ANLS theory leans heavily on the cellular distribution of monocarboxylate transporters (MCT). In the brain, the high affinity MCT2 is found predominantly in neuronal cells, while the lower affinity MCT1 and the low affinity MCT 4 are present on astrocytes and oligodendrocytes [58, 59]. The shuttle is linked to neuronal activity by modulating glucose metabolism in astrocytes via the excitatory amino acid transporter (EAAT) 1 and 2. Glutamate released by neurons is taken up by EAAT1 and 2 and stimulates glucose uptake by astrocytes, leading to an increase in astrocytic glycolysis. MCT1 and 4 transport lactate from the soma to the extracellular space, to be taken up by neurons by MCT2. Next, lactate is converted to pyruvate by lactate dehydrogenase and enters the tricarboxylic acid (TCA) cycle providing the cell with ATP [60]. While lactate has long been associated with stress responses of the brain which are characterized by increased cerebral energy demand, OXPHOS increases have been recently reported in neurodevelopment and in normal brain function [56, 61]. In in-vitro studies, exogenous lactate contribution to neuronal OXPHOS has been estimated to be around 75%, while only 25% was contributed to glucose metabolism [62].

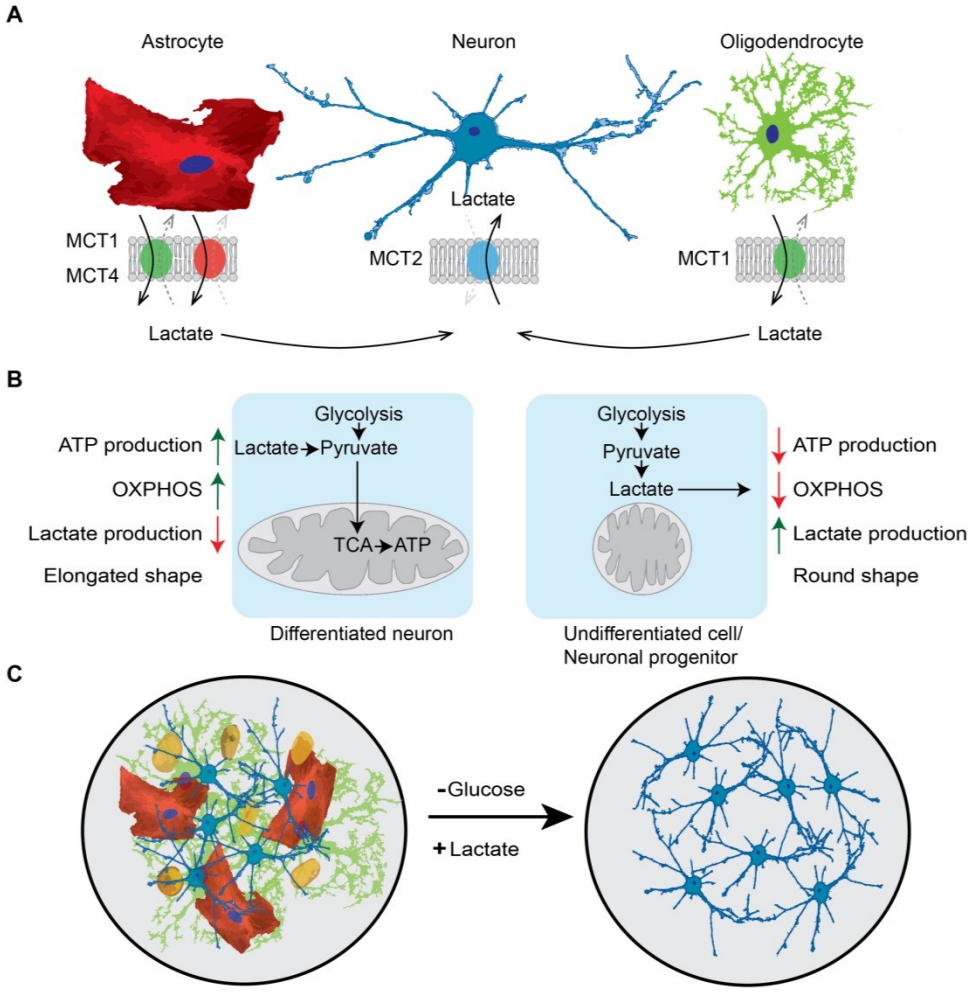

Fig 2. Metabolic selection by glucose deprivation and lactate supplementation (GDLS).

(A) *Principles of a neuronal lactate shuttle. MCT1 and 4 transport lactate to the extracellular space, to be taken up by the high affinity transporter MCT2.* ***(B)*** *While differentiated neurons are able to metabolise lactate, progenitor cells and undifferentiated cells cannot metabolise lactate. Consequently, mitochondrial OXPHOS and subsequent ATP production, are lower compared to neuronal cells.* ***(C)*** *Combining the principles from (A) and (B) using GDLS results in metabolic selection of neuronal cells.*

In GDLS, a combination of the above described processes allows the purification of neuronal populations from iPSC differentiations. Undifferentiated cells are heavily dependent on glucose, while differentiated neurons can depend on MCT2-mediated transport of lactate. Contaminating astrocytes are less efficient at transporting and metabolising lactate, leading to purified cultures of neuronal cells. GDLS thereby provides the stem cell community with a new, economical and time-efficient tool to purify neuronal cells. Furthermore, GDLS adds an important piece of evidence to the ANLS hypothesis.

Progerin-induced ageing in iPS cell culture applications

The road to pluripotency leads to many cellular alterations, including the above described metabolic alterations [43]. These alterations result in iPSCs stemness, but also rejuvenate these cells [63]. While this makes iPSCs suitable for long-term culture and transplantation purposes, it hampers the ability to use these cells in disease modelling. Removal of epigenetic marks associated with ageing, telomere extension, increased nuclear stability and increases in autophagy are all associated with the rejuvenation process and render differentiated cells less suitable to study late-onset diseases [63, 64]. To overcome this challenge, Miller et al. introduced a method to age cells using the protein progerin [65]. Progerin was discovered as the disease causing protein in the Hutchinson-Gilford Progeria Syndrome (HGPS) and its expression recaptures many hallmarks associated with cellular ageing. While the approach by Miller et al. provides an easily applicable method, there are some drawbacks to their use of modified RNA. The transfection-induced toxicity by this method causes high level of cell death even in control cultures and, consequently, can only be applied for a limited number of days [65]. To provide another toolset for cell ageing studies based on progerin expression, Chapter 5 introduces a lentiviral approach to achieve expression. Using this approach, expression of progerin can be maintained for over 30 DIV without major toxicity associated with the

expression method. This allows the cells to be studied for prolonged culture duration and shows an indirect effect on mitochondrial function. The use of cardiomyocytes (CMs) was considered for practical reasons, since these cells are relatively easy to differentiate, are post-mitotic, and have a high mitochondrial metabolism. Moreover, due their large flat soma, progerin expression and its effects can be easily observed and evaluated with immunocytochemistry. At the end of chapter 5, a conditional promoter system specific for CM is introduced, which is currently being used to validate earlier findings and assess bioenergetics function using the Seahorse XF analyser. Figure 3 captures the principles of iPSC rejuvenation, and the rationale behind progerin-induced ageing.

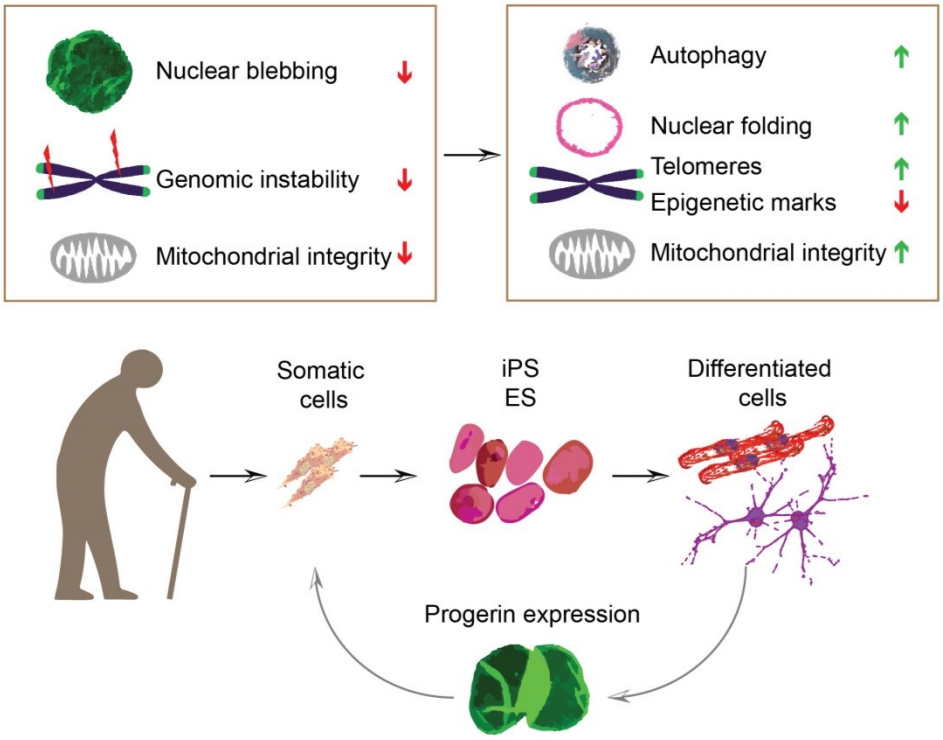

Figure 3. Progerin-induced ageing in stem cell culture applications. *Aged somatic cells are characterized by nuclear deformation, genomic instability and decreased mitochondrial integrity. The process of reprogramming effectively rejuvenates these somatic cells and their differentiated counterparts. This*

improves nuclear folding and protein homeostasis, increases telomere length and removes senescent epigenetic marks, and increases mitochondrial integrity. Using progerin expression, several of the hallmarks associated with senescent cells are recaptured.

Cellular ageing was thought to be a process governed by cell division after the Hayflick experiments in 1961 which indicated that cells do not divide indefinitely [66]. At around fifty cell divisions, fibroblast cells slow their doubling speed and eventually enter cellular senescence. The concept of replicative senescence remained and the underlying mechanisms have been well studied over the years. Amongst the complex processes underlying cellular ageing are: a decrease in mitochondrial integrity [67], nuclear instability [68], telomere attrition [69] and altered protein homeostasis [70]. Because interplay between these processes usually results in cellular senescence, the combined effects of these processes are difficult to study. Decreased nuclear stability as seen in HGPS, can indirectly lead to mitochondrial stress, which in turn can lead to increase in ROS production and DNA damage. For further reading on the processes underlying ageing, a review by Lopez-Otin et al. provides an excellent overview [71].

Chapter 5 highlights hallmarks of ageing that are more easily quantifiable, such as genomic instability and mitochondrial integrity. Skin fibroblast cells from aged individuals often present impaired protein homeostasis, nuclear deformation, genomic instability, epigenetic alterations, shortened telomeres and decreased mitochondrial integrity [72]. These hallmarks are countered by iPSC reprogramming, which increases protein homeostasis, increases mitochondrial integrity, improves nuclear folding and extends telomeres [63]. Expressing progerin reverses part of the rejuvenation process, leading to an increase in nuclear deformation and genomic instability and a decrease in mitochondrial integrity. While the model does not recapitulate all hallmarks of cellular senescence, it is more suited compared to conventional methods which often use toxins [73] or impair functions of

the DNA repair machinery [74]. In post-mitotic cell cultures, cells are less affected by DNA damage and the ability to model ageing using progerin provides a good alternative. Future experiments using progerin will focus on mitochondrial respiration to determine which complexes are most affected. In these experiments performed in collaboration with the Dept. of Experimental Cardiology UMCG, the focus will be on exposing the link between nuclear deformation and mitochondrial dysfunction.

Future research

Further investigation of mitochondrial trafficking in iPSC-derived DA neurons could make use of mitochondrial labelling in individual DA neurons. This can be achieved using a tissue-specific promoter, in this case the human synapsin promoter [75] or the human tyrosine hydroxylase promoter [76], and generating stable cell lines with this construct. Mixing labelled iPSCs with non-labelled iPSCs will allow the study of retro- and anterograde trafficking in PD DA neurons in-vitro, as it will allow mitochondria to be followed even in dense neuronal cultures. Comparing the trafficking dynamics of PD DA neurons to control DA neurons, can provide insights into the early events that lead to PD. Next, rescue of the trafficking deficiencies by davenutide might clarify involvement of the microtubule system in the observed trafficking deficiencies. Further studies of DA neurons in these settings could involve the use of brain organoids. First described in 2012, these organoids are the product of self-organization of neural stem cells, and effectively model a mini-brain in a spinning bioreactor [77]. Since then, brain organoids from different brain regions have been produced, and midbrain organoids contain functional dopaminergic and melanin-producing neurons [78, 79].

Another revolution in biomedical research recently took place involving the use of the prokaryotic clustered regularly interspaced short palindromic repeats/Cas (CRISPR/Cas) adaptive immune system of bacteria [80] to facilitate genome editing. While genome editing methods were already available [81, 82], the ease of use and efficacy of CRISPR-based genome editing have promoted its widespread use. Combining

iPSC- and CRISPR-technology will allow researchers to study disease-causing mutations in a similar genetic background. Genome-wide association studies have identified several single-nucleotide polymorphisms (SNP) in the *SNCA* and *MAPT* loci [6], but the mechanisms underlying the potential increased risks associated with these SNPs have not yet been elucidated. Using CRISPR on hESCs or hiPSCs to induce these SNPs and compare these cells to their isogenic controls, will provide new insight into the disease mechanisms. In 2016, Soldner et al. have proven the feasibility of this approach by showing that a PD-associated SNP causes increased α-synuclein expression via the modulation of a distal enhancer element [83]. Combining CRISPR technology to generate PD lines with isogenic controls and researching these cells in ventral midbrain organoids will surely lead to a better understanding of PD.

Other advancements in cell culture have come in the form of more specific cell culture media. It is now widely recognized that functional maturation of specific cell types in-vitro is dependent of the mineral and nutrient mixture provided in the medium and recently this awareness has generated a new neuronal medium that supports synaptic function [84]. By mimicking the composition of cerebrospinal fluid, the brain's normal physiological levels of salts, glucose, osmolarity and pH can be reached. This facilitates the functional maturation of differentiated neuronal cultures. However, while this media composition uses a lower glucose level compared to the widely used Neurobasal™ media, it still has a low amount of carboxylates in the form of sodium pyruvate. To more carefully mimic a brain physiological condition, lactate supplementation should be considered as an addition to this medium. In mixed culture conditions lactate can be produced and exported by astrocytic cells, but in more pure differentiations these cells are underrepresented. Furthermore, a study on the rat MCT2 illustrates that this transporter has a higher affinity for lactate [85], making it a suitable energy substrate alongside sodium pyruvate.

Finally, the second half of this decade marks the revival of nigrostriatal grafting. Similar trials as undertaken by the end of the 90's century were halted after mixed results [86-88]. Nevertheless, renewed interest partially fuelled by iPSC technology has resulted in the approval for engraftment of fetal mesencephalic dopamine neuronal precursor cells. While the number of patients enrolled is low, anticipation of these studies is high, as these studies pave the way for the use of human ESC-derived Neural Precursor Cells. Set to start in 2017, a study using these cells will run until 2020, and time will tell if the clinical benefits outweigh the potential risks. But with constant improvements in neuronal cell culture and the ever-increasing knowledge of PD, we might finally be able to prevent and/or cure the disease in at the beginning of the third century of PD research.

References

1. Kalia LV, Lang AE. Parkinson's disease. **Lancet**. 2015;386:896-912.
2. Braak H, Del Tredici K, Rub U et al. Staging of brain pathology related to sporadic Parkinson's disease. **Neurobiology of aging**. 2003;24:197-211.
3. Katzenschlager R, Lees AJ. Treatment of Parkinson's disease: levodopa as the first choice. **Journal of neurology**. 2002;249 Suppl 2:II19-24.
4. Jankovic J. Parkinson's disease: clinical features and diagnosis. **Journal of neurology, neurosurgery, and psychiatry**. 2008;79:368-376.
5. Huang Y, Cheung L, Rowe D et al. Genetic contributions to Parkinson's disease. **Brain research Brain research reviews**. 2004;46:44-70.
6. Nalls MA, Pankratz N, Lill CM et al. Large-scale meta-analysis of genome-wide association data identifies six new risk loci for Parkinson's disease. **Nature genetics**. 2014;46:989-993.
7. Takahashi K, Tanabe K, Ohnuki M et al. Induction of pluripotent stem cells from adult human fibroblasts by defined factors. **Cell**. 2007;131:861-872.
8. Thomson JA, Itskovitz-Eldor J, Shapiro SS et al. Embryonic stem cell lines derived from human blastocysts. **Science**. 1998;282:1145-1147.

9. Torrent R, De Angelis Rigotti F, Dell'Era P et al. Using iPS Cells toward the Understanding of Parkinson's Disease. **Journal of clinical medicine**. 2015;4:548-566.
10. Pacelli C, Giguere N, Bourque MJ et al. Elevated Mitochondrial Bioenergetics and Axonal Arborization Size Are Key Contributors to the Vulnerability of Dopamine Neurons. **Current biology : CB**. 2015;25:2349-2360.
11. Millecamps S, Julien JP. Axonal transport deficits and neurodegenerative diseases. **Nature reviews Neuroscience**. 2013;14:161-176.
12. DiStefano PS, Friedman B, Radziejewski C et al. The neurotrophins BDNF, NT-3, and NGF display distinct patterns of retrograde axonal transport in peripheral and central neurons. **Neuron**. 1992;8:983-993.
13. Waterham HR, Koster J, van Roermund CW et al. A lethal defect of mitochondrial and peroxisomal fission. **The New England journal of medicine**. 2007;356:1736-1741.
14. Smirnova E, Griparic L, Shurland DL et al. Dynamin-related protein Drp1 is required for mitochondrial division in mammalian cells. **Molecular biology of the cell**. 2001;12:2245-2256.
15. Chang CR, Manlandro CM, Arnoult D et al. A lethal de novo mutation in the middle domain of the dynamin-related GTPase Drp1 impairs higher order assembly and mitochondrial division. **The Journal of biological chemistry**. 2010;285:32494-32503.
16. Ishihara N, Nomura M, Jofuku A et al. Mitochondrial fission factor Drp1 is essential for embryonic development and synapse formation in mice. **Nature cell biology**. 2009;11:958-966.
17. Zuchner S, Mersiyanova IV, Muglia M et al. Mutations in the mitochondrial GTPase mitofusin 2 cause Charcot-Marie-Tooth neuropathy type 2A. **Nature genetics**. 2004;36:449-451.
18. Baloh RH, Schmidt RE, Pestronk A et al. Altered axonal mitochondrial transport in the pathogenesis of Charcot-Marie-Tooth disease from mitofusin 2 mutations. **The Journal of neuroscience : the official journal of the Society for Neuroscience**. 2007;27:422-430.
19. Pham AH, Meng S, Chu QN et al. Loss of Mfn2 results in progressive, retrograde degeneration of dopaminergic neurons in the nigrostriatal circuit. **Human molecular genetics**. 2012;21:4817-4826.
20. Weihofen A, Thomas KJ, Ostaszewski BL et al. Pink1 forms a multiprotein complex with Miro and Milton, linking Pink1 function to mitochondrial trafficking. **Biochemistry**. 2009;48:2045-2052.

21. Wang H, Song P, Du L et al. Parkin ubiquitinates Drp1 for proteasome-dependent degradation: implication of dysregulated mitochondrial dynamics in Parkinson disease. **The Journal of biological chemistry**. 2011;286:11649-11658.
22. Cheung YT, Lau WK, Yu MS et al. Effects of all-trans-retinoic acid on human SH-SY5Y neuroblastoma as in vitro model in neurotoxicity research. **Neurotoxicology**. 2009;30:127-135.
23. Borland MK, Trimmer PA, Rubinstein JD et al. Chronic, low-dose rotenone reproduces Lewy neurites found in early stages of Parkinson's disease, reduces mitochondrial movement and slowly kills differentiated SH-SY5Y neural cells. **Molecular neurodegeneration**. 2008;3:21.
24. Lee HJ, Khoshaghideh F, Lee S et al. Impairment of microtubule-dependent trafficking by overexpression of alpha-synuclein. **The European journal of neuroscience**. 2006;24:3153-3162.
25. Irrcher I, Aleyasin H, Seifert EL et al. Loss of the Parkinson's disease-linked gene DJ-1 perturbs mitochondrial dynamics. **Human molecular genetics**. 2010;19:3734-3746.
26. Fleming SM, Mulligan CK, Richter F et al. A pilot trial of the microtubule-interacting peptide (NAP) in mice overexpressing alpha-synuclein shows improvement in motor function and reduction of alpha-synuclein inclusions. **Molecular and cellular neurosciences**. 2011;46:597-606.
27. Korecka JA, van Kesteren RE, Blaas E et al. Phenotypic characterization of retinoic acid differentiated SH-SY5Y cells by transcriptional profiling. **PloS one**. 2013;8:e63862.
28. Danzer KM, Haasen D, Karow AR et al. Different species of alpha-synuclein oligomers induce calcium influx and seeding. **The Journal of neuroscience : the official journal of the Society for Neuroscience**. 2007;27:9220-9232.
29. Camilleri A, Zarb C, Caruana M et al. Mitochondrial membrane permeabilisation by amyloid aggregates and protection by polyphenols. **Biochimica et biophysica acta**. 2013;1828:2532-2543.
30. Surmeier DJ. Calcium, ageing, and neuronal vulnerability in Parkinson's disease. **The Lancet Neurology**. 2007;6:933-938.
31. Sheng ZH. Mitochondrial trafficking and anchoring in neurons: New insight and implications. **The Journal of cell biology**. 2014;204:1087-1098.

32. Kang JS, Tian JH, Pan PY et al. Docking of axonal mitochondria by syntaphilin controls their mobility and affects short-term facilitation. **Cell**. 2008;132:137-148.
33. Sousa VL, Bellani S, Giannandrea M et al. {alpha}-synuclein and its A30P mutant affect actin cytoskeletal structure and dynamics. **Molecular biology of the cell**. 2009;20:3725-3739.
34. Esposito A, Dohm CP, Kermer P et al. alpha-Synuclein and its disease-related mutants interact differentially with the microtubule protein tau and associate with the actin cytoskeleton. **Neurobiology of disease**. 2007;26:521-531.
35. Oikawa T, Nonaka T, Terada M et al. alpha-Synuclein Fibrils Exhibit Gain of Toxic Function, Promoting Tau Aggregation and Inhibiting Microtubule Assembly. **The Journal of biological chemistry**. 2016;291:15046-15056.
36. Wang G, Huang Y, Chen W et al. Variants in the SNCA gene associate with motor progression while variants in the MAPT gene associate with the severity of Parkinson's disease. **Parkinsonism & related disorders**. 2016;24:89-94.
37. Gozes I, Divinski I. NAP, a neuroprotective drug candidate in clinical trials, stimulates microtubule assembly in the living cell. **Current Alzheimer research**. 2007;4:507-509.
38. Matsuoka Y, Gray AJ, Hirata-Fukae C et al. Intranasal NAP administration reduces accumulation of amyloid peptide and tau hyperphosphorylation in a transgenic mouse model of Alzheimer's disease at early pathological stage. **Journal of molecular neuroscience : MN**. 2007;31:165-170.
39. Boxer AL, Lang AE, Grossman M et al. Davunetide in patients with progressive supranuclear palsy: a randomised, double-blind, placebo-controlled phase 2/3 trial. **The Lancet Neurology**. 2014;13:676-685.
40. Ivashko-Pachima Y, Sayas CL, Malishkevich A et al. ADNP/NAP dramatically increase microtubule end-binding protein-Tau interaction: a novel avenue for protection against tauopathy. **Molecular psychiatry**. 2017.
41. Zhang J, Nuebel E, Daley GQ et al. Metabolic regulation in pluripotent stem cells during reprogramming and self-renewal. **Cell stem cell**. 2012;11:589-595.
42. Dzeja PP, Terzic A. Phosphotransfer networks and cellular energetics. **The Journal of experimental biology**. 2003;206:2039-2047.
43. Folmes CD, Nelson TJ, Terzic A. Energy metabolism in nuclear reprogramming. **Biomarkers in medicine**. 2011;5:715-729.

44. Kida YS, Kawamura T, Wei Z et al. ERRs Mediate a Metabolic Switch Required for Somatic Cell Reprogramming to Pluripotency. **Cell stem cell**. 2015;16:547-555.
45. Varum S, Rodrigues AS, Moura MB et al. Energy metabolism in human pluripotent stem cells and their differentiated counterparts. **PloS one**. 2011;6:e20914.
46. Moussaieff A, Rouleau M, Kitsberg D et al. Glycolysis-mediated changes in acetyl-CoA and histone acetylation control the early differentiation of embryonic stem cells. **Cell metabolism**. 2015;21:392-402.
47. Ryall JG, Cliff T, Dalton S et al. Metabolic Reprogramming of Stem Cell Epigenetics. **Cell stem cell**. 2015;17:651-662.
48. Ryan SD, Dolatabadi N, Chan SF et al. Isogenic human iPSC Parkinson's model shows nitrosative stress-induced dysfunction in MEF2-PGC1alpha transcription. **Cell**. 2013;155:1351-1364.
49. Reinhardt P, Schmid B, Burbulla LF et al. Genetic correction of a LRRK2 mutation in human iPSCs links parkinsonian neurodegeneration to ERK-dependent changes in gene expression. **Cell stem cell**. 2013;12:354-367.
50. Hu BY, Weick JP, Yu J et al. Neural differentiation of human induced pluripotent stem cells follows developmental principles but with variable potency. **Proceedings of the National Academy of Sciences of the United States of America**. 2010;107:4335-4340.
51. Tsankov AM, Akopian V, Pop R et al. A qPCR ScoreCard quantifies the differentiation potential of human pluripotent stem cells. **Nature biotechnology**. 2015;33:1182-1192.
52. Woodard CM, Campos BA, Kuo SH et al. iPSC-derived dopamine neurons reveal differences between monozygotic twins discordant for Parkinson's disease. **Cell reports**. 2014;9:1173-1182.
53. Pellerin L, Pellegri G, Bittar PG et al. Evidence supporting the existence of an activity-dependent astrocyte-neuron lactate shuttle. **Developmental neuroscience**. 1998;20:291-299.
54. Chih CP, Roberts Jr EL. Energy substrates for neurons during neural activity: a critical review of the astrocyte-neuron lactate shuttle hypothesis. **Journal of cerebral blood flow and metabolism : official journal of the International Society of Cerebral Blood Flow and Metabolism**. 2003;23:1263-1281.
55. Laughton JD, Bittar P, Charnay Y et al. Metabolic compartmentalization in the human cortex and hippocampus: evidence for a cell- and region-

specific localization of lactate dehydrogenase 5 and pyruvate dehydrogenase. **BMC neuroscience**. 2007;8:35.
56. Machler P, Wyss MT, Elsayed M et al. In Vivo Evidence for a Lactate Gradient from Astrocytes to Neurons. **Cell metabolism**. 2016;23:94-102.
57. Erlichman JS, Hewitt A, Damon TL et al. Inhibition of monocarboxylate transporter 2 in the retrotrapezoid nucleus in rats: a test of the astrocyte-neuron lactate-shuttle hypothesis. **The Journal of neuroscience : the official journal of the Society for Neuroscience**. 2008;28:4888-4896.
58. Halestrap AP. The monocarboxylate transporter family--Structure and functional characterization. **IUBMB life**. 2012;64:1-9.
59. Lee Y, Morrison BM, Li Y et al. Oligodendroglia metabolically support axons and contribute to neurodegeneration. **Nature**. 2012;487:443-448.
60. Mason S. Lactate Shuttles in Neuroenergetics-Homeostasis, Allostasis and Beyond. **Frontiers in neuroscience**. 2017;11:43.
61. Goyal MS, Hawrylycz M, Miller JA et al. Aerobic glycolysis in the human brain is associated with development and neotenous gene expression. **Cell metabolism**. 2014;19:49-57.
62. Bouzier-Sore AK, Voisin P, Bouchaud V et al. Competition between glucose and lactate as oxidative energy substrates in both neurons and astrocytes: a comparative NMR study. **The European journal of neuroscience**. 2006;24:1687-1694.
63. Lapasset L, Milhavet O, Prieur A et al. Rejuvenating senescent and centenarian human cells by reprogramming through the pluripotent state. **Genes & development**. 2011;25:2248-2253.
64. Rando TA, Chang HY. Aging, rejuvenation, and epigenetic reprogramming: resetting the aging clock. **Cell**. 2012;148:46-57.
65. Miller JD, Ganat YM, Kishinevsky S et al. Human iPSC-based modeling of late-onset disease via progerin-induced aging. **Cell stem cell**. 2013;13:691-705.
66. Hayflick L, Moorhead PS. The serial cultivation of human diploid cell strains. **Experimental cell research**. 1961;25:585-621.
67. Wiley CD, Velarde MC, Lecot P et al. Mitochondrial Dysfunction Induces Senescence with a Distinct Secretory Phenotype. **Cell metabolism**. 2016;23:303-314.
68. Oberdoerffer P, Sinclair DA. The role of nuclear architecture in genomic instability and ageing. **Nature reviews Molecular cell biology**. 2007;8:692-702.

69. Allsopp RC, Vaziri H, Patterson C et al. Telomere length predicts replicative capacity of human fibroblasts. **Proceedings of the National Academy of Sciences of the United States of America**. 1992;89:10114-10118.
70. Koga H, Kaushik S, Cuervo AM. Protein homeostasis and aging: The importance of exquisite quality control. **Ageing research reviews**. 2011;10:205-215.
71. Lopez-Otin C, Blasco MA, Partridge L et al. The hallmarks of aging. **Cell**. 2013;153:1194-1217.
72. Tigges J, Krutmann J, Fritsche E et al. The hallmarks of fibroblast ageing. **Mechanisms of ageing and development**. 2014;138:26-44.
73. Shamoto-Nagai M, Maruyama W, Kato Y et al. An inhibitor of mitochondrial complex I, rotenone, inactivates proteasome by oxidative modification and induces aggregation of oxidized proteins in SH-SY5Y cells. **Journal of neuroscience research**. 2003;74:589-597.
74. Niedernhofer LJ, Garinis GA, Raams A et al. A new progeroid syndrome reveals that genotoxic stress suppresses the somatotroph axis. **Nature**. 2006;444:1038-1043.
75. Kugler S, Kilic E, Bahr M. Human synapsin 1 gene promoter confers highly neuron-specific long-term transgene expression from an adenoviral vector in the adult rat brain depending on the transduced area. **Gene therapy**. 2003;10:337-347.
76. Oh MS, Hong SJ, Huh Y et al. Expression of transgenes in midbrain dopamine neurons using the tyrosine hydroxylase promoter. **Gene therapy**. 2009;16:437-440.
77. Lancaster MA, Renner M, Martin CA et al. Cerebral organoids model human brain development and microcephaly. **Nature**. 2013;501:373-379.
78. Jo J, Xiao Y, Sun AX et al. Midbrain-like Organoids from Human Pluripotent Stem Cells Contain Functional Dopaminergic and Neuromelanin-Producing Neurons. **Cell stem cell**. 2016;19:248-257.
79. Monzel AS, Smits LM, Hemmer K et al. Derivation of Human Midbrain-Specific Organoids from Neuroepithelial Stem Cells. **Stem cell reports**. 2017;8:1144-1154.
80. Cong L, Ran FA, Cox D et al. Multiplex genome engineering using CRISPR/Cas systems. **Science**. 2013;339:819-823.
81. Cermak T, Doyle EL, Christian M et al. Efficient design and assembly of custom TALEN and other TAL effector-based constructs for DNA targeting. **Nucleic acids research**. 2011;39:e82.

82. Bibikova M, Beumer K, Trautman JK et al. Enhancing gene targeting with designed zinc finger nucleases. **Science**. 2003;300:764.
83. Soldner F, Stelzer Y, Shivalila CS et al. Parkinson-associated risk variant in distal enhancer of alpha-synuclein modulates target gene expression. **Nature**. 2016;533:95-99.
84. Bardy C, van den Hurk M, Eames T et al. Neuronal medium that supports basic synaptic functions and activity of human neurons in vitro. **Proceedings of the National Academy of Sciences of the United States of America**. 2015;112:E2725-2734.
85. von Grumbckow L, Elsner P, Hellsten Y et al. Kinetics of lactate and pyruvate transport in cultured rat myotubes. **Biochimica et biophysica acta**. 1999;1417:267-275.
86. Lindvall O. Update on fetal transplantation: the Swedish experience. **Movement disorders : official journal of the Movement Disorder Society**. 1998;13 Suppl 1:83-87.
87. Olanow CW, Goetz CG, Kordower JH et al. A double-blind controlled trial of bilateral fetal nigral transplantation in Parkinson's disease. **Annals of neurology**. 2003;54:403-414.
88. Freed CR, Greene PE, Breeze RE et al. Transplantation of embryonic dopamine neurons for severe Parkinson's disease. **The New England journal of medicine**. 2001;344:710-719.

Chapter 7

Nederlandse Samenvatting

Belangrijkste bevindingen

- Overexpressie van α-synucleïne leidt tot een afname van mitochondrieel transport en productie van zuurstofradicalen in een SH-SY5Y celmodel voor Parkinson
- Deze effecten van α-synucleïne kunnen worden tenietgedaan door toediening van davunetide, een microtubuli stabiliserend eiwit
- Glucose depletie en lactaat supplementatie kan worden gebruikt om uit iPS cellen gedifferentieerde neuronen te zuiveren en vindt plaatst via monocarboxylaat transporter 2
- Neuronen gedifferentieerd uit iPS cellen van Parkinson patiënten vertonen een afname van mitochondrieel transport
- Progerin expressie kan worden gebruikt om kenmerken van veroudering in gedifferentieerde iPS cellen na te bootsen

De ziekte van Parkinson is een progressieve neurodegeneratieve aandoening die wordt gekenmerkt door het verlies van dopaminerge neuronen in de substantia nigra pars compacta. Het tekort aan de neurotransmitter dopamine is verantwoordelijk voor de meeste symptomen, waaronder; moeite met lopen, traagheid van bewegen, spasmen, rigiditeit en een rusttremor. Daarnaast kan in de latere stadia van de ziekte dementie ontstaan en is er vaak sprake van mentale stoornissen zoals depressie. Verreweg de meeste gevallen van de ziekte zijn idiopathisch en vertonen een uiteenlopend ziektebeeld. Bij de meeste

vormen van de ziekte komen eiwit aggregaten voor die Lewy bodies genoemd worden. Dit pathologische kenmerk komt niet enkel voor in dopaminerge neuronen van de substantia nigra, maar is ook aanwezig in het enterisch zenuwstelsel en in andere delen van het centraal zenuwstelsel. In 2003 werd een patroon van verspreiding van de ziekte beschreven, dat tegenwoordig bekend staat als de Braak-hypothese. Hoewel de hypothese niet onomstreden is, heeft het de basis gelegd voor het begrijpen van het progressieve karakter van de aandoening. Voordat dopaminerge neuronen zijn aangedaan, zijn Lewy bodies zichtbaar in andere hersengebieden, zoals de pons en de medulla. Dit geeft aan dat er een verhoogde gevoeligheid lijkt te zijn in de dopaminerge neuronen van de substantia nigra. In latere stadia zijn de hogere hersengebieden aangedaan waarbij dementie kan optreden, hetgeen toont dat ook andere neuronen worden aangedaan door de aandoening. De verhoogde gevoeligheid van dopaminerge neuronen in de substantia nigra komt waarschijnlijk voort uit de unieke eigenschappen van deze neuronen. Grote intrinsieke activiteit zorgt voor een hoge metabole belasting, met als gevolg dat de neuronen meer worden blootgesteld aan zuurstofradicalen. Daarnaast worden de neuronen gekenmerkt door grote en complexe axonale structuren. Dit maakt de neuronen gevoelig voor afwijkingen in het intracellulair transport. Hoewel de oorzaak voor de idiopathische vorm niet bekend is zijn er aanwijzingen uit erfelijke vormen van de ziekte. Familiaire Parkinson werd in 1997 gekoppeld aan een mutatie in het *SNCA* gen, dat codeert voor het eiwit α-synucleïne. Kort na de ontdekking van deze vorm van Parkinson, werd α-synucleïne geïdentificeerd als een belangrijke component in Lewy bodies in de idiopathische vorm van de aandoening.

Een ander pathologisch kenmerk dat is gekoppeld aan Parkinson is mitochondriële dysfunctie. Na injectie van een verkeerd gesynthetiseerd opiaat, waarbij de stof MPTP was gevormd, vertoonden mensen Parkinson-achtige verschijnselen in het jaar 1976. MPTP werd omgezet door gliacellen in MPP+ wat werd opgenomen door dopaminerge

neuronen. De resulterende mitochondriële dysfunctie zorgde voor een selectieve dood van dopaminerge neuronen, waardoor de link werd gelegd tussen mitochondriële dysfunctie en Parkinson. Sinds deze ontdekkingen zijn vele studies naar α-synucleïne en mitochondria gedaan in relatie tot de ziekte van Parkinson, maar een mechanisme dat deze twee kenmerken verbindt is nog onduidelijk. De relatie tussen α-synucleïne en mitochondriële dysfunctie wordt in dit proefschrift verder onderzocht. Hierbij steunt het proefschrift op de hypothese dat veranderingen in intracellulair transport ten gevolge van afwijkende α-synucleïne expressie resulteren in mitochondriële dysfunctie.

Hoofdstuk 1 bevat een algemene samenvatting, waarin, naast de huidige stand van onderzoek, ook de onderzoeksgeschiedenis van de ziekte van Parkinson behandeld wordt. Daarnaast worden cellulaire onderzoekmodellen, waarvan enkele ook in dit proefschrift toegepast worden, besproken die gebruikt worden om het ontstaan en de ontwikkeling van de ziekte van Parkinson te bestuderen. De focus van de inleiding is gericht op mitochondriaal transport en de mogelijke eigenschappen van α-synucleïne die tot verstoringen in intracellulair transport kunnen leiden.

In **Hoofdstuk 2** werd gebruikt gemaakt van het meest voorkomende celmodel in Parkinson onderzoek, de neuroblastoom cellijn SH-SY5Y. In deze cellen werd normaal en gemuteerd α-synucleïne tot over-expressie gebracht, waarna ze gedifferentieerd werden tot neuronale cellen. Vervolgens werd in deze cellen gekeken naar de effecten op mitochondriaal transport. Hierbij bleek over-expressie van A53T-gemuteerd α-synucleïne een negatief effect te hebben op dit transport. Mitochondrieel transport van het axon naar het cellichaam was als eerste aangedaan en later werd ook transport van het cellichaam naar het axon aangetast. Oxidatieve stress ten gevolge van α-synucleïne over-expressie was significant verhoogd in alle over-expressie condities ten opzichte van controle cellen en was het hoogste in de A53T cellijn. Om mitochondrieel transport te herstellen, werden de cellen behandeld met

davunetide. Davunetide stabiliseert het microtubulaire netwerk, waardoor het mitochondriaal transport herstelde tot het niveau van controle cellen. Daarnaast reduceerde davenutide de oxidatieve stress die gepaard ging met over-expressie, in alle α-synucleïne condities.

Om deze experimenten te kunnen herhalen in neuronen gedifferentieerd uit geïnduceerde pluripotente stamcellen (iPS), verkregen uit huidbiopten van Parkinson patiënten, introduceert **Hoofdstuk 3** een methode om neuronale cellen te purificeren uit kweken met verschillende celtypen. Hierbij wordt gebruik gemaakt van de astrocyt-neuron lactaat transport hypothese. Kortweg beschrijft de hypothese dat astrocyten lactaat produceren uit glucose en dit afstaan aan neuronen om de neuronale energiebehoefte te ondersteunen. Bij de differentiatie van iPS cellen naar dopaminerge neuronen, worden verschillende andere celtypen geproduceerd en blijven doorgaans ook pluripotente cellen achter. Deze cellen zijn grotendeels afhankelijk van glucosemetabolisme en kunnen lactaat niet als metabool substraat gebruiken. Door kweken na 24 dagen te ontdoen van glucose en enkel te voorzien van lactaat, is het mogelijk de kweken selectief op te zuiveren voor neuronen. Daarnaast werd getoond dat deze purificatiemethode afhankelijk is van monocarboxylaat transporter 2 (MCT2). Door de werking van MCT2 te remmen met de stof 4-CIN, werd aangetoond dat neuronaal lactaat transport inderdaad plaatsvond via deze transporter. Celkweken die de selectie ondergingen vertoonden verrijking voor neuronale cellen, maar onder behandeling van 4CIN stierven er ook neuronen af.

Bovenstaande methode werd vervolgens toegepast, in **Hoofdstuk 4** op kweken van dopaminerge neuronen verkregen uit iPS cellen van Parkinson patiënten. Door deze culturen te verrijken voor neuronen was het mogelijk om de totale hoeveelheid mitochondrieel transport in Parkinson neuronen te vergelijken met die in controle neuronen. Daarnaast maakt de methode het mogelijk om neuronen tot 90 dagen in kweek te houden, zodat er gekeken kan worden naar fysiologische

processen zonder gebruik van mitochondriële toxines. Uit de analyse bleek dat mitochondrieel transport significant verminderd was in neuronen van patiënten met een A53T α-synucleïne mutatie en een α-synucleïne triplicatie ten opzichte van controle neuronen. Bovendien vertoonden de mitochondria van patiëntcellen een ronde morfologie, een uiting van mitochondriële stress, terwijl mitochondria in controlecellen in alle condities langgerekt waren.

Hoewel de data in hoofdstuk 4 een pathologisch effect lieten zien, is het kweken van iPS cellen erg lastig omdat de cellen effectief 'verjongd' worden in het herprogrammeringsproces. Cellen moeten daarom vaak lang in kweek worden gehouden en vertonen doorgaans geen ziektebeeld in een kweekschaal.

Om de effecten van veroudering na te bootsen introduceert **Hoofdstuk 5** een methode gebaseerd op de ziekte Progeria. Door progerin, het eiwit wat verantwoordlelijk is voor de aandoening, tot expressie te brengen werden cellen verouderd. Voor het opzetten van de methode werden cardiomyocyten gebruikt, omdat deze cellen makkelijker zijn te differentiëren en makkelijker met virus te infecteren zijn in vergelijking met neuronen. De experimenten met transgene progerin-expressie laten zien dat progerin DNA schade induceert. Daarnaast vindt er mitochondriële dysfunctie plaats ten gevolge van progerin-expressie. Dopaminerge neuronen uit iPS cellen van Parkinson patiënten vertoonden een hogere hoeveelheid fluorescent signaal voor α-synucleïne na progerin over-expressie in vergelijking tot controle cellen. Dit is waarschijnlijk het gevolg van een slechte eiwit huishouding en wellicht een indirecte consequentie van mitochondriële dysfunctie. De experimenten in cardiomyocyten zullen worden voortgezet met een conditionele promoter voor cardiomyocyten en zullen worden gebruikt om eerdere resultaten te verifiëren en het onderliggend mechanisme van mitochondriële dysfunctie verder te onderzoeken.

Hoofdstuk 6 sluit af met een samenvatting en discussie over de onderzoeksresultaten in dit proefschrift. De voor- en nadelen van de gebruikte celmodellen worden besproken en er wordt een visie gegeven op mogelijke toekomstige experimenten. De studies in dit proefschrift laten zien dat mitochondrieel transport is aangetast in celmodellen voor de ziekte van Parkinson, maar de onderliggende oorzaak van de dysfunctie is nog niet bekend. De introductie van een celkweeksysteem waar, onder expressie van de tyrosine hydroxylase promotor, enkel mitochondria van dopaminerge neuronen worden gemarkeerd, is een volgende logische stap om de mitochondriële dysfunctie in dopaminerge neuronen verder te onderzoeken. Daarnaast valt er een verbetering te behalen in het gebruik van neuronale cel media. De komst van specifieke media voor neuronen zorgt voor meer fysiologische kweekomstandigheden, die verder verbeterd kunnen worden door lactaat toe te voegen.

Het inzicht over de ziekte van Parkinson, dat wordt verkregen met de komst van nieuwe technieken en onderzoeksmethodes, zal de komende jaren nieuwe therapeutische kandidaten opleveren.

Dankwoord

Het volgen van een PhD traject is een weg die is gevuld met hoogte- en dieptepunten. In mijn geval heb ik flinke dieptepunten doorgemaakt, en zonder de steun van familie, vrienden en collega's was het voor mij zwaar geweest mijn promotietraject te voltooien. Een dankwoord is in mijn thesis dus zeker op zijn plek.

Allereerst wil ik mijn promotor Prof. **Erik Boddeke** en co-promotor Dr. **Sjef Copray** bedanken voor hun supervisie tijdens mijn project. Ik herinner me dat ik onwetend binnen kwam in de wereld van het stamcelonderzoek, vol optimisme en energie over de taak die voor me lag. Hoewel onze originele plannen ingrijpend gewijzigd zijn, is het toch gelukt om een goed project neer te zetten. Dit is grotendeels te danken aan de samenwerking die we in de jaren hebben gehad.

Beste **Sjef**, ik zal me eerst tot jou richten, aangezien je mij in de dagelijkse supervisie het meeste hebt geholpen. Voor een nieuwe generatie PhD kandidaten is het wellicht al niet meer bekend, maar je bent degene die iPS onderzoek in het UMCG groot heeft gemaakt. Door tal van samenwerkingen en het delen van kennis leeft het iPS onderzoek nu voort in het UMCG. Wellicht zijn we beiden af en toe wat te vrijgevig geweest in het delen van onze kennis, maar ik ben van mening dat samenwerking het belangrijkste aspect van wetenschap is. Bedankt voor alles wat je me in de afgelopen jaren hebt geleerd.

Erik, hoewel we in eerste instantie wat minder vaak contact hadden, hebben we in de laatste jaren intensiever samengewerkt. In je nieuwe functie als pro-decaan wist je toch tijd te vinden om me door het laatste stadium van mijn PhD te loodsen, waardoor ik nog meer ontzag heb gekregen voor je werklust. Mijn beste herinnering blijft toch de labdag bij je thuis, waarbij we een ontzettend gezellige barbecue hebben gehad.

Hierop aansluitend wil ik **Jon Laman** bedanken voor zijn hulp in de laatste fase van het schrijven van mijn PhD thesis. Je hebt de rol van dagelijkse supervisor op je genomen en je hebt me enorm geholpen in het 'proof readen' van mijn thesis. Een betere corrector had ik me niet kunnen wensen, en ik heb veel gehad aan al je tips tijdens dit proces.

Susanne, ook jou wil ik hier even benoemen, omdat je me erg hebt geholpen met het schrijven van mijn artikel. Het was perfect om een kamergenoot te hebben die met een kritische blik kan kijken naar je werk en die veel ervaring heeft in het schrijven en opstellen van papers. Ik heb veel van je geleerd en ik hoop dat we in de toekomst wellicht weer eens samen kunnen werken. Je bent een enorm getalenteerde wetenschapper en ik hoop dat je een mooie wetenschappelijke toekomst voor de boeg hebt!

Ik wil graag de leden van de leescommissie, Prof. Dr. **Harry Kampinga**, Prof. Dr. **Teus van Laar**, Prof Dr. **Martin Smit** bedanken voor het lezen en goedkeuren van mijn thesis.

Mijn paranimfen, **Martijn Hoes** en **Remon Holsbergen** wil ik bedanken voor het vervullen van de rol van paranimf. Beste **Remon,** sinds dag 1 op de middelbare school kunnen wij het goed met elkaar vinden en hoewel we nu ver van elkaar wonen, is er nog weinig veranderd als we elkaar weer zien. Tijdens de ziekte van Maaike was je een belangrijke steun voor me. Je hebt me laten zien dat sommige vrienden voor het leven zijn en je steun heeft me erg geholpen om alles weer op de rit te krijgen. Bedankt dat je mijn paranimf wil zijn. Ik hoop dat je een mooi stukje piano zult spelen na mijn verdediging; Chopin - Nocturne Op. 27 No. 2 kan ik nog steeds meespelen in mijn hoofd.

Martijn, ouwe bromsnor met een zachte G. Hoewel je vertelde initieel een beetje bang voor me te zijn geweest, hebben we een goede vriendschap ontwikkeld waarbij we zowel wetenschappelijk als vriendschappelijk op elkaar konden bouwen. Op het lab was je een ‘steen’ in de branding voor me, maar andersom zal je dit ook over mij beweren. Ik hoop dat we nog lang kunnen genieten van de aanwezigheid van jou, **Linda, Thijs** en **Lucas** in het noorden. Er gaat niks boven Groningen, zelfs voor iemand uit Limburg.

Mijn dank gaat ook uit naar de hele sectie van de medische fysiologie. Ik ga ongetwijfeld mensen vergeten, maar ik ga toch proberen personen te benoemen. Ik begin gewoon bij **Trix**, want zonder jou gebeurt er niks. Deze uitspraak bleek in de loop der jaren ook echt op te gaan en je hebt regelmatig je nek voor me uitgestoken. Bedankt voor al je hulp in de

afgelopen jaren. **Bart**, hoewel ik in de jaren van mijn PhD niet veel met je heb samengewerkt, heb ik altijd veel respect voor je gehad en veel van je geleerd. Succes in je komende levensfase als professor, volgens mij zit je goed op je plek. **Armagan**, bedankt voor de wetenschappelijke discussies en de heerlijke baksels die je altijd meebracht naar het werk. De sinterklaasvond bij jullie thuis was een geweldige ervaring. **Inge**, ik heb erg veel plezier gehad in het spelen voor proefkonijn in je experimenten, al was ik vrij slecht in de multitasking opgaven. Ik wil je ook bedanken voor je hulp bij vragen omtrent statistiek.

Loes, hoewel het al een tijd geleden is dat je het lab hebt verlaten, wil ik je toch benoemen. Ik had geen betere analist kunnen wensen voor het inwerken op de celkweek. De precisie waarmee celkweken volgens jou dient te geschieden is zelfs nu nog merkbaar in mijn dagelijkse routine en dit is grotendeels aan jou te danken. **Nieske**, je hebt het al vaker gehoord, maar je bent een belangrijke steunpilaar in het lab. Dank voor je hulp bij mijn experimenten en ik heb leuke herinneringen aan het pannenkoeken bakken met **Jan** bij jullie thuis. **Michel**, hoewel je soms een beetje kan brommen heb ik altijd veel lol met je gehad. Daarnaast heb je me enthousiast gemaakt voor de microscopie, iets waar ik tot de dag van vandaag in geïnteresseerd ben. **Evelyn**, dank voor je hulp in de afgelopen jaren, zeker met betrekking tot qPCRs. **Ietje**, je bent altijd een luisterend oor voor mensen en je organisatie van het immunolab heeft ervoor gezorgd dat ik daar altijd perfect kon werken. **Tjalling**, verassend genoeg lagen wij vaak op dezelfde golflengte. Of dit zich nu door de ether voortbeweegt, verklaard wordt door de klankhelix van Ans Schapendonk of simpelweg verklaard wordt door aardstralen valt nog te bezien. Voorop staat dat we altijd konden lachen om de grootste pseudowetenschappelijke onzin die we tegenkwamen. En dank je voor het repareren van mijn helikopter. **Hilmar**, great help you have been assisting me making my figures. Good person and fellow nerd you are. May the force be with you! Weledelgeleerde heer **Bakels**, ik ben verheugd dat Roeland u tegenwoordig voorziet van koffie. Ik ben blij dat ik de afgelopen jaren een goede jongen kon zijn en u kon voorzien van deze koffie. **Harry**, mede dankzij jou heb ik nu een leuke baan als klinisch embryoloog in opleiding. Dank voor je hulp en voor het enthousiasmeren voor deze baan, het deed me erg goed dat je me zo onbaatzuchtig

geholpen hebt. **Hisky**!!!!! Dank voor alle gezelligheid, en de leuke avondjes borrelen. Moeten we erin houden, alhoewel het de laatste tijd niet zo goed gaat met het plannen van borrels. **Wieb**, je hebt me meermaals laten schrikken toen ik binnen liep in de koude kamer, maar tijdens de koffie was het altijd gezellig.

Dù…..Co?, je stond altijd klaar met een kritische blik, een helpende hand of om gewoon lol te maken. Ik heb aan mijn PhD goede vrienden overgehouden, en ik ben blij dat we nog regelmatig een borrel doen. Helaas wat minder vaak nu je in Enschede zit, maar wellicht verplaats je je in de toekomst wel weer richting het noorden. Dan zouden we in ieder geval nooit te laat voor de lunch zijn. **Wanderito**, ik weet niet eens wat ik hier precies neer moet zetten. De jaren dat je mijn collega was waren episch. Het is wellicht beter geweest voor mij dat je naar Spanje vertrokken bent, want we anders hadden we nog vaker tot middernacht op de bowlingbaan gestaan. Het was geweldig om met Sabrien deel uit te mogen maken van jullie bruiloft deze zomer. Alle goeds ook voor **Laura** en jou, en we zien elkaar vast snel weer! **Ilia**, ik heb altijd enorm veel respect gehad voor je doorzettingsvermogen en je wetenschappelijke integriteit. Daarnaast was je ook een erg prettige collega en een enorme nerd. Scheelt dat ik ook een enorme nerd ben, dus dat schept een band ;) Ik hoop dat je nog lang kunt genieten van je Star Wars sokken! **Inge**, ik hoop dat dit bericht je bereikt in de Matrix en dat je het goed hebt in the States! Alle goeds voor de komende jaren, maar dat zal vast wel goed komen! **Corrie**, ondanks je grumpy cat was je een van de vrolijkste collega's die ik me kon wensen. Je hebt de rol van nestor goed over genomen. Als lab oudste mag je nu de andere studenten helpen. **Rianne**, het was altijd erg gezellig, maar met de keuze voor restaurants had je aan mij toch altijd een verkeerde ;) Die sushi was niks voor mij, maar jullie kregen het toch altijd voor elkaar om iedereen mee te krijgen. Ik wens je alle geluk toe! Beste **Laura**, ik ben ervan overtuigd dat je een goede wetenschapper gaat worden. Integriteit, gecombineerd met Deutsche Gründlichkeit, dat moet wel een goed resultaat opleveren. **Malte**, ik heb veel lol met je gehad in de relatief korte periode dat je mijn collega was. Vergeet niet elke dag te ontbijten, aardappelsalade legt een goede bodem voor de dag! Succes met je toekomstige experimenten! **Marissa**, dank je voor alle gezellige avonden bij jullie thuis. Het was ook erg gezellig om te

Mario karten met **Robert**. We zullen elkaar in de toekomst vast blijven zien. **Leroy**, oude red-faced monkey! Nooit begrepen waar dat vandaan kwam, maar deze naam blijft aan je plakken. Bedankt voor alle humor in het lab, helaas wisselden we elkaar net af, want je was een collega waar ik veel lol had kunnen hebben op de werkvloer. **Ming-San**, de filmavonden met Ilia waren altijd erg gezellig. We hebben verder niet al teveel contact gehad, omdat je altijd druk was met je vele studies! Succes de komende jaren als kaakchirurg! Beste **Ria**, ik hoop dat het boekje je op een of andere manier bereikt, want we hebben elkaar al een tijd niet gezien. Je was een erg gezellige collega, je 'quitness' die een andere collega over je had opgemerkt vond ik niet helemaal op gaan :p **Roeland**, ik ben blij dat je mijn koffietaken op het lab hebt overgenomen, je bent een goede jongen! **Alain**, je bent me net voorgebleven met je PhD. Je verhalen over de Hollandse garnaal deden mijn wenkbrauwen regelmatig rijzen en het feit dat je geen blad voor je mond nam leverde vaak komische situaties op. Succes met je toekomstige wetenschappelijke carrière. **Claudio de di papedi pupedi**, je was een leuke collega om te hebben. Bedankt voor alle avondjes klimmen! **Zhuoran,** ik weet niet of je Nederlands nog steeds zo goed is, maar voor jou schrijf ik ook gewoon wat op. Je bent een lief persoon en je was een leuke collega om te hebben. Het was geweldig dat je twee keer naar Apeldoorn bent gekomen om de midwinter minimarathon te lopen en ik ben blij dat je de kat niet opgegeten hebt. Succes met je toekomstige carrière en veel geluk met **Peilin**. De groetjes van onze huiskater Tex!

On to the English speaking crowd. **Marcin**, you were an excellent colleague during my first years of PhD, thank you for teaching me the basics of iPS research. I also enjoyed climbing, barbequing and drinking outside lab hours. **Thaiany**, thank for working together on our projects over the years. You're a hard-working person, and I think together we've done some nice research! I hope you find a good place to continue in science! **Arun**, though we sometimes had our differences over the years, I have always respected you. Especially in the last years, when we were the last people working in our ML-II lab, I enjoyed your company. **Suping** a.k.a. **Soepje**, thank you for the years you were in the lab, I always enjoyed our discussions, and the Chinese food evening you, **Zhuoran** and **Zhilin** prepared was amazing. **Thais**, thank you for annoying me over the

period of the two years you were in the lab ☺. In all honesty, your energy and personality truly brought life into the lab! **Xiaoming**, having you as a roommate has been a pleasure. Over the years you have blossomed in terms of scientific and presentation skills, and I can honestly say I have a lot of respect for your perseverance. To the rest of the colleagues from the lab, **Clarissa**, **Kumar**, **Yang**, **Jade**, **Annelies**, **Javier**, **Reinhard**, **Vischnu**, **Divya**, **Annelies**, **Khayum**, **Chairi**, **Nynke**, **Annelies** and probably some people I am now forgetting… Thanks for the great time in the department! **Japser**, a.k.a. **Stoethaspuru**, bedankt voor alle mooie avonden waarop jullie mij kwamen ophalen voor het kippen fascistisch collectief. Ik had er geen invloed op; ik moest en zou mee naar die toko van jullie. Ik wens je veel geluk in de toekomst, of het nou in Nederland of Azië is! Ook dank aan de rest van de afdeling Exp. Cardiologie, waar ik me altijd welkom voelde.

During my PhD I have supervised several students, and without any specific order I would like to thank **Christine**, **Alejandra** and **Clayton**. I had a good time in the lab having you around.

Over the years there were quite some collaborations. **Floris Foijer**, bedankt voor de samenwerking omtrent het iPS-CRISPR lab. Also hanks to **Evgenia**, **Alejandra**, **Eslie**, **Mathilde**, **Daniël** and **Stefan** for keeping things interesting in the lab. **Ale**, I'm still trying to speak Spanish, but I guess it won't progress beyond ola and si for the time being. **Daan,** bedankt voor de samenwerking en de gezelligheid in en buiten het lab. Ik wens jou, **Eva** en **Janne** een mooie toekomst! Ook de andere mensen op het ERIBA waar ik bijzonder vaak te vinden was, bedankt voor de gezelligheid! **Björn Bakker**, a.k.a. **BB8**, GGGWARRRHHWWWW!!

Ook dank aan de heren van de FACS faciliteit, in het bijzonder **Roelof Jan**, **Henk** & **Geert**. Ik heb me in de tijd altijd erg vermaakt als ik bij jullie langs kwam voor een FACS experiment.

Dr. Peter van der Meer, bedankt voor de fijne samenwerking de afgelopen jaren. Ik hoop dat het lab nog lang blijft werken met stamcel technologie, en ik kom af en toe nog eens een kijkje nemen naar de cardiomyocyten.

Ook veel dank aan de imaging faciliteit van het UMCG, en in het bijzonder **Klaas Sjollema**. Klaas, ik heb ontzettend veel plezier gehad tijdens het spelen met de apparatuur in het imaging centrum. Je expertise, nieuwsgierigheid en praktische kennis over microscopen werkte erg aanstekelijk en het onderwerp heeft me tot vandaag de dag weten te boeien. Ik zal in de toekomst nog regelmatig even langskomen om te kijken wat voor mooie apparatuur jullie hebben aangeschaft. Dank voor alle hulp en je enthousiasme.

Groningen hoef ik voorlopig nog geen gedag te zeggen en ik ben blij dat ik deel mag uitmaken van het IVF team van het centrum **VPG**. **Eus**, **Janneke** en **Anemieke**, ik kijk erg uit naar de komende jaren als klinisch embryoloog in opleiding en ik wil jullie bedanken voor het vertrouwen dat jullie me hebben gegeven door me voor deze baan aan te nemen. Aan de rest van de afdeling: het bevalt me erg goed, dus ik heb er veel vertrouwens in dat ik me de komende jaren op mijn plek ga voelen!

Jedi, **Gnaip** en **Liter**, ik noem jullie even apart. Als vrienden van AP hebben we regelmatig bakjes koffie gedaan en over ons onderzoek gepraat of geklaagd. Ik heb het altijd zeer gewaardeerd en ik hoop dat we binnenkort allemaal met een glimlach op deze periode kunnen terugblikken. **AP'ers**, dank voor alle support in mindere tijden, maar vooral bedankt voor een mooie studententijd. We gaan nog veel mooie avonturen tegemoet als groep! **Koen Pouwels**, ik ben een stuk minder gaan trainen in de tijd dat je in Londen zit. Het wordt weer eens tijd om flink te gaan bankdrukken, dus ik hou je op de hoogte van de vorderingen. **Daniël**, je bent zo ongeveer de grootste droogkloot die ik ken. Nu weer helemaal op je plek in A'dam, succes in de advocatuur daar!

Alle andere vrienden in Groningen, **Lisette** & **Lizette**, **Wout**, **Astrid**, **Moart'n Henk, Fabje, Wouter, Ramon, Stefan** en **vele anderen**, bedankt voor de mooie tijden!

Kirst, **Jan**, **Tim**, **Remon**, **Dom**, **Jorine**, **Nina**, **Isabelle**, **Rachid, Ivo & Lies** en **vele andere vrienden** van middelbare school, ik vind het geweldig dat we nog steeds contact hebben en realiseer me dat het erg bijzonder is dat we zoveel leuke mensen hebben overgehouden uit deze

tijd. **Roel** , **Jits**, **Ido**, **Josje**, **Maartje**, **Onne**, bedankt voor alle leuke tijden in onze jeugd!

Emma, jou wil ik even apart noemen, omdat je een enorme steun voor me bent geweest. Tijdens de ziekte van Maaike heb je zonder nadenken je werk laten vallen en was je er om mij, mijn ouders en vooral ook Maaike te steunen. Je hebt een enorm hart en ik ben blij dat we tot op de dag van vandaag bevriend zijn. Je bent een topper!

En dan moet ik natuurlijk jou bedanken **Sabrien**. Je kwam binnen tijdens een moeilijke periode in mijn leven en je hebt flink wat dalen met me meegemaakt. Je hebt er echter ook voor gezorgd dat ik er daar weer overheen ben gekomen. Inmiddels ben ik wat kilo's zwaarder door alle troosttaarten, maar het is een kleine prijs aangezien ik weer veel gelukkiger in het leven sta. Ik had je beloofd niet teveel op te schrijven, dus ik houd het maar bij een kus. ☺

M'n ouders, **Gert** en **Marion**. Jullie hebben Maaike en mij een prachtig leven gegeven waarin we alle ruimte kregen om ons te ontwikkelen. Naarmate ik volwassener werd besefte ik beter dat we een bijzonder onbezorgde jeugd hebben gehad. We hebben op een harde manier ervaren dat het ook anders kan lopen. Ik kan echter alleen maar positief op onze jaren samen terugkijken en ik hoop dat we gaan genieten van wat voor ons ligt. Bedankt voor alle steun de afgelopen jaren!

Daarnaast wil ik ook jullie vrienden bedanken die niet alleen jullie, maar ook mij opvingen. En de vrienden van Maaike, die onbaatzuchtig alles voor Maaik en ons wilden doen.

En dan jij lieve **Maaik**. Dit is het stuk tekst waar ik het meest tegenop zag. Je had beloofd wel bij mijn verdediging te kunnen zijn nadat je mijn masteruitreiking had gemist. Dat je er nu niet bij kan zijn is nog steeds onvoorstelbaar; Mijn grote zus die me altijd aan de hand nam zodat ik niet in gevaar kwam. En die de paden voor me baande, waardoor het voor mij allemaal wat makkelijker was. Vandaag sta ik hier in het pak en de schoenen die je tijdens je ziekte voor me hebt gekocht. Ik weet dat je apetrots op me was geweest en hoewel je er vandaag niet bij bent, draag ik je toch altijd bij me. Ik weet dat je er op hoopte dat we de draad weer zouden oppakken en ik denk dat ik na vandaag kan zeggen dat we dat weer hebben gedaan. De pijn blijft, maar ik heb je beloofd niet bij de pakken neer te zitten. Kin omhoog en we pakken door!
Je had gewild dat we ook feest zouden vieren, want het leven is te mooi om verdrietig te blijven. Dus ik zal het glas op je heffen. Misschien met een traan, maar dat moeten we met z'n allen dan maar accepteren. Liefs!